THE UNIVERSITY *of* EDINBURGH

ENHANCING GAIT REHABILITATION USING ROBOTIC ASSISTANCE AND FUNCTIONAL ELECTRICAL STIMULATION

ANDREAS CHRISTOU

Doctor of Philosophy

School of Informatics
University of Edinburgh

2024

Andreas Christou:
Enhancing gait rehabilitation using robotic assistance and functional electrical stimulation
Doctor of Philosophy, 2024

SUPERVISORS:
Prof. Sethu Vijayakumar, Ph.D., FRSE
Dr. Mustafa Suphi Erden, Ph.D.

EXAMINERS:
Prof. Kia Nazarpour
Prof. Gordon Cheng

"Humans are not disabled. A person can never be broken. Our built environment, our technologies, are broken and disabled. We the people need not accept our limitations, but can transcend disability through technological innovation."

— Hugh Herr

LAY SUMMARY

Wearable robots and assistive exoskeletons are robots designed based on the human anatomy and are intended to be worn. These robots are equipped with sensors and motors that can help people with their activities of daily living and can be extremely useful in gait re-education for people suffering from neurological disease, stroke and spinal cord injury. However, the same disease may affect individuals differently, and even the same person may change the way they walk regularly, depending on their mood, fitness and energy levels. The way a robot interacts with the human during robot-assisted rehabilitation needs to capture these changes, and the assistance it provides needs to reflect the unique needs of each individual.

From studying the brain and the central nervous system, it is evident that in order to speed up recovery, learn how to walk again, and help the brain restructure itself after injury, we need to create a safe environment where the patient can be sufficiently challenged and encouraged to repetitively use and coordinate their muscles in a healthy fashion. Using robotics and other wearable sensors, we can observe how a human walks and very systematically provide assistance at the different joints. We can even externally stimulate the muscles, using gel electrodes (that can be placed on the skin) and low-intensity electrical signals (that are harmless to the human) to induce muscle contractions and re-educate patients on how to activate and coordinate their muscles. However, it is still a challenge to formalise the rules based on which the level of assistance, type of assistance, and timing of assistance will be decided.

In this thesis, we propose different methods that can be used to formalise these rules and design controllers for robots and electrical stimulation in order to improve the collaboration between robots and humans, and capture the unique needs of neurological patients. We experimentally evaluate the proposed methods and discuss their strengths and limitations. These methods contribute towards the advancement of techniques for designing personalised interventions for gait rehabilitation, which could lead to improved functional outcomes and accelerated recovery.

ABSTRACT

Wearable robots and assistive exoskeletons have great potential as tools for rehabilitation and assisted living. By providing support to dedicated joints and body segments, these devices can foster the independence of people suffering from neurological diseases and improve quality of life. However, ensuring these devices respond appropriately to the unique needs of each patient is crucial, as it can play a decisive role in whether neural plasticity is induced. This is particularly challenging as patients suffering from stroke or incomplete spinal cord injury start regaining control of their limbs, where rigid robot-driven interventions are no longer adequate to facilitate recovery and more adaptive patient-driven interventions are required.

Motivated by the principles of neuroplasticity, this thesis delves into the integration of wearable robots in neurological gait rehabilitation, with a central focus on the design of personalised interventions for ambulatory patients. More specifically, this thesis explores methods for the optimisation of robotic controllers and collaborative functional electrical stimulation (FES) controllers, such that assistance can be provided as needed, encouraging the patient to use their residual strength and actively take part in gait training.

Firstly, we formulate the problem of providing assistance 'as needed' as an optimisation problem and propose an offline model-based optimisation method for the design of personalised rehabilitation interventions. Using motion capture and high-fidelity musculoskeletal models, we construct a personalised model of the human interacting with the robot, and we optimise the controller of the robot using forward dynamics. We describe how this method can be applied for both the design of novel near-optimal surrogate controllers in the real-world, as well as the fine-tuning of parameterised controllers with a known control structure. The effect of the offline model-based optimisation method is evaluated both in simulation and experimentally, highlighting the need for personalisation and the importance of capturing the inter-personal and intra-personal variability in human behaviour.

An alternative to model-based optimisation is human-in-the-loop optimisation, where the human response to different levels of assistance can be obtained

in real time, reducing uncertainties due to modelling bias. Human-in-the-loop optimisation has proven to be an effective method for reducing the metabolic cost in robot-assisted locomotion, but its potential in enhancing rehabilitation has not been explored. We hypothesise that with the use of the Covariance Matrix Adaptation Evolution Strategy (CMA-ES), time-dependent variations in gait may be captured, facilitating the detection of time-varying local minima. Using continuous optimisation over a two-day experimental protocol we carry out a preliminary study of human-in-the-loop optimisation and present the results obtained from healthy subjects.

Beyond the deployment of robotics in neural rehabilitation, numerous physiological benefits can be achieved with the use of functional electrical stimulation (FES). Particularly interesting is the integration of robotics with FES, as the two have several complementary characteristics. However, due to the increased complexity of hybrid robot-FES systems, controller personalisation through model-based or human-in-the-loop optimisation becomes increasingly demanding. To promote the triadic collaboration between human, robot and FES, we propose a novel hierarchical and adaptive controller. We demonstrate a hybrid system that can prioritise the voluntary contributions of the human and effectively distribute the necessary assistive forces between the robot and the FES, in order to delay the onset of muscle fatigue and provide assistance as needed.

These methods contribute towards the advancement of techniques for designing personalised interventions for gait rehabilitation, which could lead to improved functional outcomes and accelerated recovery after training.

ACKNOWLEDGEMENTS

First and foremost, I want to thank my supervisor, Prof. Sethu Vijayakumar, for all the support and guidance during my time at the Statistical Learning and Motor Control (SLMC) Group. Prof. Sethu provided me with the right environment to grow and become a better researcher, scientist and communicator. I consider myself lucky to have been part of this group, where the expectations are high, and everyone is provided with the tools and support to meet them and exceed them.

Additionally, I would like to thank Dr. Mustafa Suphi Erden and Dr. Mohsen Khadem for their valuable feedback during my annual reviews. I want to convey my appreciation towards Dr. Juan C. Moreno and Dr. Antonio J. del-Ama for their insightful comments and advice, and thank the Neural Rehabilitation Group in Madrid, for their hospitality and contagious excitement for research.

Next, I want to express my heartfelt gratitude to my colleague and mentor, Daniel Gordon. Daniel not only provided me with a treasure of code libraries to give me a head start with my research, but also offered me a shoulder to cry on and a helping hand during all the experiments in the lab; not to mention the spell-casting cards while playing board games.

In the same way, I would like to thank Theodoros Stouraitis for his unconditional support and commitment. Amidst all the uncertainty involved with starting a PhD, Theo's welcome definitely made a difference, giving me confidence in what I do and making me feel at home.

I also want to thank the remaining members of the SLMC Group who have also helped me in one way or another: Andreas, Carlo, Carlos, Chris, Christian, Elle, Elliot, Giulia, Henrique, Jiayi, João, Juan, Keyhan, Lei, Marina, Namiko, Ran, Ruaridh, Russel, Saeid, Sanghyun, Serena, Songyan, Steve, Suzanne, Traiko, Victor, Vlad, and Wenqian. I would be remiss if I did not mention the people from the University's workshop, Douglas Howie, Gilbert Inkster, and Laura Ferguson, who have fabricated the props for our experiments, fast-tracking my progress.

Last but not least, I want to thank from the bottom of my heart, my family. There are no words to express how deeply grateful I am to my parents, Christos

and Christoula, for offering the world to me and always empowering me to pursue my dreams. I want to express my wholehearted gratitude to my partner, Lenna Kovacevic, and my dearest friend, Dr. Georgios Kassapis, for keeping me sane through Covid and the ups and downs of a PhD. And finally, I want to thank Constantina, Marios, Savvas and Sophia, and all my friends back home, and in the UK, for all the memories we have shared.

PUBLICATIONS

Parts of the research leading to this thesis have previously appeared in the following peer-reviewed publications. Some passages have been quoted verbatim from the respective sources.

JOURNAL ARTICLES

- A. Christou, D. Gordon, T. Stouraitis, J. C. Moreno, S. Vijayakumar. 'A model-based approach for the personalisation of robot-assisted rehabilitation'. [Under review], 2024.
- D. Gordon, A. Christou, T. Stouraitis, M. Gienger, S. Vijayakumar. 'Adaptive assistive robotics: a framework for triadic collaboration between humans and robots'. In *Royal Society Open Science*, 2023 Jun; 10(6):221617.
- D. Gordon, C. McGreavy, A. Christou, S. Vijayakumar. 'Human-in-the-Loop Optimization of Exoskeleton Assistance Via Online Simulation of Metabolic Cost'. In *IEEE Transactions on Robotics (**T-RO**)*, 2022 Jun; 38(3):3133137.

CONFERENCE ARTICLES

- A. Christou, A. Sochopoulos, E. Lister, S. Vijayakumar. 'Human-in-the-loop optimisation in robot-assisted gait training'. [Under review], 2024.
- A. Christou, A. J. del-Ama, J. C. Moreno, S. Vijayakumar. 'Adaptive Control for Triadic Human-Robot-FES Collaboration in Gait Rehabilitation'. In *IEEE International Conference on Robotics and Automation (**ICRA**)*, Yokohama, Japan, 2024.
- D. Gordon, A. Christou, T. Stouraitis, M. Gienger, S. Vijayakumar. 'Learning Personalised Human Sit-to-Stand Motion Strategies via Inverse Musculoskeletal Optimal Control'. In *IEEE Conference on Robotics and Automation (**ICRA**)*, London, UK, 2023.

- A. Christou, D. Gordon, T. Stouraitis, S. Vijayakumar. 'Designing Personalised Rehabilitation Controllers using Offline Model-Based Optimisation'. In *IEEE International Conference on Robotics and Biomimetics (**RoBio**)*, Xishuangbanna, China, 2022.

DECLARATION

I declare that this thesis was composed by myself, that the work contained herein is my own except where explicitly stated otherwise in the text, and that this work has not been submitted for any other degree or professional qualification except as specified.

Edinburgh, United Kingdom, 2024

Andreas Christou
25th October 2024

CONTENTS

LIST OF FIGURES

LIST OF TABLES

ACRONYMS

AAN	assist-as-needed
BWS	body weight support
CMA-ES	Covariance Matrix Adaptation Evolution Strategy
CV	coefficient of variation
DOF	degree of freedom
DOFs	degrees of freedom
EEG	electroencephalography
EMG	electromyography
FES	functional electrical stimulation
FSM	finite state machine
GRF	ground reaction force
GRFs	ground reaction forces
GUI	graphical user interface
HAPC	hybrid adaptive path controller
HIL	human-in-the-loop
HILO	human-in-the-loop optimisation
ILC	iterative learning control
IMUs	inertial measurement units
IQR	interquartile range
MPC	model predictive control
MS	multiple sclerosis
NMES	neuromuscular electrical stimulation
PD	proportional-derivative
PID	proportional-integral-derivative
RAGT	robot-assisted gait training

RMSE root-mean-squared error

SCI spinal cord injury

1 INTRODUCTION

1.1 MOTIVATION

Neurological gait rehabilitation

Neurological gait rehabilitation stands at the forefront of restoring mobility and independence for individuals grappling with motor impairments. Through a combination of strengthening, motor task training and tailored interventions, neurological gait rehabilitation strives to promote plasticity in the nervous system to enhance overall well-being and quality of life. Its impact extends beyond the individual, fostering societal benefits by reducing healthcare burdens and promoting greater social participation in people affected by conditions such as stroke, spinal cord injury, Parkinson's disease, and multiple sclerosis.

In Scotland alone, an estimated 12,000 people live with Parkinson's disease [1] and every year, approximately 10,000 stroke incidences are recorded [2]. Additionally, there are approximately 400 new registrations of people with multiple sclerosis per year [3] and another 100 incidents of people experiencing spinal cord injury (SCI) [4]. In total, there is an estimate of over half a million people in Scotland living with mobility disabilities, according to the House of Commons Library (UK Parliament) [5].

Compelling evidence suggests that neurological gait rehabilitation can have a statistically significant and a clinically meaningful impact on gait ability [6]–[15]. Both acute and chronic improvements can occur in conditions such as stroke and incomplete spinal cord injury [6]–[13], while psychological benefits and effective control of the symptoms of neurodegenerative diseases such as Parkinson's disease, multiple sclerosis (MS) and cerebral palsy, can result from neurological rehabilitation [16]–[21]. Due to the ability of the central nervous system to adapt to external stimuli, improvements in the functional ability of neurological patients may be attributed to a combination of spontaneous and learning-dependent processes [22], [23]. Even though there are still several open questions surrounding the mechanisms of adaptation in

the adult brain [24], it is clear that these adaptations take place to accommodate for the feedback received during environmental interactions [25]–[28]. These neuroplastic adaptations form the stepping stone for all activities constituting neurological rehabilitation [29].

The role of technology in gait training

With the integration of technology in neural rehabilitation new possibilities to accelerate the path to recovery have emerged. Nowadays, it is possible to accurately measure ground reaction forces, joint angles and joint forces during gait, as well as muscle activity and brain activity to quantitatively analyse gait performance, and characterise pathological gait. We can now, better than ever, externally support the human body during locomotion, provide systematic assistance at weakened joints and stimulate muscle groups and/or brain regions both invasively and superficially to enhance gait training. The use of instrumented treadmills, body weight support (BWS), wearable sensors, electromechanical orthoses, and functional electrical stimulation (FES) have given new meaning to neurological rehabilitation and hope for improved performance and shorter recovery time (Figure 1).

To date, there is evidence to suggest that some forms of technology-assisted gait training are at least as effective as conventional therapist-assisted training for stroke survivors [30], [31], and individuals with SCI [32]–[34], Parkinson's disease [35], and multiple sclerosis [36]. On the one hand, this could be expected since the functionality of many of these devices is inspired by human-to-human therapy, and are thus designed to mimic what physical therapists do [37]–[39]. On the other hand, the ability of these devices to prolong the duration of therapy, to progressively increase the difficulty of training, to provide real-time (bio)feedback, and to precisely combine large amounts of data in order to personalise interventions, motivates the pursuit of a system that can prove to be superior to conventional therapy. But how do we design such a system that can provide assistance that is tailored to the unique needs of each patient? How can we make use of these data to make a machine understand the needs of the patient and maintain a challenging yet engaging environment for the patient to improve to the point where they are independent and they no longer need assistance?

(a) (b) (c)

Figure 1: Examples of gait rehabilitation using (a) a walking frame (extracted from [40]), (b) the stationary robotic platform LOKOMAT (extracted from [41]) and (c) the exoskeleton ABLE with a walker (extracted from [42]).

1.2 THESIS SCOPE

In this thesis we present new methods for the design of personalised rehabilitation controllers for robotic devices and FES. It is hypothesised that through novel patient-driven and personalised interventions, technology assistance will further improve the outcomes of physical therapy for ambulatory patients who retain voluntary control of their limbs. This becomes particularly important as patients with stroke and incomplete spinal cord injury start regaining voluntary control over their limbs. At this point, a shift is required from robot-driven interventions to patient-driven interventions. With an emphasis on the technical development of novel interventions, this thesis contributes to the development of robot controllers and hybrid robot-FES controllers that promote healthy human-robot collaboration following fundamental principles of neurorehabilitation.

1.3 APPROACH

The approach followed for this thesis has three basic components:

- Design from first principles: The task of assisted rehabilitation is formulated as a multi-objective optimisation problem and state-of-the-art optimisation techniques are exploited to find optimal solutions.

- Human-centric rehabilitation: Inspired by the highly personalised assistance provided by healthcare professionals during gait training, in this thesis we focus on delivering personalised assistance where accommodating for and encouraging the voluntary contribution of the human is fundamental.
- Technical novelty: It is common practice in medicine to run preclinical testing and evaluate new interventions first in vitro, and then in vivo, by carrying out animal testing before any experiments are carried out on humans. This is a good analogy of the process followed in the development of robotic interventions for rehabilitation. The process followed here is equivalent to the preclinical testing of medical interventions. With an emphasis on the technical novelty, the methods described are developed and tested firstly in simulation, and are then validated on healthy subjects before they are verified on neurological patients.

1.4 CONTRIBUTIONS

The main contributions of this thesis include the:

- Development of a pipeline for the offline model-based design and optimisation of personalised rehabilitation controllers (Chapter 3).
- Evaluation of human-in-the-loop (HIL) optimisation in the context of robot-assisted rehabilitation (Chapter 4).
- Design of an adaptive and hierarchical controller for the triadic collaboration of human, robot and FES (Chapter 5).

In all cases, the presented contributions have been validated on healthy subjects.

1.5 THESIS OUTLINE

This thesis consists of a total of six chapters. Chapter 2 provides an introduction to some of the fundamental concepts that have guided this research, along with a detailed description of the technologies used. A brief introduction into the history of neurological gait rehabilitation is provided, followed by

a review of the principles of neuroplasticity. Next, the available methods for motion capture and musculoskeletal modelling are presented, as well as a more detailed description of the motion capture and modelling tools used for the completion of the presented studies. The specifications of the robotic system used to provide external assistance are outlined, and a review of the literature is carried out summarising the state-of-the-art robotic controllers and their effectiveness in gait rehabilitation. Lastly, an introduction of what constitutes FES is provided and its impact on gait training is summarised. The following three chapters, Chapters 3-5, discuss the technical details of the proposed methods for the design of personalised assistive controllers.

Chapter 3 presents an offline model-based optimisation methodology for the design and personalisation of collaborative robotic controllers. By leveraging the power of high-fidelity musculoskeletal models, a method for choosing the optimal control structure and optimal control parameters for each person is described. We formulate the problem of providing assist-as-needed (AAN) as an optimisation problem and demonstrate how from the optimal behaviour of the robot, surrogate controllers can be designed. The potential of this method to improve the collaboration between human and robot in a rehabilitation task for the lower limbs is highlighted both in simulation and experimentally.

In Chapter 4 the potential of human-in-the-loop optimisation (HILO) in gait rehabilitation is evaluated. HILO provides an alternative to model-based optimisation, where the human response to different levels of assistance can be obtained in real time, reducing uncertainties due to modelling bias. A method that has been widely used for the optimisation of assistive forces in human augmentation applications, commonly relying on devices consisting of one actuated degree of freedom, is tested for the first time in a multi-degree-of-freedom robot for the purpose of gait rehabilitation. An objective function that aims to find a balance between user performance and robotic assistance is proposed, and an evolutionary algorithm is implemented to obtain the controller parameters that reflect the needs of the human. An experimental protocol that aims to capture the impact of HILO is designed, and preliminary data from healthy subjects are reported.

In Chapter 5 a novel adaptive and hierarchical controller is presented for the triadic collaboration between human, robot and FES. Due to the increased complexity associated with the modelling and optimisation of hybrid systems, a hybrid controller that provides personalised assistance through adaptive

control is studied. Based on the principles of path control and iterative learning control, a controller is developed that prioritises the voluntary movement of the user, prevents muscle fatigue, provides robotic assistance as needed, and promotes the collaboration between human, robot and FES. Simulation results from the development of the controller using musculoskeletal modelling, and experimental results from a pilot study with one healthy subject are presented, comparing our proposed hybrid adaptive controller against an exoskeleton-only controller, a FES-only controller and a hybrid non-adaptive controller.

Finally, in Chapter 6 the conclusions drawn from the presented studies are summarised, and future research directions are discussed.

2

RELATED WORK, TOOLS AND METHODS

"Every man can, if he so desires, become the sculptor of his own brain."
- Santiago Ramon y Cajal

This thesis combines concepts from the fields of neuroscience, physical therapy and robotics to formulate testable research hypotheses and experimental protocols. This chapter provides an overview of the theory upon which the research hypotheses were derived, a description of the technologies used for the completion of this research and a summary of the state-of-the-art developments in this field.

2.1 BRIEF HISTORY OF NEURAL GAIT REHABILITATION

The concept of neural rehabilitation and its application in gait therapy is a product of years of research in the fields of neuroscience and physical therapy. For many years, the ability of the nervous system to adapt to environmental stimuli has been hypothesised. The idea of brain growth as a result of mental exercise has been discussed as early as 1783 [43], [44]. This is a century earlier than the conceptualisation of the 'neuron doctrine', or 'neuron theory', by Heinrich Wilhelm Gottfried von Waldeyer-Hartz in 1891 [45], [46], and the discovery of the axonal growth cone and the ability of the neurons to grow in adults demonstrated by Santiago Ramon y Cajal in 1894 [47], [48]. However, it wasn't until the 1960s that these hypotheses regarding neural adaptation were tested more rigorously [49]–[52]. Following these groundbreaking discoveries, the field of neuroscience evolved rapidly to significantly enhance our understanding of neural plasticity and the effect of internal and external stimuli on neuron morphology and neuron generation and degeneration [27].

Shortly after these pioneering findings in neuroscience, the outbreak of the polio epidemic in Europe and America, and the two world wars that followed marked the start of the profession of physiotherapy and neural rehabilitation [56]–[59]. Early in the 20th century, the practise of corrective exercises

(a) (b)

Figure 2: Gait rehabilitation using (a) proprioceptive neuromuscular facilitation and (b) movement control therapy following the Bobath concept (extracted from [53], [54]).

and muscle re-education was explored as an alternative to casts and splints to treat muscle weakness and paralysis from poliomyelitis [57], [59]. By the 1960s, more methods and techniques for addressing neurological disorders such as stroke, cerebral palsy and traumatic injury were introduced by Berta and Karl Bobath, Margaret Rood, Margaret Knott, Dorothy Voss, and Signe Brunnstrom [58], [60]–[63]. These included proprioceptive neuromuscular facilitation (PNF) techniques [62] (Figure 2a), resistance exercise, approaches that focused on promoting normal movement patterns (Figure 2b), postural stability and more [58], [59]. In the years that followed, advancements in motion capture, electromyography, electrical stimulation and brain imaging, revolutionised neurological rehabilitation (Figure 3), by facilitating the quantitative analysis of neural and physiological adaptation, and shaping our current understanding and practises.

2.2 PRINCIPLES OF NEUROPLASTICITY

A fundamental concept that underpins the effectiveness of neurorehabilitation is neuroplasticity; the brain's remarkable ability to adapt and reorganise itself in response to experience and injury. By understanding the various principles of neuroplasticity, researchers gain insights into the mechanisms driving neural

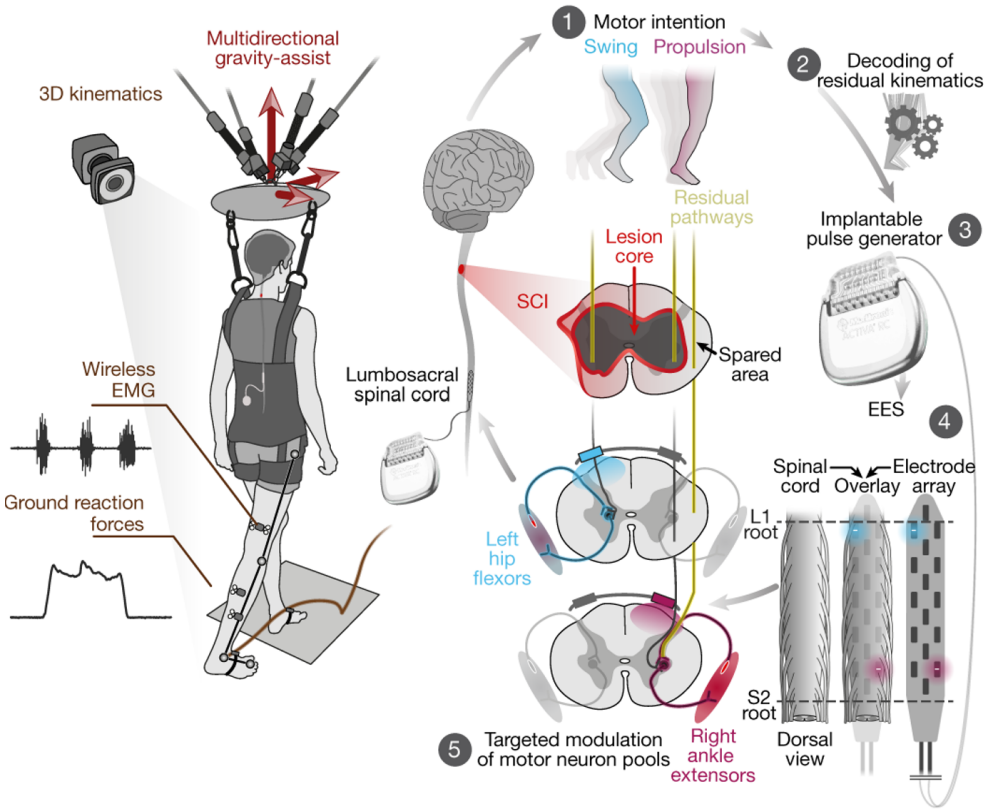

Figure 3: State-of-the-art technology-assisted gait training with multidirectional gravity assistance, motion capture and epidural electrical stimulation (extracted from [55]).

recovery and adaptation. This is crucial in designing effective rehabilitation interventions aimed at restoring function. This section discusses the principles of neuroplasticity, exploring how various factors influence the brain's capacity for adaptation.

In a highly influential review, Kleim and Jones [25] concisely summarise years of research in neuroscience as '10 principles of experience-dependent neural plasticity' (Table 1). First, the importance of the active engagement of neural circuits in task performance is highlighted. Animal studies have shown that sensory deprivation can lead to a decrease in synapse number and partial reallocation of cortical territory [64]–[67], whereas extended training can lead to increased synaptic responses and synaptogenesis [68]–[71], the effects of which are also evident in the adult human brain [22], [28], [72], [73]. It is also evident that the nature of plasticity is highly specific to the training experience [74]–[78], sensitive to the intensity of training [79]–[82] and dependent on the dose of training [83]–[85]. It has been concluded by several reviews that a higher number of task-specific repetitions and intensive training, are more

Table 1: Principles of experience-dependent neural plasticity as summarised by Kleim and Jones [25].

Principle	Description
1. Use It or Lose It	Failure to drive specific brain functions can lead to functional degradation.
2. Use It and Improve It	Training that drives a specific brain function can lead to an enhancement of that function.
3. Specificity	The nature of the training experience dictates the nature of the plasticity.
4. Repetition Matters	Induction of plasticity requires sufficient repetition.
5. Intensity Matters	Induction of plasticity requires sufficient training intensity.
6. Time Matters	Different forms of plasticity occur at different times during training.
7. Salience Matters	The training experience must be sufficiently salient to induce plasticity.
8. Age Matters	Training-induced plasticity occurs more readily in younger brains.
9. Transference	Plasticity in response to one training experience can enhance the acquisition of similar behaviors.
10. Interference	Plasticity in response to one experience can interfere with the acquisition of other behaviors.

likely to lead to improved functional outcomes [25], [74], [86]–[88], with little evidence to suggest that there is any harm in doing more, provided the timing of training is right [84], [85].

This leads to another important principle of neuroplasticity which is the timing of training. Even though it is generally accepted that reduced neuroplasticity can be expected in the ageing population as opposed to younger adults [89]–[91], several studies support the hypothesis that regardless of the age of the patient, early intervention is more likely to lead to improved functional outcomes [25], [85], [92]. However, there have also been indications to suggest that very early intensive training may lead to worse functional outcomes in people with stroke [93], [94]. Similar results have also been observed in rodent studies and have been associated with overuse and exaggerated excitotoxicity of vulnerable tissue [95]–[98], which suggests that identifying the optimal dose of training over time remains an open scientific question that requires more research.

Kleim and Jones also emphasise in their review the importance of incorporating in training, elements that can attract the subject's attention, and can increase their sense of reward, referred to as 'salience' [25]. This is also highlighted by several reviews that have discussed the important role of neurotransmitters such as dopamine, serotonin, noradrenaline and acetylcholine in neuroplasticity [99]–[102]. It is clear that while neural activation can be prompted by manipulating the mechanics of the body, permanent adaptations in the nervous system are best established when patients are in a state of alertness and wakefulness.

Moreover, it is evident that neural plasticity has the potential to both promote and inhibit subsequent plasticity. Maladaptive plasticity as a result of compensatory strategies can impede subsequent learning [103]–[105], while the combination of training with transcranial or peripheral stimulation can promote [106]–[108] or impede [109]–[111] skill acquisition depending on the relative timing of stimulation with respect to training [112].

Maier et al. [26] have elaborated on the principles of neuroplasticity to highlight the importance of a few more components including spaced practise, multisensory stimulation, explicit and implicit feedback, and motor imagery. Maier et al. [26] highlight in their review the importance of rest during training and emphasise how spaced practise, also known as distributed practise, has been found to improve skill acquisition [113]–[115]. This is also in line with recent studies that have underscored the importance of post-training quiet rest and sleep to promote neuroplasticity for memory consolidation and skill acquisition [116]–[121]. Maier et al. also elaborate on the importance of multisensory stimulation [122]–[124] and the different forms it can take to provide explicit and implicit feedback. The importance of visual feedback [125], [126], rhythmic cueing [127]–[131], mirror training [132]–[134], and action observation [135]–[137] are discussed, emphasising on their potential to enhance functional outcomes after training.

In summary, neuroplasticity or brain plasticity is what allows humans to acquire motor skills and recover from injury. Over time, researchers have identified multiple principles of neuroplasticity, reflecting the intricate and dynamic nature of the nervous system. It is clear that these principles play a crucial role in neural rehabilitation, emphasising the need for their integration into functional training [29], [138]–[140].

With the aid of technology, harnessing these principles has become more feasible, offering new avenues for innovative approaches to rehabilitation. In the following sections, we provide a description of motion capture technologies, musculoskeletal modelling, robot-assisted rehabilitation and functional electrical stimulation and their role in designing effective neural rehabilitation interventions that are tailored to the needs of the patient and are based on the principles of neuroplasticity.

Motion capture refers to the techniques that allow us to record the movement of an object, animal or person, and are widely used in recording and later analysing human biomechanics. These techniques are broadly classified into two main categories: optical and non-optical. Optical motion capture systems use optical-active or optical-passive markers [141], RGB or RGB-D cameras [142], while non-optical systems rely on other sensors such as inertial measurement units (IMUs), and magnetic systems [143], [144]. As of today, optical marker-based systems combined with ground force plates are considered to be the gold standard for three-dimensional motion capture [145]–[147].

For this thesis, a Vicon marker-based system has been used for gait analysis. During this process, reflective markers are placed on anatomical landmarks of the human body and multiple cameras are used to simultaneously record the trajectory of the markers in space. The marker trajectories are labelled, and based on the labelled trajectory of the markers, the position and orientation of the different body segments can be determined. Based on the position and orientation of the different body segments, the angular position of the joints can be calculated and analyses on the dynamics of motion can be carried out (see section 2.5).

2.3.1 *Hardware*

Vicon System

Vicon systems (UK) are among the most popular systems for high-precision motion capture and the analysis of human biomechanics. At the Gait Lab (University of Edinburgh, UK), a Vicon system consisting of 12 Vero v2.2 cameras is available, along with a Vicon Lock+ synchronisation box comprising a 64-channel analog-digital converter. The Vero v2.2 cameras are high-resolution infrared cameras that emit and capture infrared light reflected off optical-passive markers. The cameras are strategically positioned around a designated capture volume (Figure 4a), and are operated at a frequency of 100Hz. The marker data goes through the Vicon Lock+ synchronisation box which operates at 1000Hz and is processed through the Nexus software. The final output is a time series of labelled marker trajectories, which can be used for further

analysis either through Nexus or other specialised software to obtain kinematic and dynamic data including joint angles, joint moments, joint loads etc (see section 2.5).

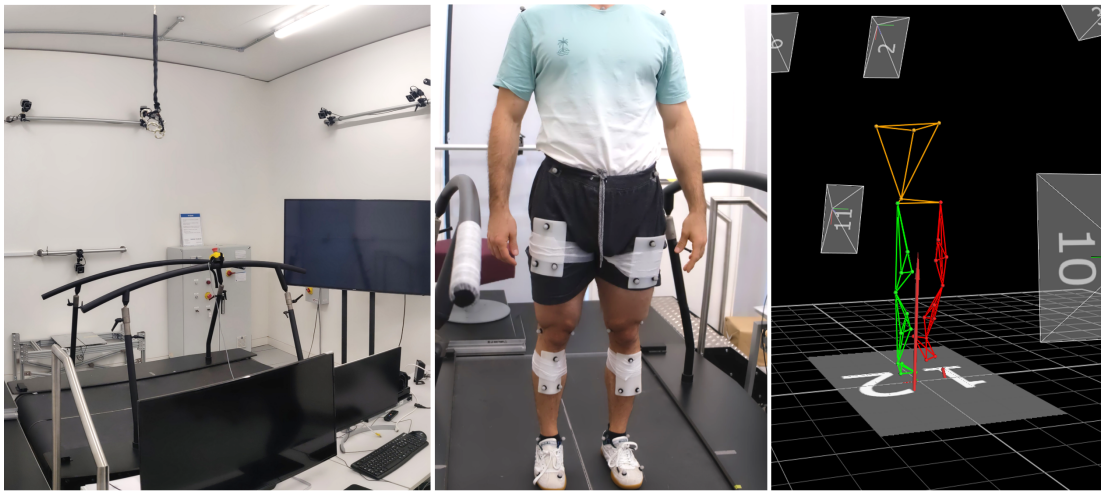

(a) (b) (c)

Figure 4: (a) The Gait Lab (University of Edinburgh, UK) including a vicon motion capture system with 12 Vero cameras positioned around the M-Gait treadmill (b) A subject wearing reflective markers while standing on the M-Gait treadmill, (c) Reconstructed figure of recorded markers during gait using the Vicon Nexus software.

Instrumented treadmill

To facilitate motion capture and force analysis within a contained capture volume, the instrumented treadmill M-Gait (Motek, Netherlands) was used. M-Gait is a dual-belt instrumented treadmill equipped with two permanent-magnet full-servo motors, enabling independent speed control of the two belts, and twelve 6-axis force-torque sensors enabling the measurement of ground reaction forces (GRFs). As an output, the magnitude of the ground reaction forces, $\mathbf{f}_g \in \mathbb{R}^3$, and ground reaction moments, $\boldsymbol{\tau}_g \in \mathbb{R}^3$, for each belt can be obtained as a time series for the x-y-z directions, along with the calculated point of action of the GRFs, known as the centre of pressure, $\mathbf{c}_p \in \mathbb{R}^3$ (Figure 5). The analogue signals of the force sensors are processed through the Vicon Lock+ box at a frequency of 1000Hz and are communicated to the Vicon motion-capture software, Nexus, and the Motek software, D-flow. Using D-flow, the speed of each of the belts of the treadmill can be controlled, dependent or independent of the outputs from the Vicon Lock+ box, and

interactive applications can be developed, such as self-paced walking, virtual reality visualisations, and unstable environments.

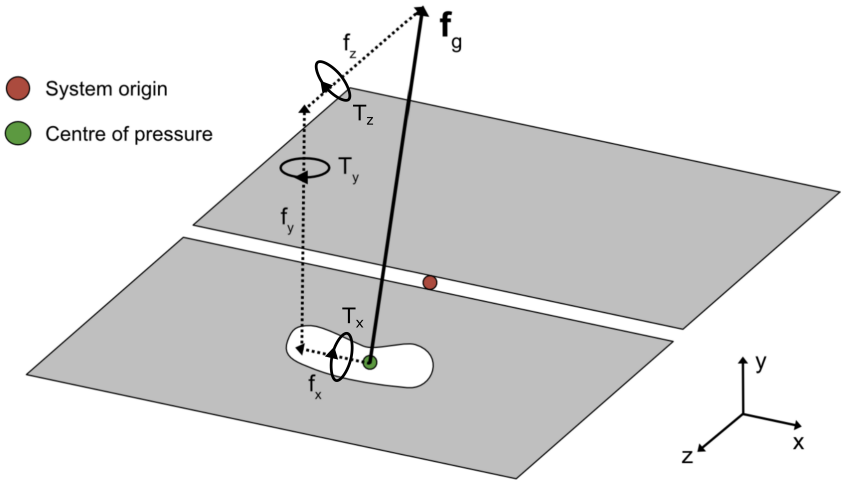

Figure 5: Diagram of the instrumented dual-belt treadmill and the measured GRFs and centre of pressure (extracted from [148]).

2.3.2 *Marker placement*

Marker placement in motion capture dictates the degree of accuracy of the recorded data. Depending on the application, the number of markers and the location of the markers can change. For example, if only the position of the human body is of interest in a three-dimensional space, then a single marker at the pelvis may suffice. For measurements of human kinematics during gait, more granularity is required to accurately track the position and orientation of the different segments of the lower limbs.

A custom marker set was used in our studies for motion capture with a focus on lower limbs. The marker set consisted of 32 markers: 20 anatomical markers placed on bony landmarks on the human body, and 12 tracking markers placed as rigid clusters at the thighs and the shanks. Figure 6 shows the marker set used for gait analysis. The anatomical markers are placed on well-defined anatomical landmarks that can be precisely located across individuals, such as the lateral and medial malleoli of the ankle joint, and can be used as a reference for processes such as model scaling and the adjustment of tracking markers in musculoskeletal modelling (see section 2.4 for more details). Tracking markers are markers that are used to further increase the accuracy of motion capture

during dynamic trials, and do not need to be placed consistently across subjects as their exact position can be identified during the post-processing of the data based on the position of anatomical markers (see section 3.3.1).

Figure 6: Placement of reflective markers for gait analysis. Tracking markers were placed on the right (1) and the left (2) shoulder and an anatomical marker was placed on the sternum (3). Three anatomical markers were used to define the pelvis with one marker on the right anterior superior iliac spine (ASIS) (4), one on the left ASIS (5) and one on the sacrum (6). A cluster of three tracking markers was used on the thighs (7a-7c) and anatomical markers were placed on the lateral (8) and medial (9) femoral epicondyles. A cluster of three tracking markers was also placed on the shanks (10a-10c). The feet were defined with five anatomical markers placed on the lateral (11) and medial (12) malleoli, the fifth (13) and the first (14) metatarsal heads and the heel (15).

2.3.3 *Data Processing*

The final step for a reliable transition from motion capture to gait analysis is data processing. While optical marker-based motion capture offers high precision and reliable measurements, the reliability of each recording may be affected by jitter and gaps in marker trajectories. To reduce errors during motion capture, a system calibration is carried out which involves the masking

of reflective parts of the lab, and the centering of the capture volume using a light-emitting wand. This system calibration is performed at least 45 minutes after initialisation, ensuring the cameras have reached a stable operating temperature. To further increase the reliability of data, a constraint is implemented that defines the minimum number of cameras required to detect the trajectory of a marker to three cameras. However, occlusions that prevent the detection of markers by at least three cameras result in gaps in the trajectories of the markers. Therefore, once the motion capture is completed, the marker trajectories are labelled and checked for gaps.

The Vicon Nexus software provides five different methods for filling up gaps in marker trajectories: spline fill, pattern fill, rigid body fill, kinematic fill and cyclic fill [149]. Spline fill uses interpolation on quintic splines generated from valid frames around the gap to predict the trajectory of a marker, while pattern fill predicts the trajectory of a marker using linear interpolation and the trajectory of a reference marker. Rigid body fill uses the trajectory of other markers to fill in trajectory gaps assuming that the marker whose trajectory is missing is part of a rigid body, while kinematic fill determines the fill based on the position and orientation of a body segment. Provided that the Vicon model has clearly defined joints and segments, the position and orientation of the model's segments can be obtained from raw marker data using direct kinematics. Lastly, cyclic fill uses patterns from a missing marker's earlier or later gait cycles to fill gaps. Depending on the recorded motion and the duration of the gap, these different methods for gap filling are used to generate continuous marker trajectories.

As a final step, smoothing of the marker trajectories is carried out using a 4th order low-pass zero-lag Butterworth filter at 6Hz [150]. This is to remove noise and artefacts due to gap filling, unstable markers, and tracking errors. The continuous smoothed marker trajectories are then exported along with the corresponding GRFs, and can be used for further processing including model scaling, and inverse kinematics and dynamics analyses that are discussed in more detail below.

Musculoskeletal modelling is a powerful tool that can play a crucial role in gait analysis. By using data from motion capture, personalised human models can be constructed that can be used to provide more insights into the biomechanics of human locomotion. These models can then be combined with the inertial properties of wearable robots, and personalised human-robot models can be constructed, which can be used to improve our understanding of the interactions between human and robot, and facilitate the design of tailored interventions for rehabilitation. For this purpose, several musculoskeletal modelling platforms are available, with the most popular being OpenSim [151] and AnyBody [152].

For this thesis, the musculoskeletal modelling software, OpenSim, was used. OpenSim offers detailed musculoskeletal models that can be adjusted to reflect the physical properties of the human [151], including any characteristics that may be a result of an injury or a neurological disorder. These include muscle properties such as the muscle attachment point, the minimum muscle activation, and the maximum isometric force, tendon properties such as tendon compliance, tendon slack length, and the tendon maximum strain, and skeletal properties such as the inertia properties of body segments, and the axis of rotation and functional degrees of freedom of joints. Based on experimental data and studies on human anthropometry [153], [154], joint anatomy [155], [156] and the properties of skeletal muscle [157], [158] a series of human musculoskeletal models of varying complexity are provided.

For the modelling of the human body in this thesis, the generic OpenSim model, *gait1018*, was used (Figure 7b). This model focuses on the lower limbs and is a dimensionally reduced version of the *gait2354* model [153] (Figure 7a), intended for simulations of high computational demands. It consists of 12 bodies and 12 joints that are represented by 10 degrees of freedom (DOFs) and are driven by 18 musculotendon units. To construct personalised models that accurately reflect the anatomical properties of the human subjects in our studies, the generic OpenSim model, *gait1018*, was first adjusted to support hip adduction and abduction. The adjusted model was then scaled using data from motion capture, and combined with the model of the exoskeleton, Exo-H3 (see section 2.6.1). More details regarding the scaling of the human model and its integration with the robot model are provided in Chapter 3.

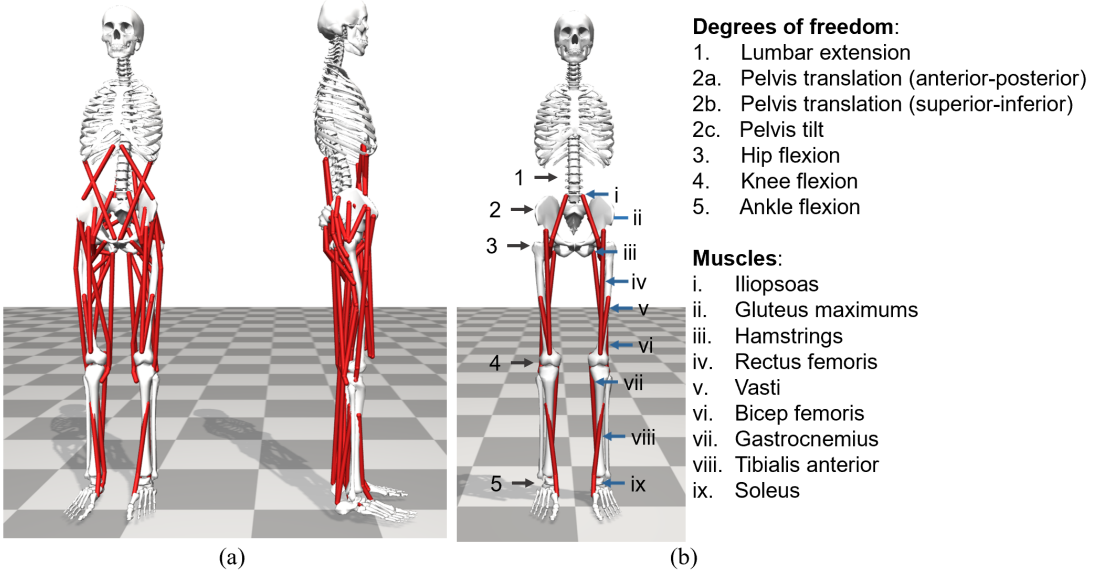

Figure 7: (a) OpenSim model, *gait2354*, (b) Dimensionally reduced OpenSim model, *gait1018*, with annotated degrees of freedom and musculotendon actuators.

2.5 GAIT ANALYSIS

The gait cycle

Using musculoskeletal models, gait analysis can be carried out to quantify clinically meaningful characteristics of gait based on the relative position and orientation of the different body segments. This is commonly performed in three spacial dimensions referred to as the frontal plane, the sagittal plane and the transverse plane (Figure 8a). To facilitate a more granular analysis of human locomotion, a temporal segmentation of gait has also been established. A gait cycle that starts and ends at well-defined discrete events such as the heel strike and toe off is being used, and the relative position in the gait cycle, ranging from $[0, 100]\%$, is often referred to during gait analysis to define an instance in the gait cycle (Figure 8b). Based on these discrete events, different phases in the gait cycle are also defined such as double stance, single stance and the swing phase, and have been used to carry out comparisons across subjects (and within subjects) to identify artefacts of neurological disease, motor training or external assistance.

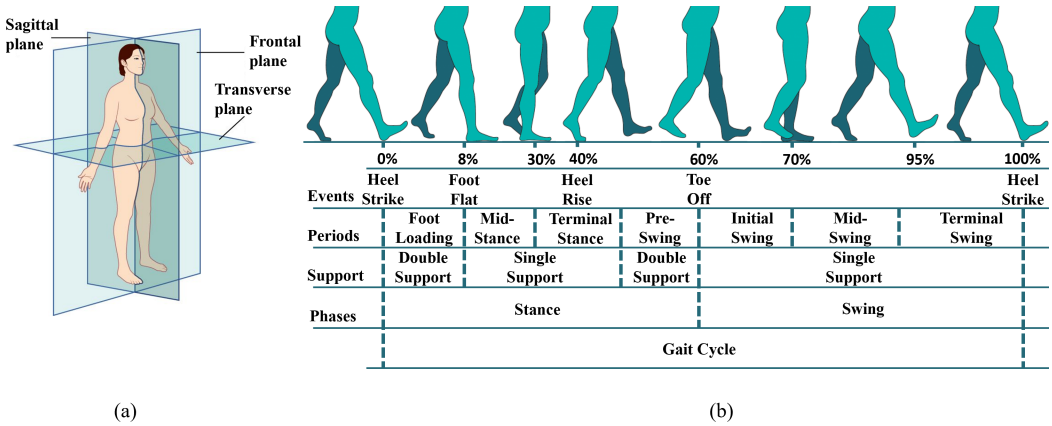

Figure 8: (a) The three planes of motion and (b) the gait cycle.

Inverse and forward analyses

For the quantification of gait characteristics, inverse and forward dynamics analyses can be carried out. During the inverse analysis, the joint angles or the joint torques of the model, respectively, can be calculated based on the marker trajectories and the ground reaction forces obtained during motion capture. Similarly, the muscle controls of the model can be computed using musculoskeletal modelling. This can be carried out through an optimisation procedure that assumes metabolic efficiency in the human body and minimises the sum of controls and joint acceleration errors. As a result, gait can be analysed using kinematic, dynamic and clinically relevant metrics such as average gait speed, average step length, duration of swing, symmetry in stance, variability in kinematics, peak load in joints, maximum activation of muscles and more.

Furthermore, forward dynamics analyses can be carried out. During forward dynamics, the differential equations of the model can be integrated to compute the future kinematics of the model. Provided that the joint torques or muscle controls of the model, as well as any other external forces acting on the model, are known at the different points in time, the future state of the model can be calculated. In the case where a wearable robot is interacting with a human, this can be a powerful tool for the prototyping and optimising of robotic controllers. This is discussed in more detail in Chapter 3.

These powerful tools for motion capture and gait analysis, along with advancements in technology and our increased appreciation towards the principles of neuroplasticity, have driven the development of innovative gait training methods. For example, treadmill training and body weight support have proven to be extremely useful for delivering task-oriented training, where a high number of repetitions can be performed in a confined and safe environment [30], [159]. Moreover, the incorporation of real-time visual feedback, electrical stimulation and robotic assistance have integrated into gait training the concepts of multisensory stimulation and salience, making gait therapy more captivating and interactive. It would thus be expected that with the use of technology, the functional outcomes of gait rehabilitation would be superior to conventional therapist-assisted rehabilitation. However, this is a very broad statement that (1) does not specify what the use of technology entails, (2) does not indicate what functional outcomes are of interest, (3) does not differentiate between neurological conditions, and (4) does not distinguish between the different stages of rehabilitation.

Several reviews have tried to investigate the effectiveness of robot-assisted rehabilitation on the different functional and clinically-relevant outcomes of training for different neurological disorders [19], [36], [160], [161], addressing points (2)-(4), but not many studies have carried out the meta-analysis on the effect of the technology used and implemented control method during robot-assisted gait training (RAGT) on the outcomes of therapy (point 1). One of the most important components of therapist-assisted gait rehabilitation, is the interaction between the therapist and the patient. Similarly, in RAGT, how the robot interacts with the patient can be a determining factor of whether RAGT is beneficial or not. Campagnini et al. [162] carried out this investigation and looked at the effect of different control strategies during RAGT on the functional outcomes of people with stroke in the subacute or chronic phase. It is concluded that due to the high heterogeneity in study design and performance metrics, it was not possible to carry out a meta-analysis to identify differences in the relative effectiveness of the different control strategies used in RAGT.

To the best of our knowledge, a similar investigation for the effect of functional electrical stimulation (FES) control on the outcomes of therapy is not available. Evidently, understanding the effects of different stimulation

profiles on muscle force generation and induced muscle fatigue was prioritised. Moreover, a much richer literature seems to exist on the neuroprosthetic applications of FES than the therapeutic applications of FES.

Here, we provide an introduction to RAGT and FES, and review the algorithms used for the control of assistive robots and electrical stimulation. The aim of this review is to offer a comprehensive understanding of the current state of the art in RAGT and FES-assisted gait training, highlighting recent advancements and identifying existing gaps in the literature. This analysis sets the stage for comparing and contextualising the contributions outlined in the subsequent chapters.

2.6.1 *Robot-assisted rehabilitation*

Robot-assisted gait training gained increasing popularity in the last two decades with the introduction of actively-controlled electromechanical devices. These devices can be programmed to safely exert guiding forces on a selection of the patient's body parts and provide partial body weight support to alleviate the strain on healthcare professionals. They can also guarantee high precision and repeatability, and provide a means for quantitatively assessing the performance of the patient.

These devices are generally classified into two categories: exoskeletons and end-effector robots (Figure 9). Exoskeletons are wearable robots that are placed on the exterior of the user's skeleton and can provide assistance at the joints of the patient. They can be integrated with a treadmill and body weight support (Figure 9a), or they can be used for overground gait (Figure 9c). End-effector robots are often stationary platforms that drive motion by attaching to the feet of the patient. Due to their distinct design features, the algorithms used to drive these devices often varies. While the control methods used for end-effector robots are often limited to position profile controllers [163]–[167], with a few exceptions where admittance control [168], [169] and impedance control [170] have been implemented, a much richer literature exists on the controllers used for exoskeletons.

The reviews carried out by Tucker et al. [172], Miguel-Fernandez et al. [173] and Baud et al. [174] summarise the controllers used to drive exoskeletons, and classify them into a hierarchical order. These include high-level controllers that

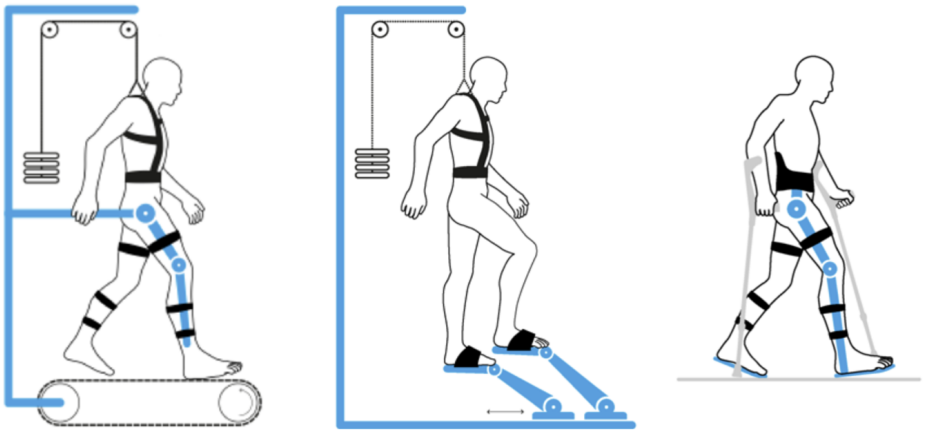

Figure 9: Types of actively-controlled electromechanical devices: (a) wearable exoskeleton integrated with a treadmill and body weight support, (b) end-effector robots and (c) wearable exoskeletons for overground gait (extracted from [171]).

aim to identify the task being executed and select the corresponding mid-level controller, mid-level controllers that are responsible for calculating the desired joint positions, velocities or torques to help with the execution of the task, and low-level controllers that are responsible for realising these commands. With our focus lying on the assistance of gait rehabilitation, the implementation of high-level controllers extends beyond the scope of this thesis. Similarly, the low-level controllers are usually dependent on the type of actuators used and are often shared across robotic devices. Thus, here we discuss the mid-level controllers developed for providing assistance in gait rehabilitation.

Baud et al. [174] further categorised the mid-level controllers into two sub-categories: the detection/synchronisation controllers and the action controllers (Figure 10). The former is responsible for estimating the gait state, gait phase or intention of the human, which is information often used by the action controller for the operation of the exoskeleton. This information includes the estimation of different events and gait phases using methods such as manual triggering via user-operated buttons [175]–[178], event triggering through ground reaction force (GRF) sensing [179]–[181], adaptive frequency oscillators [182], [183], finite state machines [184]–[186] and more. In the action controllers, methods for the calculation of the physical output of the robot are included.

The three main types of mid-level controllers identified in the sub-category of action controllers involve: position profile controllers, torque profile controllers and impedance controllers [172]–[174]. Position profile controllers aim

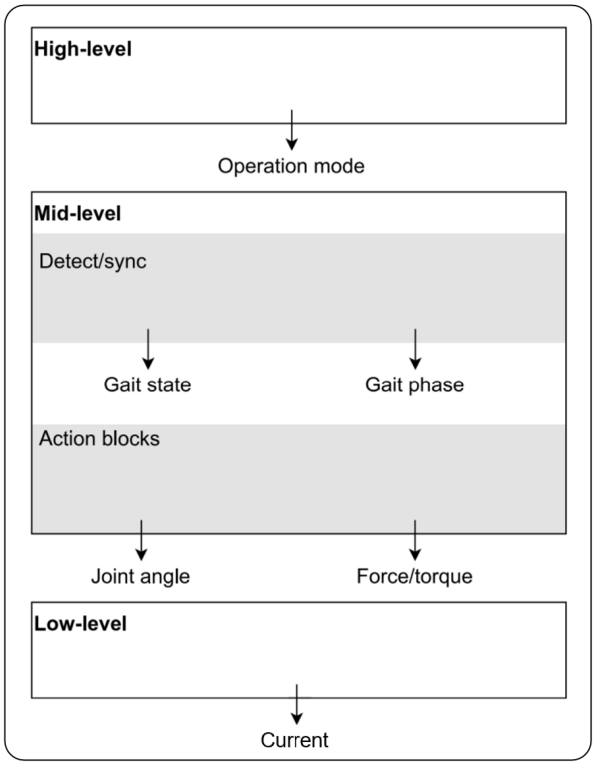

Figure 10: Classification of robot controllers into high-level, mid-level and low-level controllers (adapted from [174]).

to strictly follow an input position profile that is defined either in joint space or end-effector space. Similarly, torque profile controllers aim to generate an input torque profile, whereas impedance controllers aim to establish a relationship between joint angle and joint torque [187], [188]. Most position profile controllers rely on profiles that have been extracted from the kinematics observed in healthy people [189]–[191], with a few studies investigating methods for generating or adapting kinematic trajectories, either offline [192], [193] or in real time [175], [194]–[198]. Similarly, many torque profile controllers rely on constant torque profiles [181], [199]–[202] with some studies investigating methods for identifying the appropriate shape and/or timing of the torque profiles based on feedback from the users [6], [203]–[206]. Impedance controllers on the other hand, provide partial assistance (or resistance) and a certain degree of compliance to help patients follow a fixed [207]–[209] or adaptive kinematic trajectory [210]–[215]. In many cases, an error tolerance has also been added around the reference trajectory to create an area or a tunnel where movement remains unimpeded, providing assistance to the patient based on their needs, often referred to as 'assist-as-needed' control [213], [216], [217].

Miguel-Fernandez et al. [173] mention that the position-profile controllers can mobilise weakened limbs and can be especially beneficial for people suffering from severe impairments since they provide a means for delivering enhanced somatosensory stimulation in a safe environment for locomotion training. However, it is harder to provide partial assistance using position-profile controllers, which is important in creating a challenging and interactive environment for less affected patients. On the other hand, torque-profile controllers are most often open-loop controllers that have proven to be effective in reducing the metabolic cost of locomotion in healthy adults [6], [218], [219], but will fail to promptly react to disturbances and provide real-time haptic feedback, which is important for promoting neuroplasticity in neurological patients [25], [26]. This makes impedance controllers that provide assistance as needed particularly attractive for the rehabilitation of people with mild impairment. In all cases, the importance of controller tuning is highlighted in [173], and the need for methods that can automatically tune the open parameters of RAGT controllers to meet the needs of the patients is underscored.

The contributions presented in this thesis, involve the development of methods that can be used to optimally tune the open parameters of RAGT controllers to provide personalised assistance to ambulatory neurological patients with mild impairments who retain voluntary control of their limbs. For this, we have focused on the personalisation of assist-as-needed controllers, which are implemented on a lower limb exoskeleton. Below, we provide a description of some common elements of assist-as-needed controllers, along with a description of the exoskeleton, Exo-H3.

Path control and assist-as-needed

Assist-as-needed (AAN) control is a term used in robot-assisted rehabilitation to describe a family of controllers that aim to encourage the patient's active participation by providing tailored treatment. Path control [216], and force-field control [220], are controllers that belong to this family of AAN controllers and have some very similar characteristics. Here, we use path control as an example to present some of these characteristics. Path control uses a reference kinematic path in joint space, $\mathbf{Q}_{ref} \in \mathbb{R}^{i\times 2}$, that describes the desired relationship between the hip joint angle and the knee joint angle in the sagittal plane (where i is the number of points in the discretised domain of the reference path). Based

on this reference path, the reference point, $\mathbf{q}_{\text{ref}} \in \mathbb{R}^2$, is dynamically defined as the point on the reference path where the Euclidean distance between the reference path, $\mathbf{Q}_{ref}$, and the joint angles of the human (herein referred to as the actual point), $\mathbf{q}_{act} \in \mathbb{R}^2$, is at a minimum (Figure 11).

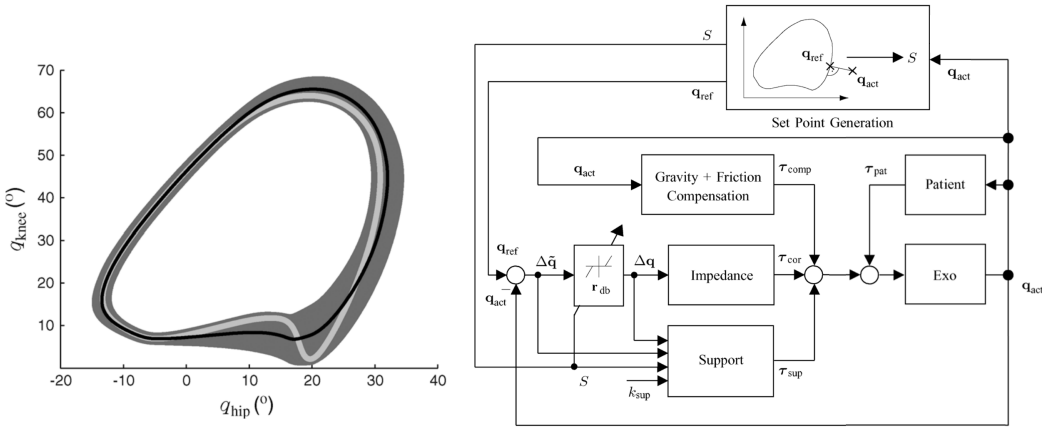

(a) (b)

Figure 11: (a) Illustration of the reference kinematic path, $\mathbf{Q}_{ref}$, defined in joint space and surrounded by the dead band region as presented in [221]. The grey line shows the reference path used by the robotic platform Lokomat during position control, and the black line shows the adapted reference path used for path control. (b) A diagram of the path controller (adapted from [221]).

This reference point can also be described by its relative position in the gait cycle, $\{S \in \mathbb{R} : 0 < S < 1\}$, and can be expressed as:

$$S = \text{argmin} \left\| \mathbf{Q}_{\text{ref}}(S) - \mathbf{q}_{\text{act}} \right\|_2, \tag{1}$$

$$\mathbf{q}_{\text{ref}} = \mathbf{Q}_{\text{ref}}(S) \tag{2}$$

The absolute joint angle error, $\Delta\tilde{\mathbf{q}} \in \mathbb{R}^2$, is then defined as the difference between the reference point and the actual point. In order to allow for some error tolerance, a dead band region of radius, r_{db}, is defined around the reference path, and the true joint angle error, $\Delta\mathbf{q} \in \mathbb{R}^2$, is defined as the difference between the reference point and the actual point, minus the error tolerance when the error tolerance is exceeded. This is expressed as:

$$\Delta\tilde{\mathbf{q}} = \mathbf{q}_{\text{ref}} - \mathbf{q}_{\text{act}}, \tag{3}$$

$$\Delta q^{(j)} = \begin{cases} 0, & |\Delta\tilde{q}^{(j)}| \leq r_{\text{db}}, \\ \Delta\tilde{q}^{(j)} - r_{\text{db}}, & \Delta\tilde{q}^{(j)} > r_{\text{db}}, \text{ for } j = 1,2 \\ \Delta\tilde{q}^{(j)} + r_{\text{db}}, & \Delta\tilde{q}^{(j)} < -r_{\text{db}}. \end{cases} \tag{4}$$

Based on the true joint angle error, $\Delta\mathbf{q}$, an assitive controller can then be defined to ensure that the patient is guided closer to the reference path and the kinematic tracking error is reduced. In the controller presented by Duschau-Wicke et al. [221] this controller comprises a number of assistive forces. These include, corrective forces, τ_{cor}, implemented using a proportional-derivative (PD) controller whose direction is perpendicular to the reference path and are used to minimise the patient's tracking error, supportive forces, τ_{sup}, whose direction is tangential to the reference path and are used to help patients overcome weaknesses, and compensatory forces, τ_{comp}, which are used to compensate for the robot's inertia and friction (Figure 11b).

Given this configuration, path control is a suitable controller for ambulatory patients with residual strength at the hips and the knees, and voluntary control of the upper limbs which can be used to provide balance. Some of these concepts of path control are revisited in the next Chapters.

The exoskeleton Exo-H3

For this thesis, the exoskeleton Exo-H3 (Technaid, Spain) is used, which is an upgrade of the exoskeleton Exo-H2 presented in [191]. The Exo-H3 exoskeleton is a multi-degree of freedom (DOF) lower-limb exoskeleton, that can provide support in hip flexion and extension, knee flexion and extension, and ankle plantarflexion and dorsiflexion. Each joint is equipped with position and velocity encoders, torque sensors, mechanical stops that limit the range of motion of the joint, and a geared electric motor with a reduction ratio of 160. Pressure sensors are also available at the heels and toes, which can be used for the detection of gait events such as the heel strike and toe off. Each leg comprises modular links of adjustable length which can be expanded or contracted to accommodate for people of different heights. An adjustable back support is also provided to accommodate for people of different waist circumference. The total weight of the exoskeleton is 17kg, including a rechargeable 19.2 V DC

lithium iron phosphate ($LiFePO_4$) battery, which weighs 2.8kg and is equipped with an emergency button (Figure 12a).

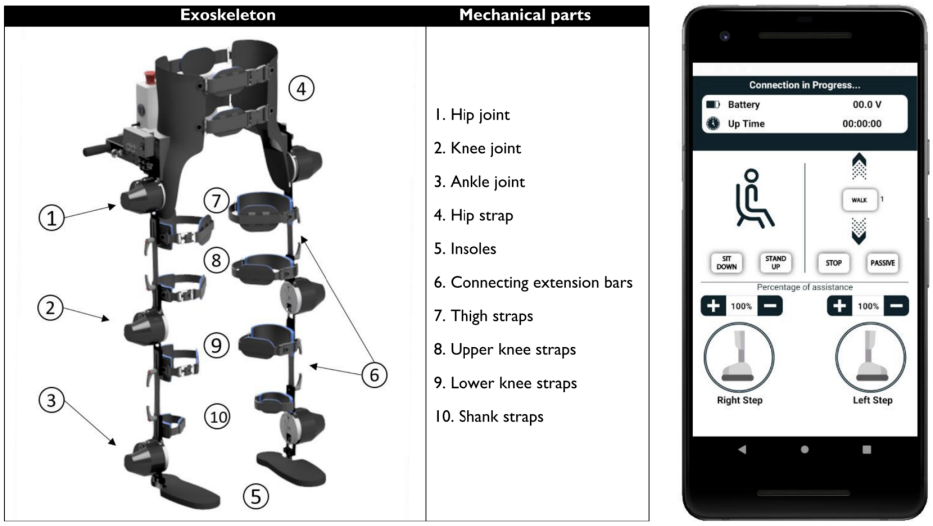

(a) (b)

Figure 12: (a) The mechanical parts of the exoskeleton Exo-H3, (b) The Android GUI for the high-level control of the exoskeleton.

The exoskeleton can be controlled using both built-in and custom mid-level controllers. The built-in controllers include position-controlled routines such as continuous steps of adjustable frequency, and sit-to-stand and stand-to-sit routines that can be accessed through an Android application and initiated through wireless Bluetooth communication (Figure 12b). A transparent controller is also available, which allows the user to freely walk with the exoskeleton while feeling little resistance from the exoskeleton's motors. This controller is implemented using torque control and compensates for the friction in the geared motors. Prototype mid-level controllers can be developed using both position control and torque control. For the development of torque controllers, two low-level controllers are available relying on proportional-integral-derivative (PID) control to define the current supplied to the motors; one uses as an input the torque measured by the strain gauges to control motor current, referred to as joint-torque controller, and the other uses as an input an estimate of the torque, based on the current provided to the motors, referred to as motor-torque controller. Both low-level controllers operate at 1000Hz.

Prior to the use of the exoskeleton Exo-H3, both low-level controllers were tested and their ability to follow the provided torque commands was examined. For this thesis, the motor-torque controller has been used for low-level control

as it more accurately matched the torques recorded by the torque sensors. A friction compensation controller was added to reduce the effect of static friction and viscous friction imposed by the motor dynamics, which further reduced the discrepancy between the commanded torques and the torques measured by the strain gauges. The addition of friction compensation was carried out using MATLAB and Simulink Real-Time Desktop, and the communication has been established using a PCAN bus at a frequency of 100Hz.

Furthermore, additional safety mechanisms have been put in place. An additional emergency button was programmed to terminate the communication between the exoskeleton and the torque controller, and lock the joints of the exoskeleton. Also, the range of motion of the exoskeleton's joints was limited to [-25°, 100°] for the hips, [0°, 100°] for the knees and [-25°,25°] for the ankles.

2.6.2 *Functional electrical stimulation*

FES is another popular and well-researched intervention for the rehabilitation of neurological impairments. FES is a special case of neuromuscular electrical stimulation (NMES), which involves the artificial stimulation of muscles by delivering low-energy electrical impulses to motor neurons in order to generate force and facilitate the completion of a functional task [222] (Figure 13). Electrodes can be placed either over the skin, known as transcutaneous (surface) stimulation, or through the skin, also known as percutaneous stimulation, and requires the nerves on the target muscles to be intact and the muscles not to be dystrophic or atrophic [223].

This external stimulation of motor units can have both neuroprosthetic and therapeutic benefits. Neuroprosthetic benefits, also known as orthotic benefits, are the instantaneous functional improvements observed during the use of electrical stimulation such as increased ankle dorsiflexion, improved symmetry in gait and increased single-stance duration in paretic limbs [225], [226]. Therapeutic benefits are the functional and/or physiological improvements observed after the use of electrical stimulation that may be associated with neuroplastic changes in the central nervous system [227]–[231], potentially resulting from the increased sensory stimulation and afferent signals to the spinal cord [232], [233]. These benefits include muscle strengthening, improved muscle fatigue resistance [234]–[236], and reduced spasticity [237]–[239], all of which may

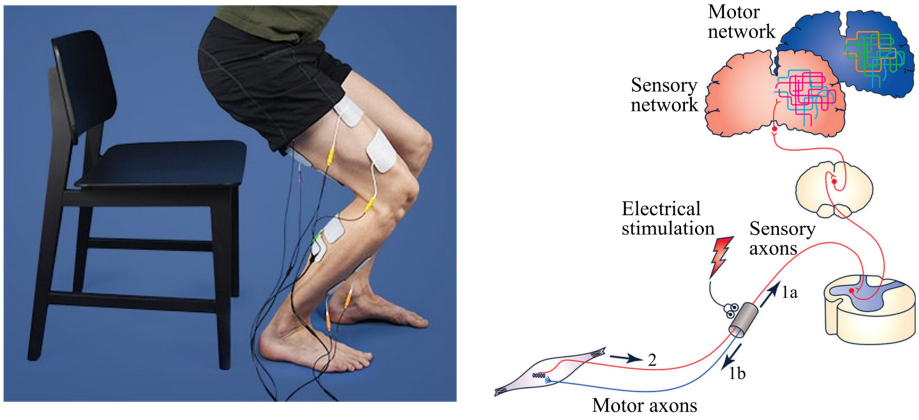

Figure 13: (a) Application of functional electrical stimulation on the lower limbs. (b) Schematic of neuromuscular electrical stimulation with (1a) and (1b) indicating direct sensory stimulation and muscle excitation, respectively, and (2) indicating sensory feedback due to muscle contraction (extracted from [224]).

eventually lead to an increase in walking performance and community mobility [238]–[242], which can be maintained even in the absence of electrical stimulation.

A major limitation of FES when it comes to gait rehabilitation is the rapid onset of muscle fatigue and the limited control of the resultant limb movement. The nonlinear muscle response to FES makes accurate modelling, control and trajectory tracking hard to achieve [232], [243], while the sub-optimal and non-physiological recruitment of the stimulated motor units can quickly induce muscle fatigue and a subsequent reduction in the duration of therapy and its effectiveness [231], [234], [244], [245]. To address some of these limitations, efforts have been made to create better models of FES [246], [247], to understand the relationship between electrode placement and muscle force [248], and to identify control strategies that will both ensure the accurate control of the limbs [249] and reduce muscle fatigue [244], including strategies where FES is combined with robotic assistance [250].

In this case, on top of the control of the robot, the control of FES involves the tuning of several parameters to adjust the stimulation intensity. These include the current amplitude, pulse width, and pulse frequency. In order to achieve tetanic muscle contractions using surface stimulation these parameters usually range between 0-120mA for current amplitude, 0-400μs for pulse width, and 0-100Hz for frequency [234], [236]. Moreover, the adjustment of pulse waveform

is also possible. Pulse waveforms can be described as monophasic/monopolar or biphasic/bipolar. In monophasic waveforms, current flow is induced only in one direction, whereas in biphasic waveforms each pulse is accompanied by a second pulse in the opposite direction which can be symmetric or asymmetric in amplitude, and balance or unbalanced in charge [231], [251] (Figure 14). These pulses can take different shapes, with the most common being rectangular and quasi-rectangular, where a smooth ramp up towards the peak amplitude is included along with a ramp down towards zero current.

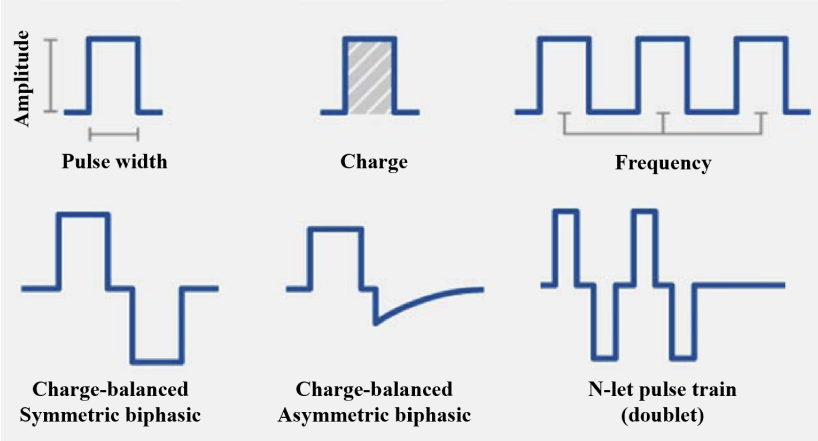

Figure 14: The characteristics of electrical pulses in neuromuscular electrical stimulation (adapted from [252]).

Many studies looked at the effect of these parameters on muscle fatigue. In their systematic review, Ibitoye et al. [244] suggest that modulating the stimulation frequency, pulse width and amplitude may be a viable strategy for reducing muscle fatigue, but due to high heterogeneity in the identified studies, determining the optimal strategy for reducing muscle fatigue remains a challenge. For example, the use of submaximal stimulation [253], [254], as well as the use of mixed stimulation frequencies [254] and variable frequency trains (stimulation trains starting with a doublet – two closely spaced pulses – followed by single pulses at a constant frequency) [255]–[257] seem to lead to less relative force loss in fatiguing muscles. On the other hand, it is still unclear whether the stochastic modulation of stimulation parameters can delay the onset of muscle fatigue [258], [259]. A few studies have also shown that the use of higher stimulation frequencies may lead to a quicker onset of muscle fatigue [260]–[263].

For the control of generated muscle force and limb movement, a variety of feedforward and feedback controllers have been studied [264], [265]. Feed-

forward control, where fixed stimulation sequences are delivered based on the state of the patient, have been quite successful in facilitating stepping and standing in people with spinal cord injury (SCI) [266]–[268], but the need to be able to address muscle fatigue and more accurately drive the resultant kinematics towards healthier patterns led to the investigation of feedback controllers [269], [270]. Feedback control, where information about the state of the patient is used to appropriately adjust the intensity of the stimulation trains, demonstrated the ability to facilitate movement in paralysed limbs, increase the duration of standing, and accurately track trajectories during gait and cycling [269]–[272]. Methods including fuzzy logic control [273], [274], PID control [275], [276], sliding mode control [277] and the use of artificial neural networks [278], [279] are examples of controllers that have been used to incorporate a feedback loop in the control of FES. However, in most cases, the neuroprosthetic effect of FES was emphasised, where the aim was to control the motion of fully paralysed limbs. The use of collaborative controllers that emphasise the therapeutic effect of FES on people who retain control of their limbs have not been studied extensively.

Two main classes of collaborative FES controllers have been identified: biosignal-driven control and iterative learning control (ILC). In biosignal-driven control, signals obtained either from the muscles via electromyography (EMG) or the brain via electroencephalography (EEG), have been used to control the intensity of stimulation in order to complement the voluntary efforts of the patient [280]–[282]. Similarly, ILC [271] has been used to adjust the stimulation intensity in order to ensure that enough assistance is provided, on top of the patient's voluntary efforts, for the completion of cyclical events. However, with the use of FES as the only intervention, the only control option available when it comes to maintaining a low trajectory tracking error as fatigue progresses is to increase the stimulation intensity in order to recruit deeper muscle fibres and maintain a high output force. As a result, fatigue progresses at a faster rate [253], [254], and gait training becomes uncomfortable, necessitating an interruption of training for the muscles to recover. For this reason, the hybridisation of FES with robotic assistance has been gaining increasing attention [250]. In Chapter 5, the relevant state-of-the-art hybrid robot-FES controllers will be discussed and a novel adaptive and hierarchical controller will be presented.

RehaMove3 ScienceMode

For this thesis, the RehaMove3 stimulator has been used. RehaMove3 is a medically approved multi-channel stimulator (Hasomed GmbH, Germany) that can be programmed using an external device through the ScienceMode communication protocol. Each RehaMove3 stimulator can control up to four channels and can deliver transcutaneous electrical stimulation using surface gel electrodes. Current amplitude can range from [-130,+130]mA, pulse width can be set anywhere between [20,16000]μs and frequency can vary from [1,500]Hz. Up to 16 points can be used to adjust the discretised pulse waveform and real-time feedback control can be established through an interface with Simulink.

(a) (b)

Figure 15: (a) The RehaMove3 stimulator connected to an external controlling device. (b) The RehaMove3 stimulator connected to the thigh muscles using rectangular surface gel electrodes.

2.7 SUMMARY

In summary, this chapter discussed the intricate landscape of neurorehabilitation, underscoring the importance of understanding the mechanisms of neuroplasticity in enhancing the functional outcomes of therapy. The dynamic and multi-disciplinary nature of neurorehabilitation has been explored, integrating concepts from neuroscience, robotics, and physical therapy to address the diverse needs of individuals with neurological disorders. Central theme

of this chapter, has been the transformative impact of technology in neurorehabilitation, ranging from motion capture, gait analysis, and gait training. The importance of choosing the right technology and the right intervention for each patient is highlighted, differentiating between robot-driven interventions, which may be more appropriate for people with complete SCI, and patient-driven interventions, which may be more appropriate for people who retain voluntary control of their limbs. As we move forward, it becomes apparent that, in both cases, harnessing the therapeutic advantages of neurorehabilitation is a particularly challenging problem, influenced by a multitude of variables, including the type of disability, the severity of disability, the patient's perceived level of disability, the type of technology incorporated in training, the way it is controlled and the way it is integrated with other technologies and/or other interventions. Inspired by seminal contributions in this field, as discussed above, the following chapters propose three different methods for approaching neurological gait rehabilitation in people who retain voluntary control of their limbs in order to provide personalised assistance and promote neural plasticity.

3

OFFLINE MODEL-BASED OPTIMISATION

3.1 INTRODUCTION

In rehabilitation for locomotion, the main effort has been to help the patients learn how to reproduce a healthy gait pattern. In the early rehabilitation stage, robot interventions that strictly guide the patient along a predefined kinematic trajectory are often implemented [283]. This robot-driven approach can be useful to induce physiological muscle activation, reduce spasticity, increase blood flow, support the function of the internal organs and potentially induce brain plasticity through increased somatosensory stimulation [160], [161], [171], [284], [285]. However, for ambulatory patients who retain some voluntary control over their limbs, this approach may not be as effective. The use of robot-driven interventions for the rehabilitation of ambulatory patients may induce patient slacking and passive participation, which may prohibit or delay their recovery [286]. The concept of patient-driven rehabilitation is thus given more attention during the later stages of rehabilitation, and controllers are studied that aim to capture the patient's attention and encourage them to actively participate during their therapy [283], [287].

Several studies have highlighted the importance of providing assistance as needed, and encouraging patient participation for the treatment of ambulatory people with gait disabilities [287]–[290]. However, even though there are several control strategies that can be used to provide assistance as needed [216], [291]–[294], it is still unclear whether there is a single control strategy that is superior to other strategies [162]. One common denominator among the studies investigating the efficiency of assist-as-needed controllers, is the fact that often a controller is designed and tuned based on the performance of a healthy participant and the same controller is tested across several patients. As a result, contrary to the highly personalised human-human intervention provided by physicians, many of the human-robot interactions are not tailored to the needs of the user. Given the highly inter-personal and intra-personal variability in gait among people with neurological disorders, the same controller may not

be optimal for everyone. It is therefore prudent to look for methods that can be used to adjust these controllers to meet the needs of the patients.

This process of personalising a controller to the needs of the patient is an optimisation problem where often a balance between two or more competing objectives needs to be satisfied. In this chapter, we describe an offline model-based optimisation approach for the design and optimisation of personalised assistive controllers, where we leverage the power and advances in musculoskeletal modelling in order to reduce the requirement for extensive human data collection (Figure 16). Firstly, we present our offline optimisation framework in a generalised form to highlight its utility in similar fields where the optimisation of human-robot interaction is important, such as human augmentation and/or (industrial) human-robot collaboration. Next, we demonstrate the ability to optimise an assist-as-needed controller of a lower-limb exoskeleton to the needs of the user as a case study. We formulate the concept of 'assistance as needed' as an optimisation problem, and we illustrate how we can obtain a personalised controller for each individual. With the help of eighteen healthy participants, we then evaluate the effect of our proposed optimisation approach on the collaboration between the participants and the robot. The key contributions of this work involve, firstly, the introduction of an innovative methodology for the optimisation of robotic controllers in human-robot collaboration utilising musculoskeletal modelling, and secondly, the evaluation of this methodology, specifically for personalising an assist-as-needed controller, through testing on healthy individuals.

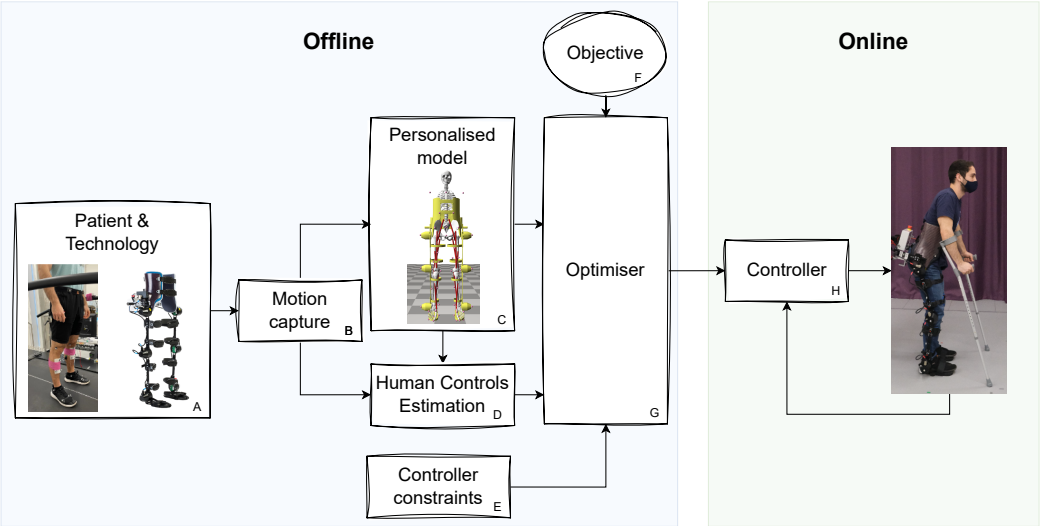

Figure 16: Offline model-based optimisation pipeline.

This chapter describes the different components of our proposed method as illustrated in Figure 16. The generic optimisation framework is described first, followed by a description of the motion capture and modelling process (B-C), the estimation of the human controls (D), and the controller objectives and constraints that can be used (E-F). Two methods for solving the generic optimisation problem are then discussed (G). In the first instance, a case is discussed where the unconstrained optimisation problem is addressed. This is the case where a controller structure is not imposed through the constraints, and the decision variables consist of purely the controls of the robot. In the second instance, a case is discussed where an impedance controller is considered, and thus a more constrained optimisation problem is solved to obtain the optimal controller parameters for the impedance controller. The optimisation of the impedance controller is then verified in simulation and experimentally.

3.2 GENERALISED PROBLEM FORMULATION

The aim of our model-based optimisation framework is to minimise a set of (rehabilitation) objectives, C, given a model of the combined human-robot system, S, in order to obtain a set of personalised controller parameters, P^*. This can be expressed as a multi-objective optimisation problem with equality, $g(\cdot) = 0$, and inequality constraints, $h(\cdot) > 0$, in the following generalised form:

$$\min_{\mathbf{P}} \sum_{i=1}^{N} w_i C_i(S) \tag{5}$$

$$g(\mathbf{x}, \mathbf{u}) = 0, \tag{6}$$

$$h(\mathbf{x}, \mathbf{u}) > 0, \tag{7}$$

$$\mathbf{x}^- < \mathbf{x} < \mathbf{x}^+, \tag{8}$$

$$\mathbf{u}^- < \mathbf{u} < \mathbf{u}^+, \tag{9}$$

where w represents the weight of the associated cost terms, for N number of costs. $\mathbf{u}$ is the vector of controls of the human model and the robot model, and $\mathbf{x}$ is the vector of states of the human-robot model, such as the joint positions

and velocities. $[\mathbf{x}^-, \mathbf{x}^+]$ and $[\mathbf{u}^-, \mathbf{u}^+]$ are the lower and upper bounds of the model's states and controls, respectively.

3.3 OPTIMISATION PIPELINE

As shown in Figure 16, the proposed optimisation pipeline involves the construction of a personalised human-robot model and a human behaviour model based on motion capture and the technical specifications of the robot. Using these models, the optimal robot controls are obtained, which can be used for the tuning of the respective rehabilitation controller. In this section, this pipeline is presented, starting from the construction of a personalised human-robot model, moving onto the estimation of human behaviour, the definition of the appropriate controller objectives and constraints, the selection of the optimisation method and the tuning of the real-time robot controller.

3.3.1 *Human model scaling*

With the use of musculoskeletal modelling software, such as OpenSim and AnyBody, a personalised human-robot model can be constructed [152], [295]. These platforms offer detailed musculoskeletal models with variable levels of complexity that can be adjusted to reflect the physical properties of the human (see section 2.4).

For this study, the generic OpenSim model, *gait1018*, was used (section 2.4). The generic model was adjusted to allow hip adduction and abduction, and was scaled using motion capture (Figure 16B). A static pose of the human was recorded and OpenSim's scaling tool was used to scale the model's geometry and inertial properties using measurement-based scaling (Appendix A). To do this, marker pairs placed on bony landmarks, were defined for each segment of the body in order to compute the x-y-z scale factors for the corresponding segments (Figure 6). At the same time, a marker adjustment process was carried out. For this, a weight was assigned to each marker in order to indicate the confidence level of the marker's relative position on the model with respect to its real position on the human. Using these weights, the marker positions of the tracking markers were adjusted using OpenSim's inverse kinematics optimisation pipeline (Appendix B) in order to minimise the error between

the virtual model markers and the experimental markers. The accuracy of the scaled model was evaluated using OpenSim's graphical user interface (GUI), where the model's joint coordinates were reviewed as well as the mean and maximum root-mean-squared error (RMSE) achieved by the marker adjustment process.

3.3.2 *Human-robot modelling*

This adjusted human model can then be combined with the model of the robot in order to create a personalised human-robot model (Figure 16C). This involves the adjustment of the robot's configuration in order to align with the human pose, and the modelling of the interaction forces between the human and the robot. The coupled dynamics of this model are a fundamental constraint of the optimisation problem (Equation 6) and are expressed as:

$$\mathbf{M}_{hr}(\mathbf{q})\ddot{\mathbf{q}} + \mathbf{C}_{hr}(\mathbf{q}, \dot{\mathbf{q}}) + \mathbf{G}_{hr}(\mathbf{q}) = \boldsymbol{\tau}_h + \boldsymbol{\tau}_r + \sum_{i=1}^{n} \mathbf{J}(\mathbf{q})_i^T \mathbf{f}_{\text{ext}}^{(i)}, \tag{10}$$

where $\mathbf{q}, \dot{\mathbf{q}}, \ddot{\mathbf{q}} \in \mathbb{R}^n$ are the generalised joint positions, velocities and accelerations of the model, respectively. $\mathbf{M}_{hr}(\mathbf{q}) \in \mathbb{R}^{n \times n}$ is the mass matrix of the human-robot model, $\mathbf{C}_{hr}(\mathbf{q}, \dot{\mathbf{q}}) \in \mathbb{R}^n$ is the vector of Coriolis and centrifugal forces, and $\mathbf{G}_{hr}(\mathbf{q}) \in \mathbb{R}^n$ is the vector of gravitational forces for a system with n degrees of freedom (DOFs). $\boldsymbol{\tau}_h \in \mathbb{R}^n$ represents the human's voluntarily generated joint torques and $\boldsymbol{\tau}_r \in \mathbb{R}^n$ are the assistive forces provided by the robotic device. $\mathbf{J} \in \mathbb{R}^{6 \times n}$ is the system's Jacobian and $\mathbf{f}_{ext} \in \mathbb{R}^6$ represents any external force or torque that may be applied to either the robot or the human model, including forces due to the human-robot interaction and ground reaction forces.

For this study, the exoskeleton's position and orientation were first adjusted in the frontal plane, and the exoskeleton's hip joint centre was aligned with the hip joint centre of the human model in the sagittal plane. With the hip joints aligned, the length of the exoskeleton's limbs was adjusted sequentially from top to bottom in order to achieve a good alignment between the rest of the joints of the two models. This exoskeleton adjustment was performed according to the constraints imposed by the hardware, and the fitness of the final human-robot model was evaluated using OpenSim's GUI. For the

interactions at the points of contact, linear bushing forces were used. These are translational and rotational triaxial springs and dampers that can model force transmission losses due to skin and muscle elasticity. These forces were placed at the torso, the thighs (lower and upper thigh strap), the shanks (lower and upper shank strap), and the feet (heel contact and foot strap). The stiffness of the bushing forces was selected using OpenSim's GUI to ensure a firm contact between the exoskeleton model and the human model. The values of the bushing forces chosen for the different contact points are presented in Table 2.

Table 2: Stiffness of translational (x, y, z) and rotational (θ, ϕ, ψ) bushing forces for the modelling of human-robot contact, where K and B are the stiffness and damping coefficients, respectively.

Bushing force properties	Torso	Thighs, Shanks & Feet
$[K_x\ K_y\ K_z]$ (kN/m)	[40 40 40]	[10 10 10]
$[B_x\ B_y\ B_z]$ (kN/m/s)	[0.2 0.2 0.2]	[0.1 0.1 0.1]
$[K_\theta\ K_\phi\ K_\psi]$ (kN/rad)	[1 1 1]	[0.1 0.1 0.1]
$[B_\theta\ B_\phi\ B_\psi]$ (kN/rad/s)	[0.03 0.03 0.03]	[0.01 0.01 0.01]

Lastly, to reduce computational demands and speed up the convergence of optimisation, the model's muscles were replaced by ideal joint actuators. The upper and lower limits of the joint actuators were defined based on the values reported in [296]–[298].

3.3.3 *Human controls estimation*

In the context of human-robot collaboration, human behaviour becomes a primary contributor to task completion. Contrary to other scenarios of human-robot interaction where human behaviour may be considered a disturbance, here it is increasingly important to recognise it as a central element in the collaborative dynamics. Therefore, for the model-based optimisation of the

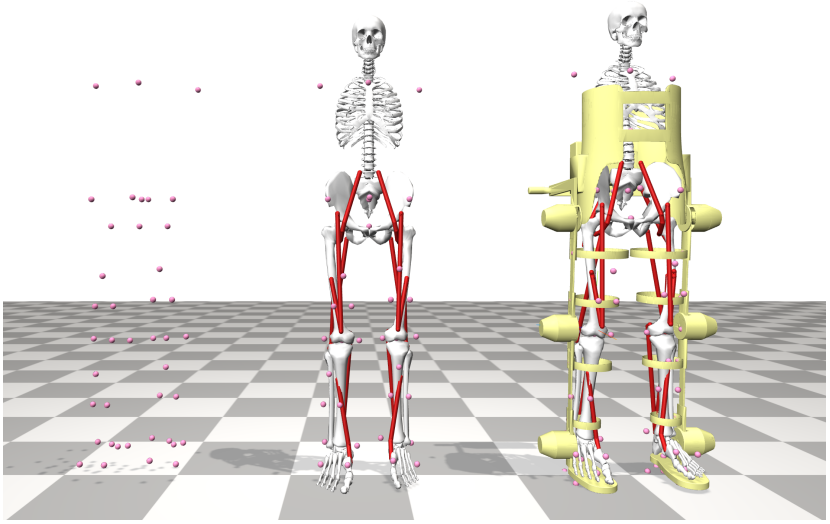

Figure 17: Creating a human-robot model based on the recorded posture of the human and the robotic description file of the exoskeleton.

robot controller, a reliable model of the human behaviour, τ_h, is required (Figure 16D). In many cases, human behaviour has been characterised by a combination of feedforward and feedback processes with both long-term and short-term adaptations [299]–[302]. Computational models that describe the adaptation of human motor control in environments with high uncertainty and environments with predictable external perturbations have been proposed in [303]–[305], while efforts have been made to also capture human behaviour during gait and sit-to-stand using inverse optimal control [306]–[309].

For this study, a feedforward model was used (Figure 16D). To do this, the motion of the human was recorded while performing the desired task (see section 3.4.1), and while wearing the exoskeleton in transparent mode, ($\tau_r = 0$). Five consecutive cycles were extracted from the recorded data and a proportional-derivative (PD) controller was used at the joints of the human model, in a forward dynamics analysis, to estimate the human joint torques that are necessary to reproduce, in simulation, the recorded motion. This process was carried out using the Residual Reduction Algorithm (RRA) available in OpenSim (Appendix C). The obtained joint torques, τ_h, were then used as a constraint in the optimisation pipeline to replace this human PD controller (Equation 9), and form the feedforward human model. To prevent any biases introduced from the short-term adaptation of the human, a training period was prescribed prior to the data collection, and due to the short duration of

the study, it was assumed that adaptation beyond the training phase will be insignificant.

Parallel to this study, we also investigated the potential of inverse optimal control for learning personalised human motion strategies [306]. This work, led by Daniel F. N. Gordon, focused on the sit-to-stand task, and is based on the assumption that human motion for a given task, as perceived by kinematic and dynamic metrics, is governed by an objective function which aims to minimise a set of biomechanical performance metrics, C. Based on this assumption, personalised human motion strategies can be learnt using motion capture, musculoskeletal modelling, and bi-level optimisation. At the lower level of this optimisation, optimal control is used to carry out a predictive simulation of the task, which is defined by a number of constraints and an objective function consisting of the relevant *weighted* performance metrics, such as balance, energy expenditure, joint loading and more. At the upper-level, optimal control is used to obtain the relative magnitude of the weights, $\mathbf{w}$, that need to be used in the lower-level objective, such that the difference between the simulated kinematics, $\mathbf{x}$, and the experimentally observed kinematics, $\tilde{\mathbf{x}}$, is minimised. This process is summarised in Figure 18 and can be formally expressed as:

$$\min_{\mathbf{w}} \quad \frac{1}{n}\sum_{i=1}^{n}\sqrt{\frac{1}{mT}\int_0^T\left(\sum_{j=1}^{m}\tilde{x}_j^i(t)-x_j(t)\right)^2 dt}, \tag{11}$$

$$\text{s.t. } \mathbf{w}^- \leq \mathbf{w} \leq \mathbf{w}^+, \tag{12}$$

$$\min_{\mathbf{x},\mathbf{u}} \quad \sum_{k=1}^{z} w_k C_k(\mathbf{x}(t),\mathbf{u}(t)), \tag{13}$$

$$\text{s.t. } g(\mathbf{x},\mathbf{u}) = 0, \tag{14}$$

$$h(\mathbf{x},\mathbf{u}) > 0, \tag{15}$$

$$\mathbf{x}^- < \mathbf{x} < \mathbf{x}^+, \tag{16}$$

$$\mathbf{u}^- < \mathbf{u} < \mathbf{u}^+, \tag{17}$$

where n is the number of observed motion samples, m is the number of degrees of freedom observed during motion, T is the finite time horizon of motion, $[\mathbf{w}^-, \mathbf{w}^+]$ represent the lower and upper bounds of the weights, respectively, and z is the number of lower-level objectives.

Using this method, a personalised set of weights can be obtained that reflects the strategy adopted during motion. In [306] we also demonstrated that

through inverse optimal control, changes in the human motion strategy due to environmental changes, such as external forces applied to the human body or the anticipation of external forces, can also be captured. Albeit computationally expensive, this approach provides an alternative for the estimation of human controls and could be used to learn personalised human motion strategies in robot-assisted gait.

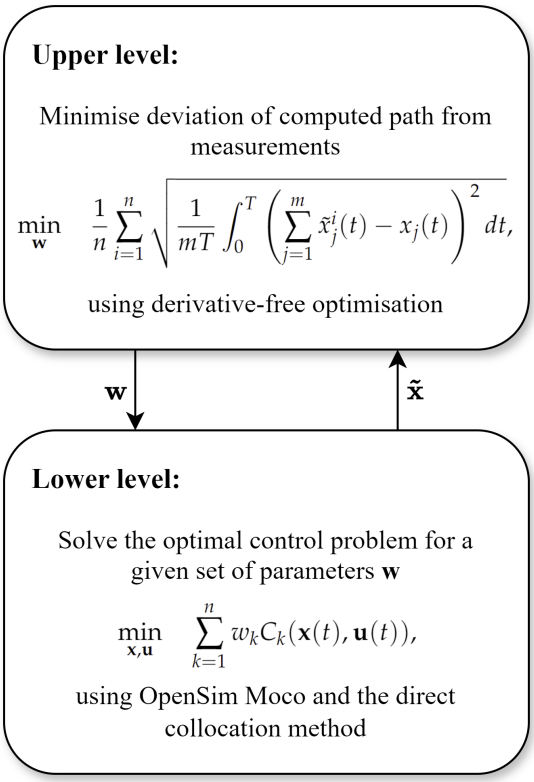

Figure 18: Diagram of the inverse optimal control problem which can be solved using bi-level optimisation to obtain personalised models of human motion strategies.

3.3.4 *Controller constraints and robot control model*

Given the human-robot model and a model for the human behaviour, it is then possible to identify in simulation the optimal robot behaviour, τ_r. To do this, the appropriate constraints need to be defined. Firstly, the boundary constraints are implemented. These include the upper and lower boundaries of the assistance to be provided, $\mathbf{u}$, and any limits that may be present in

the states, $\mathbf{x}$ (i.e. range of motion) of the patient or the robot. These can be expressed as inequality constraints:

$$\mathbf{x}^- < \mathbf{x} < \mathbf{x}^+, \tag{18}$$

$$\mathbf{u}^- < \mathbf{u} < \mathbf{u}^+. \tag{19}$$

For this study, the range of motion of the exoskeleton was constrained to [-25°, 100°] for the hips, [0°, 100°] for the knees and [-25°,25°] for the ankles, the joint torques for the hips and the knees of the exoskeleton were constrained to [-40,+40]Nm and the joint torques for the human model were constrained as described in section 3.3.2.

Additionally, a robot control model with the respective constraints can be defined (Figure 16E). This would impose additional constraints regarding the controller's structure and/or limits (Equations 6-7). Unlike the upper and lower safety boundaries of the states and controls, these constraints are optional, since it is possible to solve the unconstrained optimisation problem without such constraints, from which the optimal controller structure or appropriate limits may be inferred. These cases are discussed in more detail in sections 3.4.2 and 3.4.3.

3.3.5 *Objective*

For the optimisation of rehabilitation controllers that provide assistance as needed, a fine balance between two objectives is needed (Equation 5). These include the amount of assistance provided to the patient and a performance metric that describes their ability to accurately complete the desired task with the provided assistance (Figure 16F). In the case where robotic assistance is provided, $\mathbf{u}_r$, and the desired task involves the tracking of a desired kinematic trajectory, this can be expressed as:

$$\min_{\mathbf{P}} \quad \frac{w_1}{J_1} \frac{\sum_{i=1}^{N-1} (\mathbf{u}_{r_i}^T \mathbf{I} \mathbf{u}_{r_i})}{N-1} + \frac{w_2}{J_2} \frac{\sum_{i=1}^{N} \epsilon_i^2}{N}, \tag{20}$$

where w_1 and w_2 are the weights of the two costs, ϵ is the kinematic tracking error, $\mathbf{P}$ is the vector of decision variables, $\mathbf{I}$ is the identity matrix, N is the number of time steps for the completion of the task and J is a scaling factor. The

scaling factor is used to normalise the cost terms to the maximum exoskeleton assistance and the maximum expected trajectory error, respectively, such that the magnitude of the two costs is comparable. Similarly, N is used to normalise the two cost terms to the length of the simulated cycles and w is used to adjust the relative importance of the two normalised costs.

3.3.6 *Forward dynamics*

Using the human-robot model, the expected human joint torques, and the constraints implemented due to the robot controller, forward dynamics simulations can be carried out to obtain the robot behaviour that minimises the desired cost. Using forward dynamics, the kinematics of the human-exoskeleton model can be predicted for different levels of assistance as follows:

$$\ddot{\mathbf{q}} = \mathbf{M}_{hr}^{-1}(\mathbf{q})(\boldsymbol{\tau}_h + \boldsymbol{\tau}_r + \mathbf{J}(\mathbf{q})^T \mathbf{f}_{\text{ext}} - \mathbf{C}_{hr}(\mathbf{q}, \dot{\mathbf{q}}) - \mathbf{G}_{hr}(\mathbf{q})). \tag{21}$$

Based on this predicted trajectory, the objective function value can be obtained (Equation 20) and the optimal robot behaviour can be calculated.

3.3.7 *Optimisation*

The described optimisation problem can be solved in a number of ways. Optimal control methods such as model predictive control (MPC) could be used to obtain the optimal exoskeleton controls to assist with gait. However, implementing such a real-time controller in practise would be extremely challenging due to high computational demands. Yet, the outputs of the offline optimisation could be used to design a surrogate controller. By identifying the appropriate control models, simple state-feedback controllers can be derived from the outputs of the offline optimisation to approximate the behaviour of the optimal controller. An alternative is to further constrain this problem by including a robot control model in the problem constraints and solve for the open parameters of the robot controller. For this, gradient-free optimisation methods such as Bayesian optimisation, surrogate optimisation or genetic algorithms can be used.

Next, two methods for solving the generic optimisation problem are discussed. In the first instance, a case is discussed where the unconstrained optimisation problem is addressed using MPC. This is the case where a controller structure is not imposed through the constraints and the decision variables consist of purely the controls of the robot. In the second instance, a case is discussed where an impedance controller is considered, and thus a more constrained optimisation problem is solved to obtain the optimal controller parameters for the impedance controller. These cases are demonstrated using concepts from path control as described below.

3.4 CASE STUDY: PERSONALISED PATH CONTROL

For the verification of the proposed pipeline, we rely on the principles of the assist-as-needed controller, path control [216] (see section 2.6.1). For this, a reference path, $\mathbf{Q}_{ref} \in \mathbb{R}^{i\times 2}$, is defined in joint space, which describes the desired relationship between the hip joint and the knee joint in the sagittal plane. This reference path is defined using the kinematic data collected from a healthy subject and is adapted to a path with less pronounce loading response, including a deadband with a radius of 2 degrees (Figure 19)[1]. Following the principles of path control, the reference point on the reference path, $\mathbf{q}_{ref} \in \mathbb{R}^2$, is dynamically defined based on the pose of the human, $\mathbf{q}_{act}$, from which the trajectory tracking error, $\Delta\tilde{\mathbf{q}}$, can be obtained. As a result, common to the two cases described below for the verification of the proposed pipeline, are the path control constraints regarding the time-independent definition of trajectory tracking error. These constraints are expressed as:

$$\Delta\tilde{\mathbf{q}} = \mathbf{q}_{\text{ref}} - \mathbf{q}_{\text{act}}, \tag{22}$$

$$\Delta q^{(j)} = \begin{cases} 0, & |\Delta\tilde{q}^{(j)}| \leq r_{\text{db}}, \\ \Delta\tilde{q}^{(j)} - r_{\text{db}}, & \Delta\tilde{q}^{(j)} > r_{\text{db}}, \text{ for } j = 1,2 \\ \Delta\tilde{q}^{(j)} + r_{\text{db}}, & \Delta\tilde{q}^{(j)} < -r_{\text{db}}. \end{cases} \tag{23}$$

1 This reference path is used as a means of verifying the optimisation procedures proposed and it is not implied that this path is in any way ideal for all or any of the participants of the following experiments. Identifying a suitable reference path, or the optimal reference path if one exists, for a person or group of people, with or without neurological disease, is still an open research question which extends beyond the focus of this thesis [310], [311].

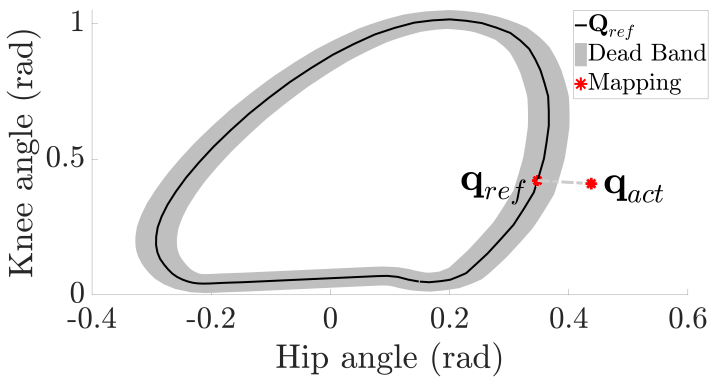

Figure 19: Illustration of the reference kinematic path, $\mathbf{Q}_{\text{ref}}$, surrounded by a deadband and an example of the mapping between the pose of the human, $\mathbf{q}_{\text{act}}$, and the reference point, $\mathbf{q}_{\text{ref}}$.

3.4.1 *Simulation & experimental setup*

For this study a 12-camera Vicon system was used for the recording of the human posture, which was used for the scaling of the human model (see sections 2.3-2.4). The open-source software, OpenSim, was used for the modelling of the human-robot system where the intertial properties of the exoskeleton, Exo-H3, were used (section 2.6.1). To carry out dynamic simulations, an interface between OpenSim and MATLAB was used. Ideal exoskeleton actuators were assumed, ($\boldsymbol{\tau}_r = \mathbf{u}_r$), and motion was analysed in the sagittal plane. To reduce the computational demands of the optimisation, and uncertainty involved with the optimisation of balance, a unilateral tracking task was considered and a human model with ideal joint actuators was used, where the model was pinned at the pelvis and contact with the ground was prevented. These conditions were also matched during the experimental study, where the participants were asked to perform a trajectory tracking task with their right leg, while their left leg was used to support their weight on an elevated platform (Figure 26a). Side rails were provided to help the participants maintain their balance, and the exoskeleton Exo-H3 (Technaid, Spain) was used to provide assistance. The exoskeleton's joint position sensors were used to record the joint angles of the legs and provide real-time visual feedback to the user. Simulink Desktop Real Time was used for the real-time control of the exoskeleton at 100 Hz.

3.4.2 *Solving the unconstrained problem*

To demonstrate the ability of the proposed method to find the optimal control actions, $\mathbf{u}_r^*$, for a given human-robot model and human behaviour model, a simulation pipeline was implemented to first solve the unconstrained problem. By solving the unconstrained problem, personalised *surrogate* controllers, H_r, can potentially be learnt based on the outputs of the optimiser. Given a model of the patient, P, and a model of the rehabilitation robot, R, the aim is to obtain the optimal behaviour of the robot, $\mathbf{u}_r^*$, that will minimise a set of rehabilitation costs, C. This can be expressed as:

$$H_r = \phi(\mathbf{u}_r^*), \tag{24}$$

$$\mathbf{u}_r^* = \underset{\mathbf{u}_r}{\operatorname{argmin}}\, f(P, R, C, \mathbf{u}_R), \tag{25}$$

where $\phi(\cdot)$ and $f(\cdot)$ are generalised functions.

For this case, the generalised function, $f(\cdot)$, involves the objective function described by equation 20, the dynamic model of the human and the robot (equation 10), with their respective boundary constraints (equations 18-19), and the path control constraints as described by equations 22-23. This is referred to as the 'unconstrained' problem where a robot control model is not explicitly defined and can be expressed as:

$$\min_{\mathbf{u}_r} \quad \frac{w_1}{J_1}\frac{\sum_{i=1}^{N-1}(\mathbf{u}_{r_i}^T \mathbf{I} \mathbf{u}_{r_i})}{N-1} + \frac{w_2}{J_2}\frac{\sum_{i=1}^{N}\Delta\mathbf{q}_i^T \mathbf{I} \Delta\mathbf{q}_i}{N}, \tag{26}$$

$$\text{s.t.} \quad \mathbf{M}_{hr}(\mathbf{q})\ddot{\mathbf{q}} + \mathbf{C}_{hr}(\mathbf{q}, \dot{\mathbf{q}}) + \mathbf{G}_{hr}(\mathbf{q}) = \boldsymbol{\tau}_h + \boldsymbol{\tau}_r + \sum_{i=1}^{n} \mathbf{J}(\mathbf{q})_i^T \mathbf{f}_{\text{ext}}^{(i)}, \tag{27}$$

$$\Delta\tilde{\mathbf{q}} = \mathbf{q}_{\text{ref}} - \mathbf{q}_{\text{act}}, \tag{28}$$

$$\Delta q^{(j)} = \begin{cases} 0, & |\Delta\tilde{q}^{(j)}| \leq r_{\text{db}}, \\ \Delta\tilde{q}^{(j)} - r_{\text{db}}, & \Delta\tilde{q}^{(j)} > r_{\text{db}}, \text{ for } j = 1, 2 \\ \Delta\tilde{q}^{(j)} + r_{\text{db}}, & \Delta\tilde{q}^{(j)} < -r_{\text{db}}, \end{cases} \tag{29}$$

$$\mathbf{x}^- < \mathbf{x} < \mathbf{x}^+, \tag{30}$$

$$\mathbf{u}^- < \mathbf{u} < \mathbf{u}^+. \tag{31}$$

In simulation, where computational constraints are less relevant for the control of the exoskeleton, this can be solved using optimal control methods. The outputs of the offline optimisation can then be used to construct a surrogate controller that will satisfy any computational constraints.

Here, we demonstrate how MPC with a finite time horizon can be used to calculate the optimal robot controls for a given model behaviour in order to provide assistance as needed and guide the model towards the reference path. Using a finite difference method, OpenSim's integrator was used to predict the future trajectory of the human-robot model for different levels of robot assistance.

In this case, a healthy subject was fitted with the exoskeleton and was asked to follow the kinematic path shown in Figure 19. The exoskeleton was controlled by a compliant/transparent controller ($\boldsymbol{\tau} = \mathbf{0}$) and the kinematic trajectory of the subject was recorded using the exoskeleton's joint sensors. A cycle of the recorded trajectory was used for the analysis and for the calculation of the actions of the human model (Figure 20a). The recorded trajectory was also scaled to observe the outputs of the optimiser to a human behaviour that results in a higher tracking error (Figure 20b).

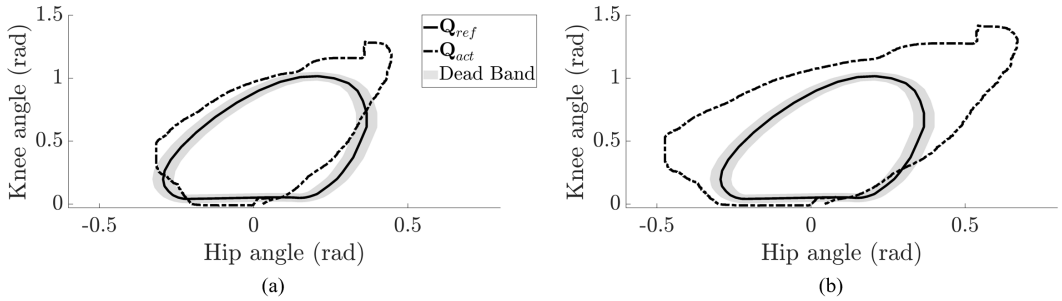

Figure 20: (a) Recorded gait cycle (dashed line) compared to the reference path (solid line). (b) Scaled gait cycle used in simulation.

Simulation results

Figure 21 shows the results obtained from the offline optimisation using MPC. It can be seen that with very small assistive forces, mostly within the range of [-10,10]Nm, the exoskeleton can support the motion of the model, such that the kinematic tracking error is substantially reduced. It can also be noticed, that for the hip joint, a linear relationship between the joint angle error and the assistance provided by the robot may explain the optimal policy

calculated by the model-based optimisation, especially in the case where the modelled human behaviour leads to higher tracking error (Figure 21b). This may indicate, that at least for the hip joint, a proportional control law may be a good surrogate controller to provide assistance as needed in a near optimal way. However, the relationship between the knee joint error and the assistance at the knee is less linear. This may be due to the relative magnitude of the weights in the objective function, the magnitude of the human controls at the two joints, and the ability of the optimiser to prevent future states of high error by exploiting the model's dynamics.

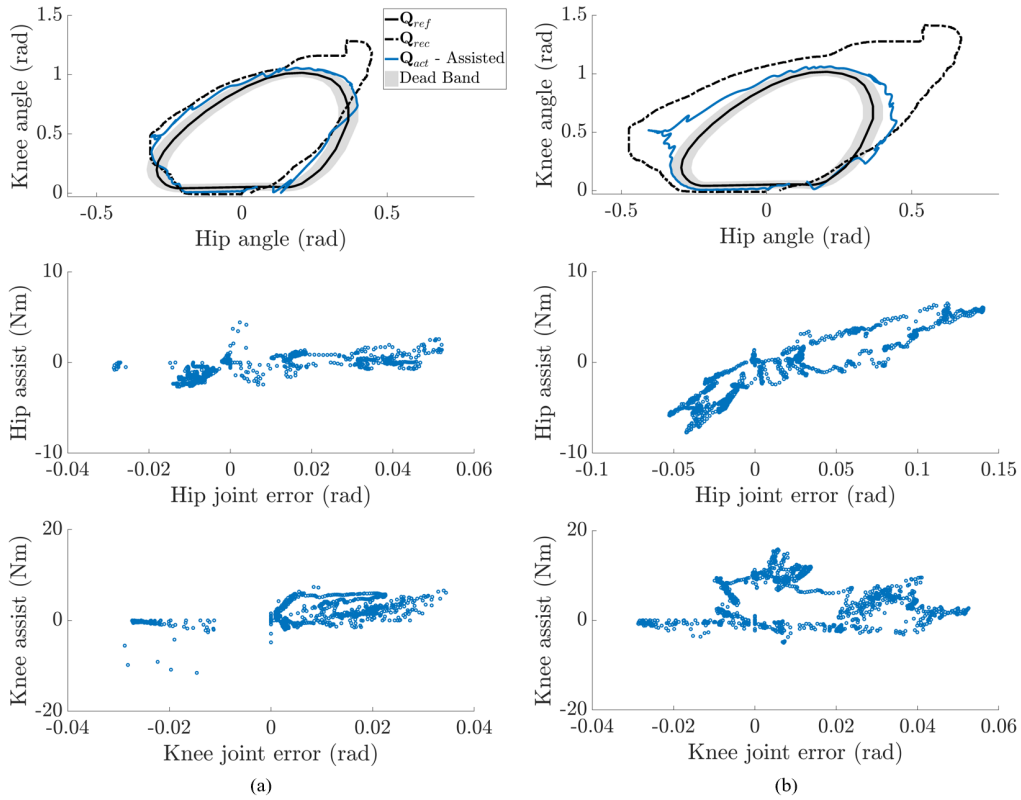

Figure 21: Providing assistance as needed using MPC in simulation. The predicted trajectory with and without assistance is plotted against the reference path, and the optimal assistive forces for each joint are plotted against the tracking error for each joint: (a) for a human model whose unassisted trajectory results in low tracking error and (b) for a human model whose unassisted trajectory results in high tracking error.

One way to obtain this surrogate controller when a relationship between the optimal asssitive forces and the model state is not clear, is through data-driven methods. Using artificial neural networks, the optimal assistive forces obtained from the MPC can potentially be learnt as a non-linear function of a number of features. By using as inputs the kinematic tracking error of the hip joint

and the knee joint, as well as the rate of change of this error, a neural network can be trained to predict the optimal assistive forces that are generated by the MPC. Figure 22 shows the predicted trajectory obtained when MPC is used, overlayed by the trajectory obtained when a neural network trained on 80% of the outputs of the MPC is used. It can be seen that the two are well aligned indicating that the neural network can create a surrogate controller of the MPC through a non-linear combination of the joint errors and the rate of change of the joint errors. However, in the absence of an analytical dynamic model, this process is computationally expensive, making its implementation in real life harder, and offers limited safety guarantees. For these reasons the optimisation of a more constrained problem was investigated.

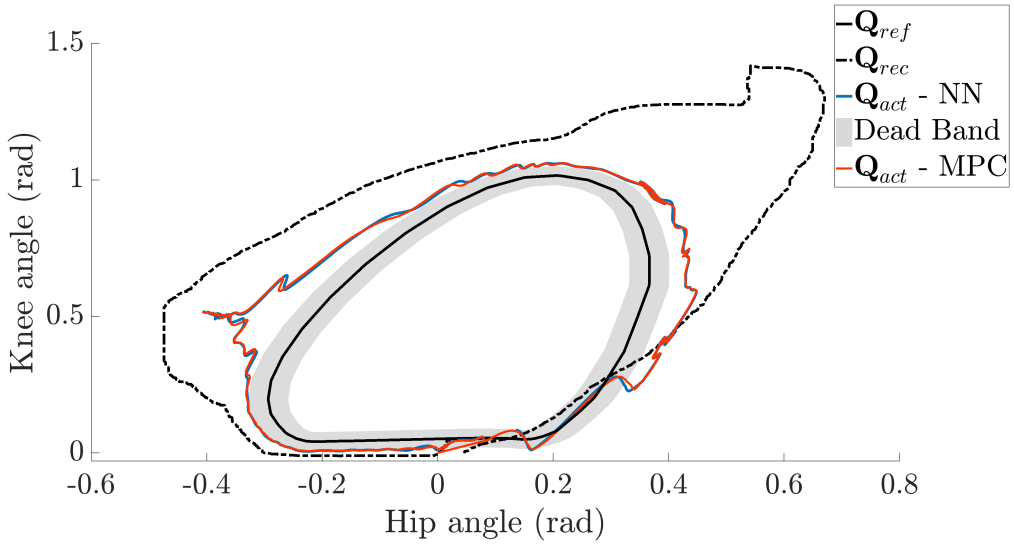

Figure 22: Providing assistance as needed using both MPC in simulation (red line) and a MPC-based NN (blue line). The output trajectories can be compared to the reference path (solid black line) and the unassisted trajectory of the human model (dotted black line).

3.4.3 *Solving the constrained problem*

Further to the constraints imposed by the human-robot model and the human behaviour model, constraints regarding the robot control model can be imposed if a specific controller structure is desired. This can help simplify the problem in order to speed up the optimisation process and lead to the optimisation of a controller which can be more reliable and predictable. In the case of path control, the desired controller structure may be the structure of an impedance

controller (section 2.6.1). As such, a PD controller can be used to ensure that assistive forces are provided by the exoskeleton in order to guide the user closer to the reference path based on the true joint angle error, $\Delta\mathbf{q}$ (equation 23). This can be expressed as:

$$\boldsymbol{\tau}_r = \mathbf{K}\Delta\mathbf{q} + \mathbf{B}\Delta\dot{\mathbf{q}}, \tag{32}$$

$$\mathbf{B} = \mathbf{c}_{cr}\sqrt{\mathbf{K}}, \tag{33}$$

where $\mathbf{K}$ and $\mathbf{B}$ are the joint stiffness and damping matrices of the exoskeleton's joints, and $\mathbf{c}_{cr}$ is the matrix of the critical damping coefficients. As a result, the open parameters for the given controller and the decision variables, $\mathbf{P}$, of the optimisation problem (Equation 5), consist of two parameters: the robot stiffness at the hip joint, K_h, and the knee joint, K_k.

To solve this problem using OpenSim, where the analytical form of the dynamics is not available, gradient-free optimisation was used. For this purpose Bayesian optimisation, *bayesopt* [312], and surragote optimisation, *surrogateopt* [313], were used (Figure 16G). *Bayesopt* and *surrogateopt* are global solvers available in MATLAB, which are designed for computationally expensive functions that may not be smooth. Given finite bounds on the decision variables, the optimisers explore the unknown optimisation landscape, using an acquisition function or radial basis functions, respectively, to create a surrogate model of the unknown function. After a predefined number of iterations, or time, this process terminates and the arguments of the minimum observed point are provided. The following pseudocode describes the way this optimisation process was carried out for the personalisation of the exoskeleton's rehabilitation controller:

Algorithm 1 Pseudocode for offline controller optimisation

Require: $0 < \mathbf{w} < 1$
1: $\mathbf{S} \leftarrow \{\}$; $N \leftarrow 150$; $i \leftarrow 1$
2: **while** $i < N$ **do**
3: $\quad \mathbf{K}_i \leftarrow$ gradient_free_opt$(\mathbf{S}, \mathbf{x})$
4: $\quad \ddot{\mathbf{q}} \leftarrow$ forward_dynamics$(\boldsymbol{\tau}_h, \mathbf{K}_i)$
5: $\quad \mathbf{O}_i \leftarrow$ objective_fcn_value$(\Delta\mathbf{q}, \mathbf{u}_r, \mathbf{w})$
6: $\quad \mathbf{S} \leftarrow \{\mathbf{S}; [\mathbf{K}_i, \mathbf{O}_i]\}$
7: $\quad i \leftarrow i + 1$
8: **end while**
9: $\mathbf{K}^* \leftarrow \mathbf{S}$ such that $\mathbf{O}^* = \min \mathbf{S}$

At a first instance, Bayesian optimisation was used, and a series of simulations were carried out to observe the ability of the proposed optimisation pipeline to converge to a set of exoskeleton stiffnesses that will minimise the objective function. These include: (1) simulations where variation in the strength of the model is considered, (2) simulations where variation in the model mass is considered, and (3) simulations where variation in the model's actions is considered. Lastly, the effect of adjusting the relative weights of the objective function costs is presented in order to highlight the ability of the proposed method to provide personalised controller parameters that reflect the relative importance of the different rehabilitation tasks. The output of these simulations is the value of the personalised exoskeleton stiffness for the impedance controller (equation 32). The personalised controller is then used to assist the human model and three metrics are used to evaluate the ability of the controller to provide assistance as needed: the normalised mean squared value of the trajectory error, hereafter referred to as the *error metric*, C_e, the normalised mean squared value of the exoskeleton assistance, hereafter referred to as the *assistance metric*, C_a, and their weighted sum, as described by equation 20, which is referred to as the *total cost*, C_T. These values are compared to the corresponding values obtained when a baseline stiffness of magnitude $\mathbf{K} = [340, 340]$ Nm/rad is used [314]. For this case, the behaviour of the human model was obtained based on the trajectory shown in Figure 20a.

Simulation results

Here we demonstrate how variations in the user's musculoskeletal properties may affect the outputs of the model-based optimisation and how they compare to the outputs obtained from a baseline controller.

VARIATION IN STRENGTH This experiment simulates the effects of weakness, which may be the result of neurological injury. It is expected that muscle weakness due to neurological disease will result in inadequate range of motion and thus higher assistive forces will be needed. Yet, the exoskeleton stiffness of an impedance controller that will keep the objective function value to a minimum is unknown. To investigate this, muscle weakness was simulated as a decrease in the maximum joint torque the model can generate, which

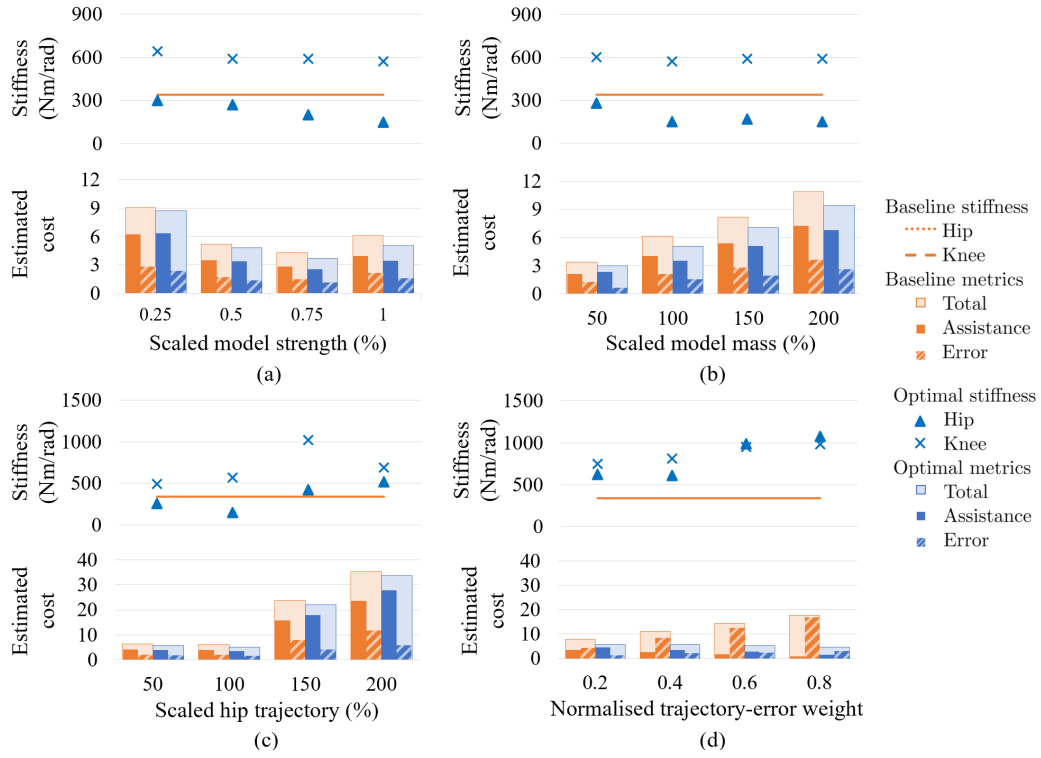

Figure 23: Results from the simulation experiments. The dependent variables include the optimal exoskeleton stiffness, the error metric, the assistance metric and the total rehabilitation metric, while the independent variables include (a) the model's strength, (b) the model's mass, (c) the model's actions and (d) the relative weights of the two costs.

results in the scaling of the input human controls, τ_h. Forward dynamics simulations were carried out for the cases where the model's maximum joint torque was scaled by 25%, 50%, 75% and 100%. Figure 23a shows how the optimal exoskeleton stiffness and the three rehabilitation metrics change as the model strength changes.

It can be seen that as the strength of the model increases, the exoskeleton's stiffness for both the hip joint and the knee joint decreases. Compared to the baseline stiffness, a higher knee stiffness and a lower hip stiffness appear to result in a lower value for the total cost, C_T. In all cases, it can be seen that the value of C_T that results from the use of the personalised exoskeleton stiffness is lower than the value of C_T achieved when the baseline stiffness is used.

VARIATION IN BODY MASS This experiment simulates how variability in human body weight may affect the outputs of the optimiser. It is expected that as the mass of the patient increases, higher assistive forces will be needed to

help them follow a reference kinematic path, however the way this is reflected on the optimal exoskeleton stiffness and the value of the objective function is unclear. To test this, the mass of the human-exoskeleton model was scaled to simulate individuals of lower and higher body weight. The mass of the model was scaled by 50%, 100%, 150%, and 200% and the human controls required to generate the motion (Figure 20) based on the new model mass were recomputed (section 3.3.3). The results from the optimisation using the updated model and human controls can be seen in Figure 23b.

It can be seen that the value of the exoskeleton stiffness does not vary notably with variations in the model's mass. Yet, the value of the weighted assistance, C_a, seems to proportionally increase as the mass of the model increases, which suggests that higher assistive forces are required to correct the motion of the model as the mass increases. It is also evident that the value of the optimal exoskeleton stiffness is different to the baseline stiffness. An impedance controller with higher knee stiffness and lower hip stiffness than the baseline stiffness appears to result in a lower tracking error, C_e, and a lower overall cost, C_T, for all cases.

VARIATION IN HUMAN BEHAVIOUR This experiment simulates how variability in human controls may affect the outputs of the optimiser. Each person has a unique kinematic pattern when they walk which is reflected in the joint torques they generate. It is expected that the closest the kinematic trajectory of the patient is to the reference path, the lower the required assistance will be. However, it is not clear how the stiffness of the rehabilitation technology may need to be adjusted at the different joints given an increased trajectory error in either, or all the dimensions of the trajectory. In these simulations, the kinematic trajectory of the motion (Figure 20), was scaled by 50%, 100%, 150%, and 200% in the direction of the hip motion and the corresponding joint torques were obtained using the human control estimation method described in section 3.3.3. The results of the optimisation are presented in Figure 23c. Figure 24a illustrates the resultant kinematic trajectory when the hip range of motion is scaled by 50% and Figure 24b presents how the RMSE of the unassisted, scaled trajectory varies over the different model actions.

From Figure 23c it can be seen that the value of the optimal exoskeleton stiffness varies substantially over the different model actions. By comparing the variability of the optimal exoskeleton stiffness to the RMSE of the unassisted

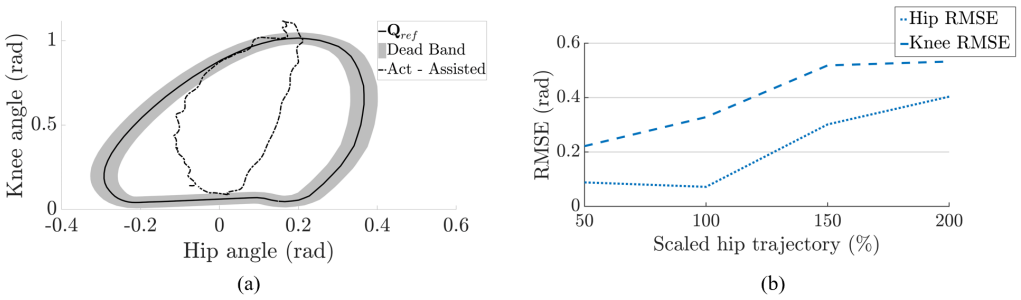

Figure 24: (a) The resultant kinematic trajectory that corresponds to the scaled version of the recorded motion when the range of motion of the hips is scaled by 50%. (b) RMSE of the hip and knee joint for the unassisted scaled trajectory.

trajectories, it is evident that the optimal exoskeleton stiffness changes according to the trajectory error generated by the different model actions. It can be seen that as the RMSE increases, so does the optimal exoskeleton stiffness. In all cases, it is obvious that the value of both the error metric, C_e, and the total cost, C_T, are lower when the optimal exoskeleton stiffness is used compared to when the baseline stiffness is used.

PRIORITISING REHABILITATION TASKS Depending on the severity of the injury and the patient's residual strength, different levels of assistance may be desired. By changing the weights of the costs in the objective function, the relative importance of the different rehabilitation tasks can be adjusted. It is expected that as the relative weight of the trajectory error cost is increased, the optimal exoskeleton stiffness will also increase. Figure 23d shows how the absolute value of the exoskeleton's stiffness, and the total cost, C_T, change when the weights of the objective function are adjusted to progressively prioritise the controller's goal of achieving accurate trajectory tracking, starting from left to right.

It can be seen that as the weight related to the trajectory tracking error increases, the optimal exoskeleton stiffness increases for both the hip joint and the knee joint. In all cases, the value of the total cost, C_T, is lower when the optimal exoskeleton stiffness is used. It can be noticed that in all cases, the value of the weighted assistance, C_a, is slightly higher when the optimal stiffness is used, which results in a reduced tracking error, C_e.

3.4.4 *Experimental validation*

To verify whether the benefits observed in simulation can be realised in real life, an experimental study with eighteen healthy subjects was carried out. In this case, in order to increase the potential improvements due to optimisation, the search space of the optimisation was increased. This was implemented by dividing the reference path into two phases based on the motion capture data used to define the reference path. As a result, the reference path was divided into the stance phase (ST), and the swing phase (SW), and a PD controller with constant stiffness was used for each phase:

$$\mathbf{K} = \begin{cases} \mathbf{K}_{st}, & \text{ST phase} \\ \mathbf{K}_{sw}, & \text{SW phase} \end{cases} \tag{34}$$

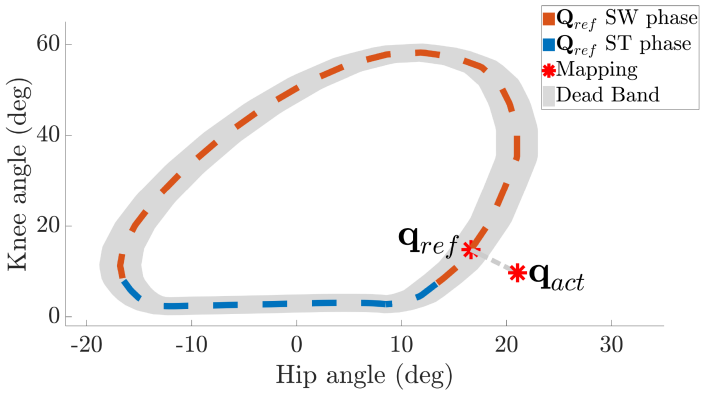

Figure 25: Illustration of the dual-phase reference path, $\mathbf{Q}_{ref}$, defined in joint space, and an instance of the dynamic allocation of the reference point, $\mathbf{q}_{ref}$, based on the pose of the human, $\mathbf{q}_{act}$.

Evaluation with healthy subjects

SUBJECTS The effectiveness of this optimisation approach was studied with the help of eighteen healthy volunteers (15 male, 3 female, age = 26 ± 4, weight = 74.6kg ± 10.4kg). All participants were first-time users of a wearable robot and had no prior knowledge of the task to be completed. The experimental pipeline was approved by the University of Edinburgh, School of Informatics Ethics Committee (ID 2021/46920) and all participants provided written consent.

EXPERIMENTAL SETUP The participants were first fitted with reflective markers, as explained in section 3.3.2, to enable the modelling of the human-exoskeleton system. Once a scaled model was constructed, the markers were removed and the participants were fitted with the exoskeleton. The exoskeleton was adjusted to the dimensions of each participant to ensure a tight and comfortable fit, and a good alignment between the joints of the exoskeleton and the joints of the participant. While wearing the exoskeleton, the participants were asked to perform a trajectory tracking task with their right leg, while their left leg was used to support their weight on an elevated platform which was used to avoid contact between the user's right leg and the ground (Figure 26). Side rails were provided to help the participants maintain their balance. This task was selected in order to reduce the computational demands of the optimisation, and uncertainties involved with the optimisation of balance.

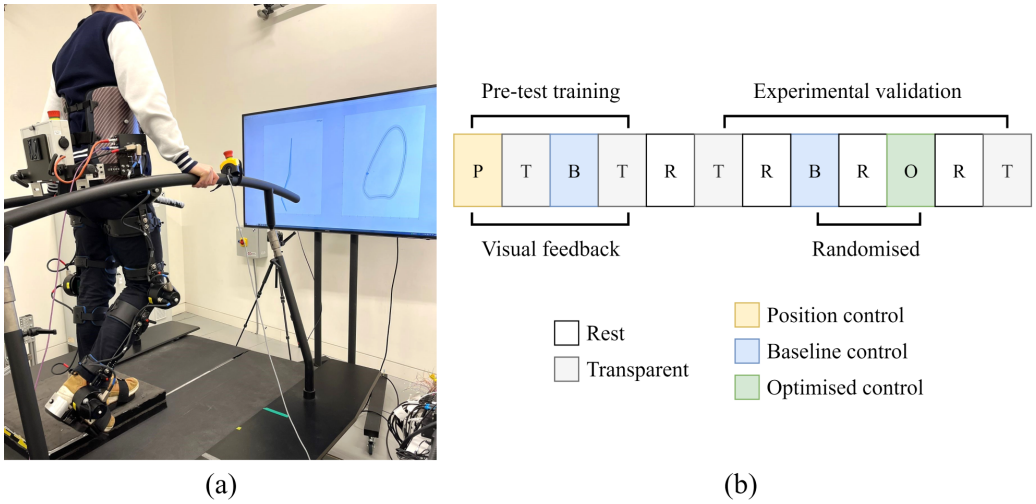

Figure 26: (a) Data collection setup. Participant wearing the Exo-H3 exoskeleton and performing a unilateral tracking task with the help of visual feedback. (b) Experimental protocol including four phases of pre-test training with visual feedback and the experimental validation where the baseline controller and the optimised controller were tested in a randomised order.

Prior to recording the performance of the participants, a training period was prescribed to allow the participants to get familiar with both the desired task and the exoskeleton (Figure 26). This training period included four phases complemented by visual feedback: (1) a position controlled exoskeleton ($\mathbf{q}_{exo}(t) = \mathbf{q}_{ref}(t)$), (2) a transparent exoskeleton ($\tau_e = 0$), (3) an assistive exoskeleton ($\tau_e \neq 0$), and (4) a transparent exoskeleton again. Each training phase lasted between 2-5 minutes, depending on the user's confidence level. The

visual feedback included a virtual image of the exoskeleton's leg, as well as a graphical representation of the reference kinematic path in joint space together with the real-time pose of the exoskeleton and the corresponding reference point (Figure 26). The visual queues were explained to the participants and the participants were instructed to follow the reference path as accurately as possible. After the training period, the visual feedback was removed in order to prevent further learning of the task, and to capture the participant's kinematics reflecting the internal model of motor control constructed by the participant during this period. The participants were then asked to repeat the task with the exoskeleton in transparent mode and their motion was recorded. This recorded motion was then used for the estimation of the human behaviour model as explained in section 3.3.3. A total of ten cycles were performed by each participant and a sample of five cycles was selected from the recorded motion in order to reduce computational demands.

Based on this recorded motion, a personalised exoskeleton stiffness was obtained for each participant through offline model-based optimisation. In this case, *surrogateopt* was used [313] (algorithm 1) to obtain the personalised stiffness for each participant. The obtained stiffness was used to adjust the controller of the exoskeleton and the participants were asked to perform the desired task, while wearing the exoskeleton in assistive mode. Their performance while using the exoskeleton with both their personalised stiffness and a baseline stiffness was recorded and analysed. The baseline stiffness was set to 340Nm/rad which is in line with the stiffness used in [314] and approximately half of the maximum stiffness used in [216]. The order at which the participants experienced the baseline controller and the optimised controller was randomised. The metrics used to verify the effectiveness of the optimisation approach included the kinematic tracking error of the participants, the level of assistance they received, and the weighted sum of the two, which formed the objective function of our optimisation problem (Equation 20). At the end of the experiment the participants were asked to perform the task while wearing the exoskeleton in transparent mode once again. This was done to assess any changes that may have occurred during the experiment in the behaviour of the participants, and test the validity of our previous assumption that the participants' behaviour will not significantly change during the experiment beyond the training phase.

ANALYSIS Given the recorded motion of the participants, paired-samples t-tests were used to test for statistical significance in performance changes across the group of participants and within participants. To test for normality in the data, Shapiro Wilk tests were carried out. The null hypothesis tested was that the performance of the participants using the exoskeleton with the baseline stiffness has the same distribution as the performance of the participants using the exoskeleton with the optimised stiffness. The median and the interquartile range (IQR) of the two distributions were calculated to identify any outliers based on the 1.5IQR rule. To quantify the variability in performance among individuals and within individuals the standard deviation and the coefficient of variation (CV) was used. Similarly, paired-samples t-tests were used to check whether the behaviour of the participants when using the exoskeleton in transparent mode changed significantly beyond the training phase. A statistical analysis was not carried for the simulation results since an infinite number of repetitions can be carried out in simulation which will affect the outcome of the statistical analysis.

Simulation results

Figure 27 shows the resultant stiffness obtained for each participant from the offline optimisation for the two phases of the cycle. It can be seen that a wide range of stiffness outputs were obtained for the different participants, ranging from 20 Nm/rad (almost no assistance), to 560 Nm/rad, which corresponds to a stiff exoskeleton. It can be observed that, for the given task, the stiffness for both the hip joint and the knee joint, for the ST phase, are almost always lower than the stiffness of the two joints during the SW phase.

Similarly, Figure 28a shows the kinematic error and exoskeleton assistance that correspond to each participant as predicted in simulation using these optimal exoskeleton stiffnesses[2]. It can be seen that in all cases, the offline optimisation can find an exoskeleton stiffness for the hip and the knee joints that can reduce the weighted sum of the overall tracking error of the model and the assistance provided by the exoskeleton. This consistent improvement that is predicted for the objective function value, predicts a mean improvement of approximately 30.4% (Figure 29a) in the controller's ability to provide assistance as needed.

2 Error bars on Figure 28a are not provided since different number of repetitions can be carried out in simulation which will affect the results.

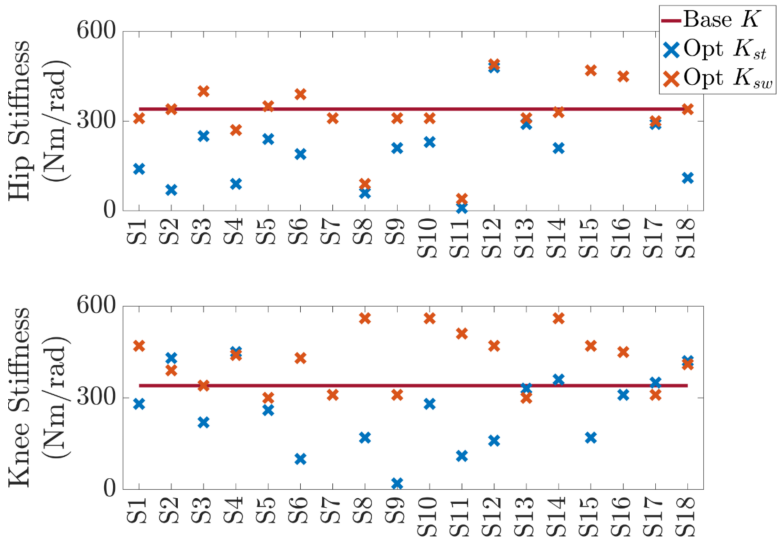

Figure 27: Personalised stiffness obtained for each participant for the two phases of the cycle for both the hip joint and the knee joint of the exoskeleton.

With the exception of S11, the obtained exoskeleton stiffness is expected to reduce both the tracking error and the levels of assistance provided. For S11, a very low stiffness was obtained for the hip joint (Figure 27), for both phases of the cycle, with a relatively high stiffness of the knee during the swing phase. This is expected to result in a slightly higher tracking error but significantly lower assistive forces from the exoskeleton (Figure 28a). With respect to the expected performance of the rest of the participants, the expected performance of S11 using the baseline stiffness is considered an outlier based on the 1.5 IQR value (Figure 29a). However, when the optimised stiffness is used, the expected performance of S11 lies within the 1.5 IQR value and is no longer considered an outlier (Figure 29b).

Experimental results

TASK PERFORMANCE Once the optimised exoskeleton stiffness was obtained for each participant, the participants tested the exoskeleton's controller with both the baseline stiffness and the optimised stiffness in a randomised order. Their ability to follow the desired kinematic path and the levels of assistance they received from the exoskeleton are presented in Figure 28b. In contrast to the idealised simulation environment, during the experimental validation of the proposed offline optimisation method, not all participants performed better with the optimised exoskeleton stiffness. While for some participants the optimised exoskeleton stiffness resulted in a significant im-

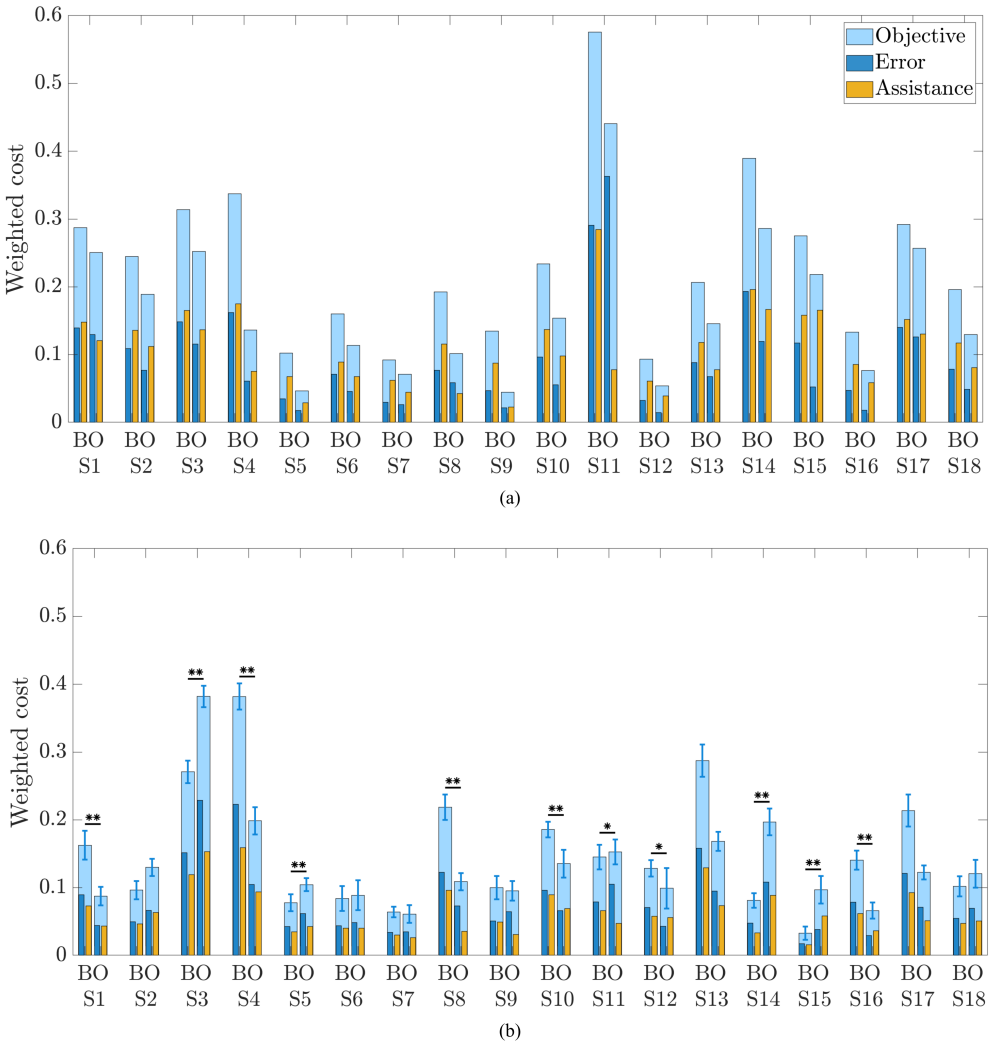

Figure 28: (a) Simulation results, (b) Experimental results obtained when assistance from the exoskeleton was provided using the baseline controller, B, and the optimised controller, O, for the total number of cycles performed during testing. Error bars denote standard error. Statistical significance denoted with asterisks *P<0.05, **P<0.01.

provement in performance, as recorded by their performance per cycle, such as S1, S4, S8, S10, S12, and S16, for some participants it had no significant effect (S2, S6, S7, S9, S13, S17, and S18), whereas for some it resulted in significantly worse performance (S3, S5, S11, S14 and S15). As a result, the effect of offline optimisation on the performance of the 18 subjects is not statistically significant.

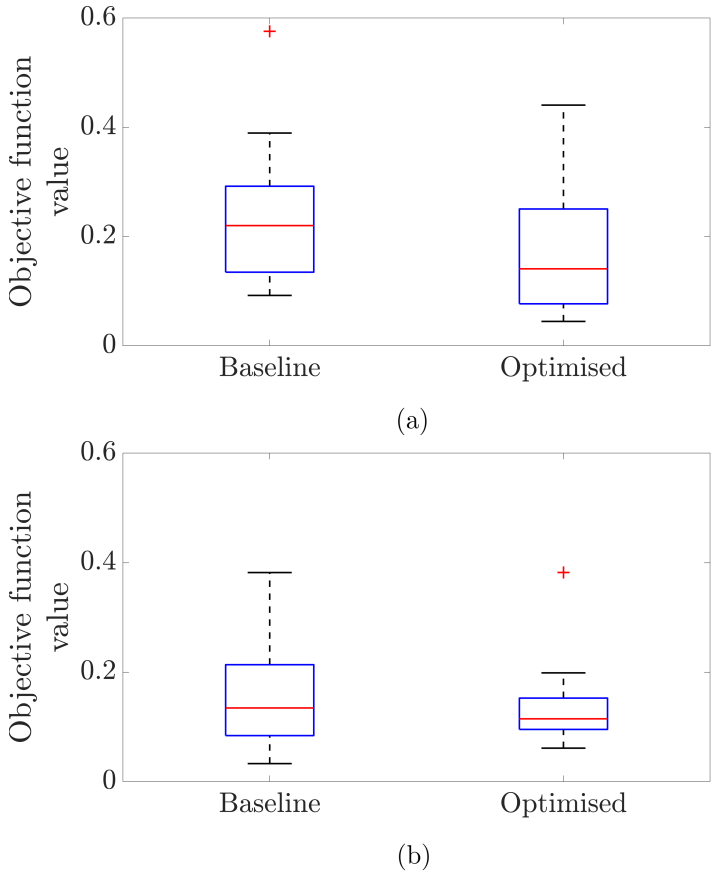

Figure 29: (a) Distribution of the expected objective function value (simulation results), (b) Distribution of the experimentally measured objective function value (experimental results).

Throughout the experiment, some participants experienced difficulty in completing some cycles. These events led to an increased and sustained trajectory tracking error and assistance from the exoskeleton. This was in turn reflected in their performance as an increase in the recorded objective function value. The frequency of these events was recorded by calculating any outliers in the performance of the participants as recorded per cycle. 19 such events were observed when participants used the baseline controller, and 9 such event were observed when participants used the optimised controller. Even though cycles

where such an event occurred may seem as outliers, it is unclear whether these events are independent from the choice of exoskeleton stiffness. These events were therefore not excluded from the analysis. This helps to better understand the results presented in Figure 29 and cases, such as S13 and S17 that may seem significantly different when in fact they are not. For reference, the performance of subjects S10, S13 and S17, as recorded per cycle, is presented on Figure 30. Three cycles of high objective function value can be observed for S13 and one such cycle can be observed for S17 when the baseline controller is used (Figure 30a). In contrast, more consistent results were obtained for these subjects when the optimised stiffness was used (Figure 30b).

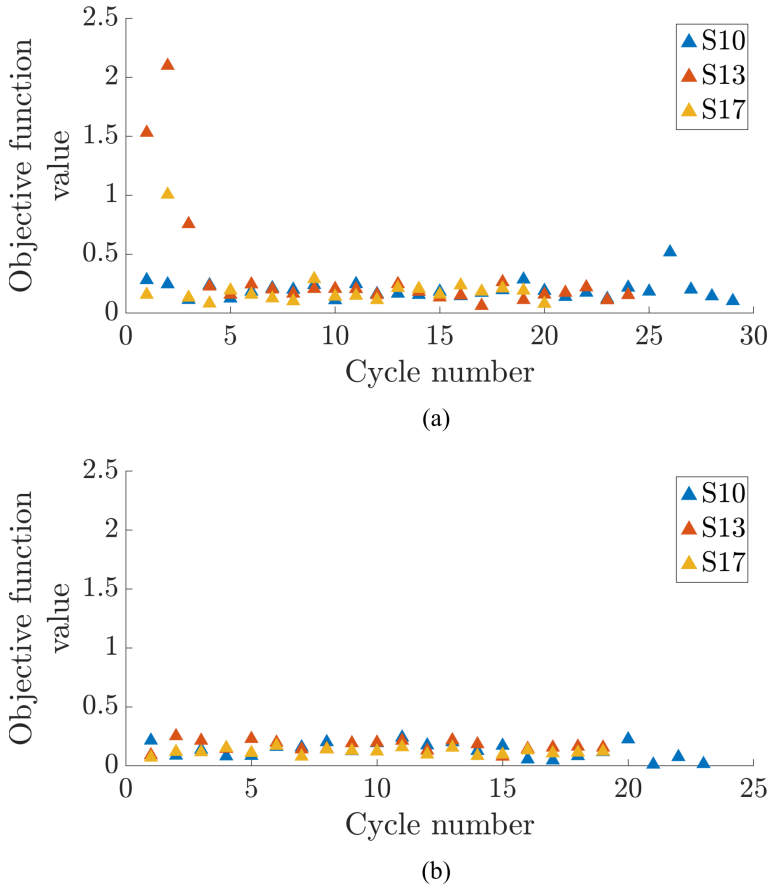

Figure 30: The performance of subjects S10, S13, S17 as recorded per cycle when (a) using the baseline controller and (b) the optimised controller.

It is also interesting to note that for some participants, the optimised stiffness that they experienced was very similar to the baseline stiffness of the exoskeleton, yet their performance was significantly different (S3, S5). In fact, the performance of S3 with the optimised stiffness was worse than the performance of all other participants, which may be considered an outlier according

to the 1.5 IQR value (Figure 29b). This suggests that the performance of each participant may not be entirely dependent on the stiffness of the exoskeleton controller but other exogenous parameters too. These may include some form of motor learning or the participant's levels of concentration and fatigue.

To quantify this variability in performance among individuals, and within individuals, the standard deviation and the CV was calculated ($CV = \sigma/\mu$) for their performance during the assistive trials. A standard deviation of 0.059 and 0.071 and a CV of 0.60 and 0.56 was obtained for the performance of the participants while using the baseline controller and the optimised controller, respectively. This high value of CV indicates a high inter-personal variability, where the standard deviation is more than half the average performance of the participants. Similarly, the standard deviation and the CV were calculated for the performance of each participant independently and as it was recorded per cycle during the assistive trials. The standard deviation of the participants' performance and the corresponding CV using the two controllers ranged from 0.019-0.077 and 0.17-0.83, respectively. This indicates that some participants performed more consistently than others, while some participants had significant variations in their motor commands during the execution of the task, which were independent of the controller used. For reference, Figure 31 shows the performance of two individuals with similar performance, as quantified by their ability to follow the reference path, but with different variability in performance. When this variation in performance is compared to the expected 30% improvement due to the optimisation of the controller parameters as observed in the results obtained in simulation, a low signal-to-noise ratio can be noticed.

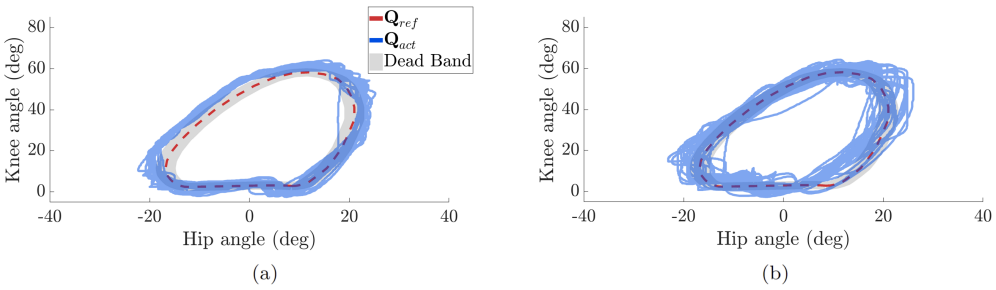

Figure 31: Recorded motion of two participant with similar performance, as quantified by their ability to follow the reference path while wearing the exoskeleton in assistive mode. (a) The recorded motion of a participant who had less variable movement (S5), (b) The recorded motion of a participant who had more variable movement (S11).

TASK LEARNING VARIABILITY After the participants experienced the exoskeleton's assistive controllers, they were asked to perform the task with the exoskeleton in transparent mode once again. This was to investigate any behaviour changes that may have occurred during the experiment and test the validity of our assumption that the behaviour of the participants will not significantly change beyond the training phase. The results can be seen in Figure 32. While the performance of some individuals was observed to significantly change, the change in the overall performance of the participants as a group was not statistically significant. A high variance is also noticeable reflecting the fact that some participants were able to more accurately track the reference path than others. This again may be a result of external factors such as concentration, fatigue and potentially even some motor learning, affecting the behaviour of the participants.

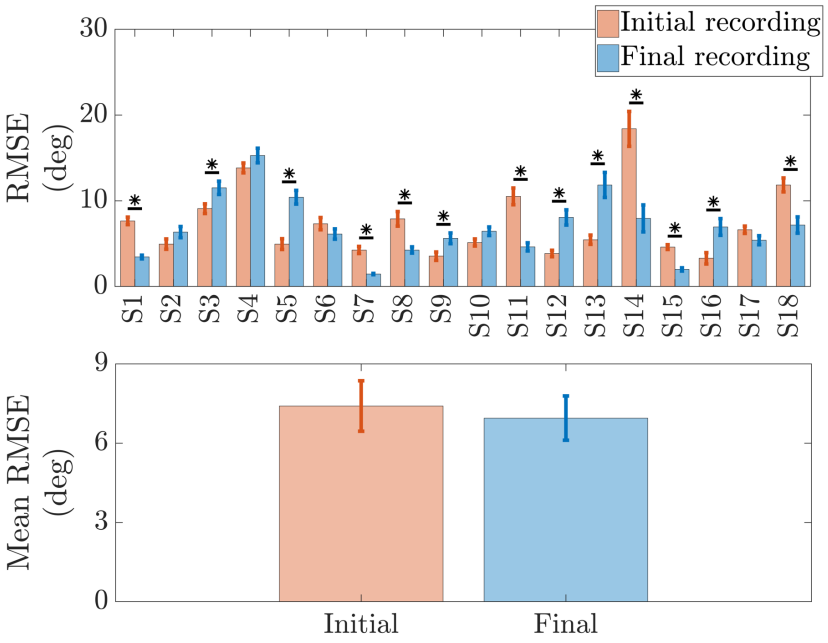

Figure 32: Kinematic tracking error of participants at the beginning of the experiment and at the end of the experiment. Error bars denote standard error. Statistical significance denoted with an asterisk for $P<0.05$.

For reference, Figure 33 illustrates the recorded motion of two participants before and after the experiment; one participant who had no evident change in their motor commands (S2), and one participant who had a significant change in their motor commands throughout the experiment (S11). It can be seen that while initially both participants demonstrated an exaggerated hip flexion and knee flexion during the SW phase, after approximately 5 minutes of testing,

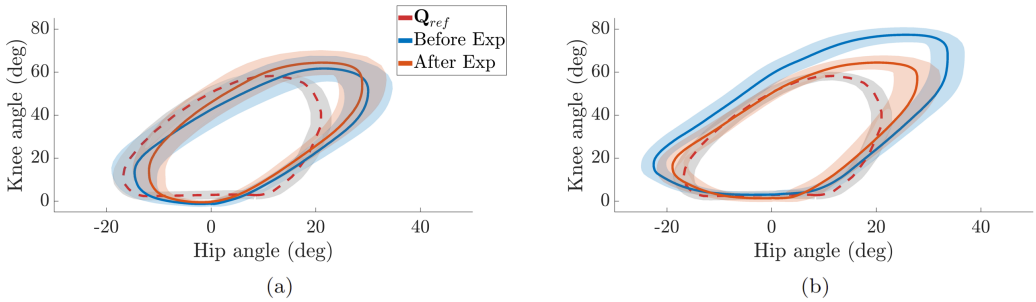

Figure 33: Recorded motion of two participants before and after the experiment while wearing the exoskeleton in transparent mode. (a) The recorded motion of a participant who had no significant improvement in their performance (S2), (b) The recorded motion of a participant who had a significant improvement in their performance (S11).

subject S2 had no obvious change in their kinematics, while subject S11 had a significant decrease in their range of motion during the SW phase, which more accurately follows the reference path.

3.5 DISCUSSION

Here, we presented an offline model-based approach for the design and optimisation of robotic controllers that focus on human-robot collaboration. Solving this problem in simulation demonstrated that this approach can enable the design of rehabilitation controllers which can be personalised to the patient's mass, residual strength and motion patterns. It is shown that for patients who are more severely affected and suffer from muscle weakness, an impedance controller with higher stiffness may be better at providing assistance as needed. On the other hand, the patient's weight does not appear to have an obvious impact on the optimal controller stiffness. Moreover, depending on the patient's actions, a different stiffness may be required. It is shown that for patients whose range of motion is either limited or exaggerated for one or more of their joints, a unique set of exoskeleton stiffnesses for the hip joint and knee joint may be required. Lastly, depending on which rehabilitation tasks need to be prioritised, adjustments may need to be carried out on the hyperparameters of the optimisation.

With the help of eighteen healthy participants, we also demonstrated how this approach can be applied to the optimisation of a real-time exoskeleton controller. Based on the musculoskeletal models of the participants, it is clear

that a unique exoskeleton stiffness can be obtained for each participant that is expected to improve their ability to follow the desired path more accurately, and with less robotic assistance. This implies an improved ability to provide assistance as needed in order promote patient-driven rehabilitation. During our experimental validation, this improvement was not uniform across all the participants. Inter- and intra-personal variability was evident. Performance variability, especially among individuals whose personalised stiffness was similar to the baseline stiffness, suggests that other factors such as concentration, fatigue and motor learning ability may be influencing the results.

The accuracy of the proposed approach is dependent on the quality of the models used. Accurately modelling an integrated human-exoskeleton system can be challenging. Here, we considered the scaling of a generalised musculoskeletal model with ideal joint actuators to match the subjects' geometric and inertial characteristics, and combined this model with the exoskeleton model, Exo-H3, which was also modelled as an exoskeleton with ideal joint actuators, generating torques that perfectly match the input torque commands. In this case, modelling uncertainty could be reduced, for example by incorporating into the model the muscle excitation and activation dynamics, the identified maximum isometric force for the different muscle groups of the subject, the exoskeleton's motor dynamics, and interaction torque losses between the human and the exoskeleton. However, many of these parameters can be particularly difficult to estimate, may require specialised equipment to measure and can significantly increase computational demands.

One other way in which model uncertainty can be reduced, is through a more accurate representation of the contact dynamics between human and exoskeleton. In many studies, fixed contact points have been used [315], [316], but this approach does not take into account force transmission losses and may result in restricted motion in the presence of joint misalignment. In other studies, kinematic constraints have been used [317]–[319]. This method avoids constraints that may arise due to joint misalignment but may rely in unrealistic interaction forces between the human and the exoskeleton. In this study, bushing forces have been used at the interaction points between the human model and the exoskeleton, which are a combination of translational and rotational elastic and viscous forces (section 3.3.2). This allows for the use of plausible human-exoskeleton interaction models, where factors such as transmission losses and skin elasticity can be considered [320], [321]. However, an accurate

value of the stiffness and the damping coefficient of these bushing forces is hard to obtain. In [322], Serrancoli et al. proposed a method for estimating human-exoskeleton contact forces, as well as ground contact forces in sit-to-stand movements. Such calibration routines could improve the accuracy of the human-exoskeleton models and the effectiveness of the controller optimisation.

One of the main challenges that may have also contributed to modelling uncertainty, is the modelling of human behaviour. In this study, a feedforward model of human behaviour was constructed based on the recorded motion of the participants. A short sample of five cycles was selected from the recorded motion and it was assumed that the human behaviour can be accurately captured within these cycles. However, it is likely that movement variability and the participants' response to assistive controllers of varying stiffness have challenged this assumption. It is expected that with a better estimation of the human behaviour and movement variability, the improvements observed in simulation will more closely match the observed improvements in real life. One way to improve the estimation of human control is either through inverse optimal control, as described in section 3.3.3, or through computational models of motor control.

Computational models of human motor learning have been proposed in [303]–[305] based on the ability of healthy people to adapt their strategy to achieve a motor task in environments where disturbances are provided in the form of either unpredictable perturbations or predictable force fields with or without stochastic catch trials. These models describe how muscle activations and limb stiffness can change in such environments. However, it is unknown whether these models can capture the adaptation of human behaviour in the presence of a predictable force field in a collaborative task. Emken et al. [170], [323] used these computational models to describe the adaptive behaviour of unimpaired participants when subjected to a virtual impairment in the form of a robotic force field. Using an objective function that included an error cost and an assistive cost, Emken et al., proceeded to analytically derive a robotic controller that provides assistance as needed. This led to an error-based adaptive controller that bounds kinematic errors and reduces its assistance as the performance of the user improves [170]. This is different to the presented framework where the emphasis is on optimising such controllers to the needs of the user. In fact the approach adopted by Emken et al., provides another example of where the presented framework could be useful to facilitate the

optimisation of the open parameters of the adaptive controller with the help of personalised musculoskeletal models.

Lastly, it is prudent to consider the usability and acceptance of the proposed pipeline by all stakeholders. While the need for improved modelling accuracy has been highlighted in order to improve the effectiveness of model-based optimisation, the need for computational efficiency is equally as important to facilitate its deployment in the real world. Compared to conventional robotic interventions that are not personalised to the needs of the user, the proposed pipeline may be able to lead to improved outcomes, but at the cost of a slightly increased workload for both the operator and the patient. This is in order to personalise the robotic controller to each patient. Given the already overloaded schedule of healthcare providers, it is important to consider methods for improving modelling accuracy through computationally efficient algorithms, to then be able to investigate the usability and acceptance of model-based optimisation through clinical experiments.

3.6 CONCLUSION

In this chapter we presented a framework for the design and optimisation of personalised robotic controllers utilising musculoskeletal models. The proposed method offers a means to reduce the reliance on extensive human-in-the-loop testing and improve the collaboration between human and robot in order to increase productivity, comfort, safety, and the functional outcomes of therapy. Illustrated through a case study focusing on a collaborative lower-limb task, the presented simulation results highlight that the same controller parameters may not be optimal for everyone and that with our proposed optimisation pipeline, rehabilitation controllers can be designed and fine-tuned based on the needs of the patient. We demonstrated that a different exoskeleton stiffness may be needed in order to maximise the desired rehabilitation objectives depending on the user's residual strength, the user's weight and the user's actions. We observed that the tuning of a robotic controller can indeed have a significant impact on the ability of the robot to support the user. In the real world, modelling uncertainty and exogenous effects such as concentration, fatigue and interpersonal and intra-personal variability in motor control and motor learning can partly inhibit the expected improvements. This further

highlights the importance of methods that will more accurately capture these interpersonal and intra-personal variations. Future studies that will contribute towards our understanding of human behaviour and adaptive human motor control in collaborative tasks with robots are needed. The presented study thus constitutes a promising proof of concept laying the foundation for further exploration into model-based approaches for the design and optimisation of personalised human-robot collaboration. With improvements in the dynamics modelling of human-robot interaction and human behaviour, this pipeline can be used to design and optimise more complicated controllers for rehabilitation, injury prevention and human augmentation.

4

HUMAN-IN-THE-LOOP OPTIMISATION

4.1 INTRODUCTION

Human-in-the-loop optimisation (HILO) presents an alternative approach to providing personalised assistance in gait. As the name suggests, this approach considers the optimisation of the open parameters of robotic controllers, where the human contributions are integrated into the system's dynamics, and design choices are driven by human-centric metrics. Consequently, the need for high-precision musculoskeletal modelling reduces. This method leverages the cyclic nature of gait, where adjustments to robot controllers are made iteratively (Figure 34). Based on this continuous feedback loop, HILO tailors robotic controllers in real time, providing finely tuned individualised assistance.

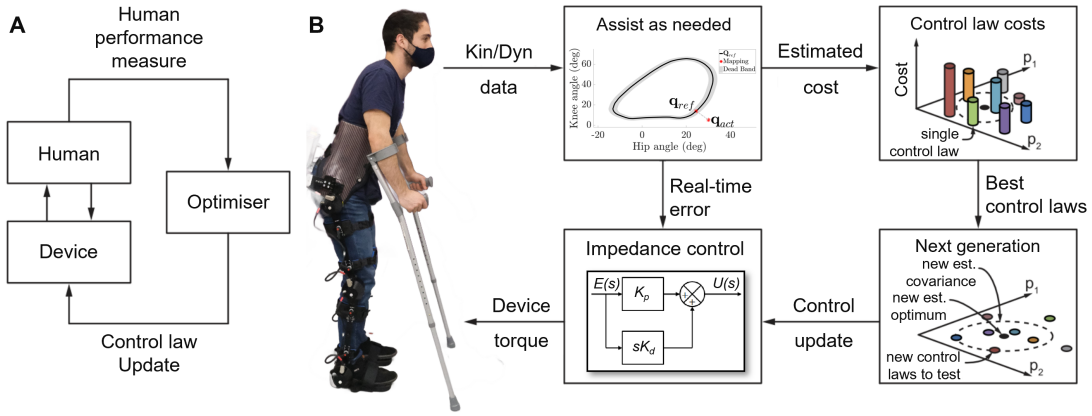

Figure 34: A. Diagram of the HILO process B. A method for providing personalised assistance in rehabilitation using the CMA evolution strategy (adapted from [180]).

To date, HILO has been successful in adjusting the assistance provided by wearable robots in order to reduce the metabolic cost of gait [180], [324], [325], and increase the self-selected speed of walking [218], [326] in healthy adults. Using one-degree of freedom (DOF) robots, studies have focused on the optimisation of parameterised assistive torque profiles for mainly the hip joint and the ankle joint. However, the effectiveness of HILO for the personalisation of rehabilitation controllers has not been studied. It is hypothesised here

that HILO could be used for the personalisation of the open parameters of rehabilitation controllers in order to provide assistance as needed.

To carry out HILO, two main algorithms have been used: the Covariance Matrix Adaptation Evolution Strategy (CMA-ES) and Bayesian optimisation. Both methods, are sample-based derivative-free optimisation methods that search for the global optimum within a constrained space. However, their underlying assumptions differ which will likely affect the efficacy of HILO, particularly when applied to gait training where time-dependent gait variability is expected to be higher.

In Bayesian optimisation, a surrogate model of a continuous function is constructed based on sampled observations. Using Gaussian process regression, the posterior probability distribution of the unknown function, $f(x)$, is iteratively updated, and is used to update the acquisition function, $a(x)$. The updated acquisition function is then used to compute the next best sample point, x_i, and this process repeats. After N number of observations, this process terminates and the point where the value of $f(x)$ is highest (or lowest) is obtained. To do this, a common acquisition function used is the *expected improvement* function, which balances exploration and exploitation. Using the *expected improvement* acquisition function the next best sample point is computed as the point with the highest expected quality and the highest posterior standard deviation, based on the assumption that $f(x)$ (given observations $y_{1:n}$ at points $x_{1:n}$) is normally distributed [312]. This implementation assumes noise-free evaluations and a constant function f. However, when it comes to HILO, where f represents the response of humans to an external force, some of the assumptions may be violated. It is important when using Bayesian optimisation to incorporate methods for updating the acquisition function based on realistic values for expected noise, and account for time-dependent changes in human behaviour due to fatigue, concentration and/or motor learning, which are often hard to predict.

In CMA-ES a stochastic search for the global optimum of an unknown function, f, is pursued iteratively through a series of generations, g. On every generation, λ sample points, $\{x_k^g | k \in \mathbb{N}, 1 \leq k \leq \lambda\}$, are generated by sampling a multivariate normal distribution with mean, $\mathbf{m}^g$, and covariance, $\mathbf{C}^g$, and are evaluated. Based on the observations, the new mean of the search distribution, $\mathbf{m}^{g+1} \in \mathbb{R}^n$, the new covariance matrix, $\mathbf{C}^{g+1} \in \mathbb{R}^{n \times n}$, and the new step size, $\sigma^{g+1} \in \mathbb{R}_{>0}$, are updated, where n is the dimension of the search space. A step

of size, σ, in a direction dictated by the sampled observations is performed, a new sample population is generated around the new mean and this process is repeated for G generations. This process does not assume that the unknown function, f, is constant and does not prevent resampling of the same points, which allows for any time-dependent changes in function f and noise in the sampled observations to be captured.

Therefore, here we propose the personalisation of a lower-limb assist-as-needed controller using HILO and the CMA-ES. Through an experimental study, we observe the ability of HILO to adjust the open parameters of a gait training controller in order to help the users accurately follow a predefined kinematic path with minimal assistance. A continuous optimisation protocol is followed over a multi-day trial as described in [324]. The preliminary results obtained from six healthy subjects are presented and discussed.

4.2 HILO AND ASSISTANCE AS NEEDED

Results from our previous study (Chapter 3) showed that the choice of stiffness of an impedance controller can have a 30% impact on the controller's ability to provide assistance as needed. However, obtaining the right stiffness for each subject remains a challenge. In our model-based method, a bottleneck was the estimation of human behaviour in a dynamic setting where the stiffness of the exoskeleton controller changes. The benefit of HILO, is that the human behaviour does not need to be estimated. On the contrary, in HILO the human behaviour is observed and is a principal component of the optimisation process.

For this reason, here we propose the optimisation of the stiffness of an impedance controller using HILO in order to provide assistance as needed. Following the principles of path control, as described in section 2.6.1, a reference kinematic path is prescribed, a dead band is defined around the reference path and an impedance controller is used to ensure the user's trajectory stays close to the reference. Iteratively, the stiffness of the hips and the knees of the two legs is adjusted and a measure of the objective function value is obtained. With the aim to provide assistance as needed, the objective function is defined as:

$$\min_{\mathbf{K}} \quad \frac{w_1}{J_1}\frac{\sum_{i=1}^{N-1}(\mathbf{u}_{r_i}^T\mathbf{I}\mathbf{u}_{r_i})}{N-1} + \frac{w_2}{J_2}\frac{\sum_{i=1}^{N}\Delta\mathbf{q}_i^T\mathbf{I}\Delta\mathbf{q}_i}{N} + \frac{w_3}{J_3}\sum_{j=1}^{4}K_j, \tag{35}$$

where $\mathbf{K}$ includes the stiffness for the hip and the knee joints, $\mathbf{u}_r$ is the exoskeleton assistance, $\mathbf{I}$ is the identity matrix, ϵ is the kinematic tracking error, and N is the number of time steps recorded in one observation. $\mathbf{w}$ are the weights of the three costs, and J is a scaling factor. The scaling factor is used to normalise the cost terms to the maximum exoskeleton assistance, the maximum expected trajectory error and maximum exoskeleton stiffness, respectively, such that the magnitude of the costs is comparable. Similarly, N is used to normalise the costs to the length of the recorded time steps and w is used to adjust the relative importance of the normalised costs. In this case, the decision variables $\mathbf{K}$ are also added in the objective function with a small weight, w, relative to the other two costs, to ensure that solutions with a lower stiffness are preferred among cases where the sum of error and assistance is similar.

4.3 THE CMA EVOLUTION STRATEGY

To speed up the convergence of the optimisation through an efficient sampling method, the CMA-ES is used as described in [327]. The mean value of the search distribution at the first generation is defined, $\mathbf{m}^0$, and λ sample points, $\{x_k^1 | k \in \mathbb{N}, 1 \leq k \leq \lambda\}$ are generated based on a multivariate normal distribution with zero mean and covariance, $\mathbf{C}^0$. The performance of the subject at the generated sample points is observed and the value of the mean point is updated based on a number of the sampled points, $\{\mu | \mu < \lambda\}$, which are weighted according to the subject's performance. This can be expressed as [327]:

$$\mathbf{x}_k^{g+1} \sim \mathbf{m}^g + \sigma^g \mathcal{N}(0, \mathbf{C}^g) \text{ for } k = 1, 2, ..., \lambda, \tag{36}$$

$$\mathbf{m}^{g+1} = \mathbf{m}^g + c_m \sum_{i=1}^{\mu} w_i (\mathbf{x}_{i:\lambda}^{g+1} - \mathbf{m}^g), \tag{37}$$

where the symbol $\sim$ denotes the same distribution on the left and right side, σ is the step size, c_m is the learning rate for the mean and $\mathbf{x}_{i:\lambda}^{g+1}$ is the i-th best sample out of all samples, $\mathbf{x}_k^{g+1}$, with the index $i : \lambda$ denoting the index of the i-th ranked sample such that $f(x_{1:\lambda}^{g+1}) \leq f(x_{2:\lambda}^{g+1}) \leq ... \leq f(x_{\lambda:\lambda}^{g+1})$, where f is the objective function to be minimised.

On every generation, an update of the covariance matrix, $\mathbf{C}^g$, and the step size, σ^g, is also carried out. The covariance matrix is updated such that it retains information from both the entire population, and the correlations between

generations. To do this, the *cumulative* evolution path, $\mathbf{p}_c^{g+1}$ is utilised, which is the sequence of steps CMA-ES takes over a number of generations. This is expressed as [327]:

$$\mathbf{C}^{g+1} = (1 + c_1\delta(h_\sigma) - c_1 - c_\mu)\mathbf{C}^g + c_1\mathbf{p}_c^{g+1}\mathbf{p}_c^{g+1^T} + c_\mu \sum_{i=1}^{\mu} w_i \mathbf{y}_{i:\lambda}^{g+1}\mathbf{y}_{i:\lambda}^{g+1^T}, \quad (38)$$

$$\mathbf{p}_c^{g+1} = (1 - c_c)\mathbf{p}_c^g + h_\sigma\sqrt{c_c(2 - c_c)\mu_{eff}} \sum_{i=1}^{\mu} w_i \mathbf{y}_{i:\lambda}^{g+1}, \quad (39)$$

$$\mathbf{y}_{i:\lambda}^{g+1} = (\mathbf{x}_{i:\lambda}^{g+1} - \mathbf{m}^g)/\sigma^g, \quad (40)$$

where c_1 and c_μ are the learning rates for the rank-*one* and rank-μ updates of the covariance matrix, respectively, c_c is the learning rate for the *cumulative* evolution path, μ_{eff} is the effective sample size of the selected samples defined as $\mu_{eff} = 1/\sum_{i=1}^{\mu} w_i^2$, and $\delta(h_\sigma)$ is defined as $\delta(h_\sigma) = (1 - h_\sigma)c_c(2 - c_c) \leq 1$, where h_σ is a Heaviside function that stalls the update of the *cumulative* evolution path depending on the size of the *conjugate* evolution path. The *conjugate* evolution path, $\mathbf{p}_\sigma^g$, is independent of the direction of the successive steps performed, and is used to update the step size, σ^g. The function, h_σ, and the *conjugate* evolution path are defined as [327]:

$$h_\sigma = \begin{cases} 1, & \text{if} \frac{||\mathbf{p}_\sigma^{g+1}||}{\sqrt{1-(1-c_\sigma^{2(g+1)})}} < (1.4 + \frac{2}{n+1})\mathbb{E}||\mathcal{N}(\mathbf{0}, \mathbf{I})||, \\ 0, & \text{otherwise}, \end{cases} \quad (41)$$

$$\mathbb{E}||\mathcal{N}(\mathbf{0}, \mathbf{I})|| \approx \sqrt{n}(1 - \frac{1}{4n} + \frac{1}{21n^2}), \quad (42)$$

$$\mathbf{p}_\sigma^{g+1} = (1 - c_\sigma)\mathbf{p}_\sigma^g + \sqrt{c_\sigma(2 - c_\sigma)\mu_{eff}}\mathbf{C}^{g^{-\frac{1}{2}}} \sum_{i=1}^{\mu} w_i \mathbf{y}_{i:\lambda}^{g+1}, \quad (43)$$

where c_σ is the learning rate for the *conjugate* evolution path.

Using the *conjugate* evolution path, the step size of the next generation is adjusted. This is to ensure a faster convergence and either increase the step size if the steps recorded are pointing in the same direction or decrease the step size if the steps recorded are not converging and move in opposite directions. This is achieved by comparing the length of the *conjugate* evolution path, $\mathbf{p}_\sigma^{g+1}$,

with its expected length, $\mathbb{E}||\mathcal{N}(\mathbf{0}, \mathbf{I})||$. The adaptation of the step size can then be expressed as [327]:

$$\sigma^{g+1} = \sigma^{g} \exp\left(\frac{c_\sigma}{d_\sigma}\left(\frac{||\mathbf{p}_\sigma^{g+1}||}{\mathbb{E}||\mathcal{N}(\mathbf{0}, \mathbf{I})||} - 1\right)\right), \tag{44}$$

where d_σ is a damping parameter.

The implementation of CMA-ES used for this study is summarised in the following algorithm.

Algorithm 2 Pseudocode for CMA evolution strategy

Require: $0 < \mathbf{w} < 1$

$\mathbf{C} \leftarrow \mathbf{I}$
$\mathbf{p}_c \leftarrow \mathbf{0}$
$\mathbf{p}_\sigma \leftarrow \mathbf{0}$
$g \leftarrow 0$
$G \leftarrow 10$
$\lambda \leftarrow 6$
$K_{max} \leftarrow 400$
$\mathbf{m} \leftarrow \frac{1}{2}\mathbf{K}_{max}$
$\sigma \leftarrow 100$
while $g < G$ **do**
    $\mathbf{x}^g \leftarrow$ sample_population$(\mathbf{m}^g, \sigma^g, \mathbf{C}^g)$
    $f(\mathbf{x}^g) \leftarrow$ evaluate_population(HIL experiments)
    $\mathbf{x}_{i:\lambda}^g \leftarrow$ sort_population$(\mathbf{x}^g, f(\mathbf{x}^g))$
    $\mathbf{m}^{g+1} \leftarrow$ update_mean$(\mathbf{m}^g, \mathbf{w}, \mathbf{x}_{i:\lambda}^g, \sigma^g)$
    $\mathbf{p}_c^{g+1} \leftarrow$ update_cum_path$(\mathbf{p}_c^g, \mathbf{m}^g, \mathbf{w}, \mathbf{x}_{i:\lambda}^g, \sigma^g)$
    $\mathbf{p}_\sigma^{g+1} \leftarrow$ update_conj_path$(\mathbf{p}_\sigma^g, \mathbf{C}, \mathbf{m}^g, \mathbf{w}, \mathbf{x}_{i:\lambda}^g, \sigma^g)$
    $\sigma^{g+1} \leftarrow$ update_step_size$(\sigma^g, \mathbf{p}_\sigma^{g+1})$
    $\mathbf{C}^{g+1} \leftarrow$ update_covariance$(\mathbf{C}^g, \mathbf{p}_c^{g+1}, \mathbf{m}^g, \mathbf{w}, \mathbf{x}_{i:\lambda}^g, \sigma^g)$
    $\mathbf{S} \leftarrow \{\mathbf{S}; [\mathbf{x}^g, f(\mathbf{x}^g)]\}$
    $g \leftarrow g + 1$
end while
$\mathbf{x}^* \leftarrow \mathbf{S}$ such that $f(\mathbf{x})^* = \min \mathbf{S}$

4.4 EXPERIMENTAL VALIDATION

4.4.1 *Subjects*

The effectiveness of the HILO was tested on six healthy subjects (Age = 30 ± 4.6, 2 females). The experimental pipeline was approved by the University of

Edinburgh, School of Informatics Ethics Committee (ID 2021/46920) and the participants provided written consent.

4.4.2 *Hardware*

The instrumented treadmill M-Gait (Motek Medical, Netherlands) was used to enable self-paced gait during the experiment (section 2.3) and the exoskeleton Exo-H3 (Technaid, Spain) was used to provide assistance during gait (section 2.6). The exoskeleton's joint position sensors were used to record the joint angle of the legs and provide real-time visual feedback to the user (Figure 35a). Simulink Desktop Real Time was used for the real-time control of the exoskeleton at 100 Hz.

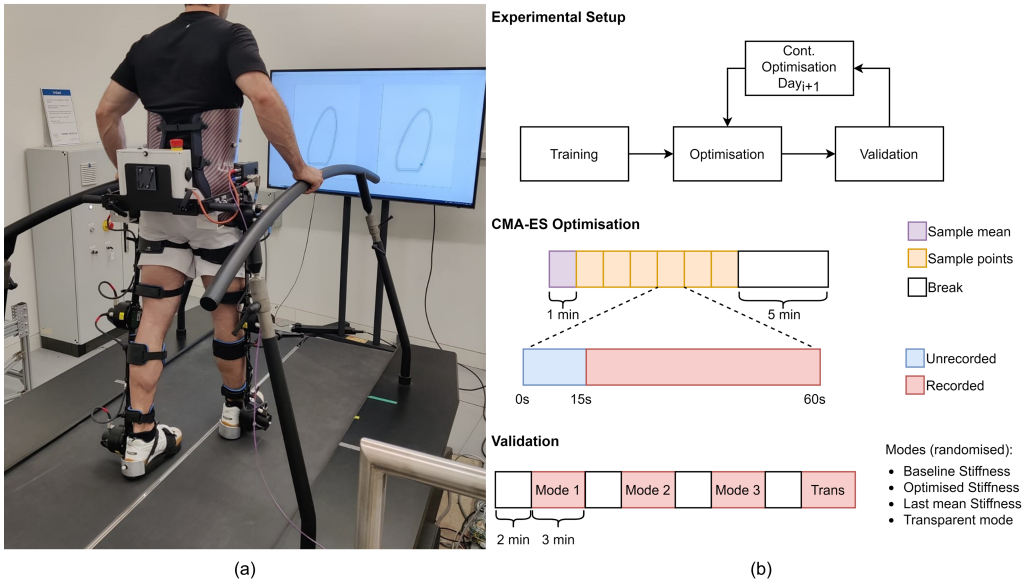

Figure 35: (a) Healthy participant walking on a self-paced treadmill with real-time visual feedback and assistance from the lower limb exoskeleton, Exo-H3. (b) Experimental protocol for HILO following a continuous optimisation protocol over multiple days.

4.4.3 *Experimental setup*

The experiments involved assisted gait training at different levels of exoskeleton stiffness. The participants were fitted with the exoskeleton and were asked to walk on the treadmill at their preferred speed in order to track the reference path as accurately as possible. The recorded kinematics of a healthy subject

were used as the reference path, and the path was adjusted to a path of a less pronounced loading response. Adjustments to the reference path were also carried out to increase comfort for each subject.

Prior to optimisation, a training period was included to familiarise the subjects with the task and the visual feedback. At all times, real-time visual feedback was provided to allow the participants to compare their kinematics to the reference, and inform them about their performance and the remaining duration of the experiment. During optimisation, a new exoskeleton stiffness was tested on every minute and the performance of the subjects was measured as described by equation 35. To reduce bias from the changing exoskeleton stiffness, the first 15 seconds of each trial were discarded. One generation of the CMA-ES included 7 sample points, making up a 7-minute bout. After each 7-minute bout, a 5-minute break was allowed to reduce bias from fatigue. A total of 5 generations were performed per day, resulting in a total of 10 generations, or 70 sampled points, over the two-day experiment. At the end of each day three rounds of 3-minute validation trials were carried out in a randomised order to evaluate the effectiveness of the HILO. These included a trial with the baseline stiffness ($\mathbf{K}_{base} = [200, 200]$ Nm/rad), a trial with the best identified stiffness and a trial with the last mean stiffness obtained from the last CMA-ES generation (Figure 35b). Lastly, a trial with no assistance was carried out.

To reduce the risk of overwhelming participants with sensory information, subjects were asked to perform the experiment for only one of the two legs (while the other leg was controlled using a constant low stiffness $K = 0.25 * K_{base}$). The convergence of the HILO and its effect on the performance of the participants are observed and discussed.

4.5 RESULTS

Figure 36 shows the adaptation of the CMA-ES for all subjects. A continuous adaptation of the CMA-ES can be seen. In most cases this led to an assistive controller which involved a higher stiffness at the knee joint. This suggests that despite the variability in gait between and within individuals, for the majority of the 2-day trial the participants were able to follow the reference path more accurately when the stiffness of the knee joint was higher than the

baseline stiffness and higher than the hip stiffness. It can also be seen that some participants were more consistent with their performance than others, which led to a more gradual convergence of the CMA-ES. This is revealed by the direction in which the mean points of the CMA-ES progressed. For example, the progression of the generated mean points for subjects S1, S2, S4 and S5 appears to be smoother and more gradual, than subjects S3 and S6. This also led to a gradually decreasing covariance and step size, which is less evident in the results obtained for subjects S3 and S6.

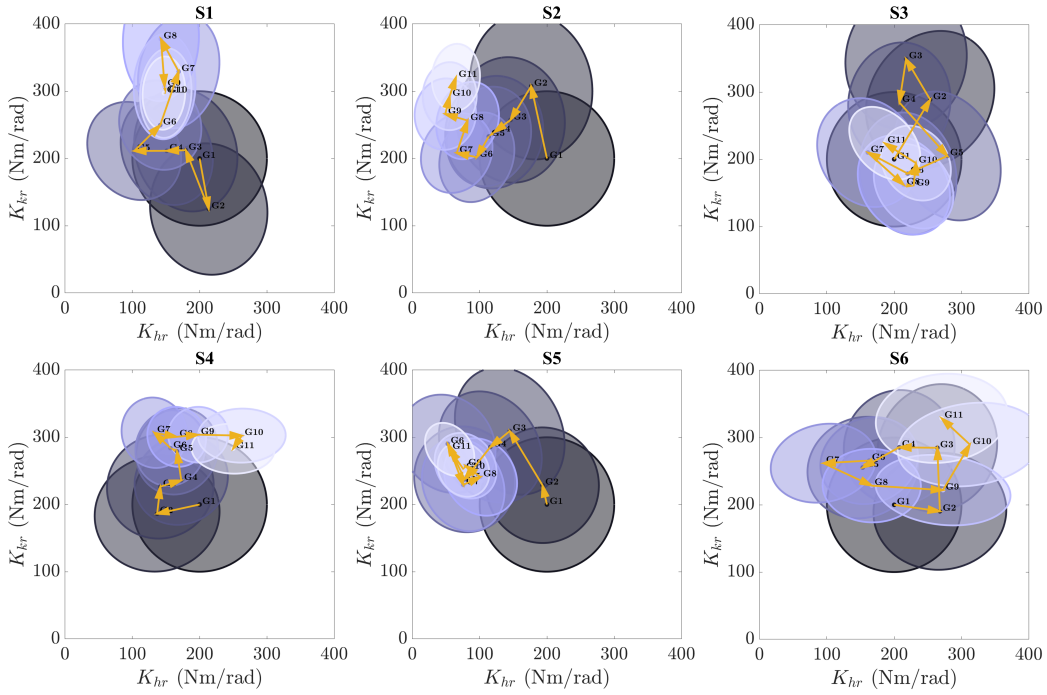

Figure 36: Adaptation of covariance matrix and the CMA-ES generation mean for all subjects. Yellow arrows show the CMA-ES step size and direction.

In Figure 37 the results from the validation trials are presented. It can be seen that a within-group difference can be observed between the validation results from day 1 and the validation results from day 2 (Figure 37a). The performance of the subjects has significantly improved from day 1 to day 2 both when the baseline stiffness and the optimised stiffness were used. However, a significant between-group difference was not evident when the performance of the subjects using the different stiffnesses was compared (Figure 37b). High performance variability was observed both between and within subjects which may have detracted from the benefits due to the adjusted controller stiffness.

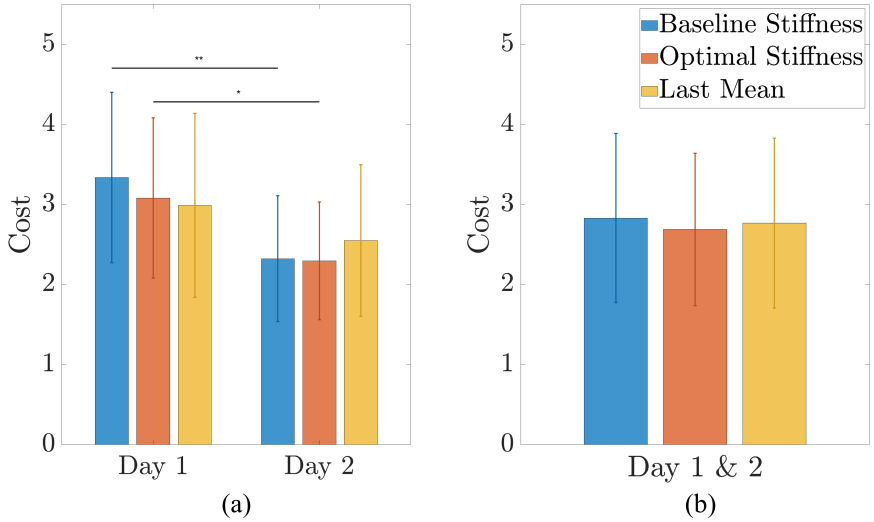

Figure 37: (a) Results from the validation trials for day 1 and day 2, separately. (b) Combined results from the validation trials from day 1 and day 2. Error bars show the standard deviation of cost. Statistical significance denoted with asterisks *P<0.05, **P<0.01.

4.6 DISCUSSION

Here, an implementation of HILO is proposed for the personalisation of robot-assisted gait training. For this purpose the deployment of the CMA-ES is used and a continuous optimisation protocol is suggested to allow enough time for the optimiser to converge over multiple days. This aligns with the needs of gait training, where gait trials may need to be interrupted for rest and safety. To the best of our knowledge, this is the first time HILO has been tested for the personalisation of assistive controllers in gait rehabilitation and for robots with multiple degrees of freedom (DOFs). It was hypothesised that with the human in the loop, the robot controller can be iteratively optimised based on the user's performance in order to provide assistance as needed. This could in turn allow ambulatory patients to benefit from personalised robot-assisted gait training (RAGT) in order to increase independence and gait efficiency.

Results from six healthy subjects are obtained indicating that the CMA-ES can adapt the stiffness of the robot controller based on the performance of the subjects to personalise gait training. However, conclusive results regarding the effectiveness of this personalised stiffness in improving the robots ability to provide assistance as needed could not be obtained. One major challenge in HILO, and in the personalisation of closed-loop robotic controllers, is intrapersonal variability. Variability within individuals may be both time-dependent

and random, which poses a significant challenge in the design of personalised interventions. For an adaptive control algorithm to prove effective, the time-dependent changes in human behaviour need to be captured and the benefits of adaptation need to outweigh any effects due to unpredicted behaviour variability. This appears to be especially hard when the adaptation of rule-based controllers is considered since such controllers are expected to be effective within a range of control parameters.

Moreover, one underlying reason that likely contributes towards the observed variability within individuals is the human-robot coadaptation. On the one hand, adjustments to the stiffness of the robot are carried out to provide support to the human in an optimal way (as defined by the objective in equation 35), but on the other hand, the human behaviour concurrently changes to utilise this stiffness perhaps for a different subject-specific objective (e.g. comfort or metabolic efficiency). This makes HILO particularly challenging as these sources of bias appear to be significant, outweighing the benefits of robot adaptation. Adjustments to the experimental protocol can help reduce this bias, but a systematic way of making these adjustments is hard to establish. For example, increasing the duration of each trial could provide a more representative recording of the human response to the new stiffness, but would also increase the duration of the experimental protocol, delay convergence and increase bias from fatigue and discomfort.

HILO and musculoskeletal modelling

In this chapter HILO has been presented as an alternative to model-based optimisation. This does not mean that the two approaches cannot be used together. While relying on direct readings from the human is considered one of the advantages of HILO, it is also one of the main limitations of this approach. Due to the inherent delays associated with some biological processes, the number of samples available to reach convergence during HILO is proportional to the duration of the experiment and therefore it is often limited.

A clear example of this, is the optimisation of robotic assistance for the minimisation of energy expenditure. Measuring the effects of an adaptive controller on the metabolic cost of gait, commonly involves the measurement of noisy, low-frequency calorimetric data, which requires large measurement

times in order to produce accurate readings [328]. This presents two issues: first, as the time spent walking increases, so too does the likelihood that the subject will become fatigued, introducing bias to measurements obtained later in the experiment, and second, limitations to the complexity of the optimisation problem are introduced, necessitating a reduction in the dimensionality of the problem. With the use of musculoskeletal modelling, these problems can be addressed to reduce excessive runtimes in HILO. By utilising dynamic models driven by musculotendon actuators [153]–[156] combined with models of muscle energetics [329], [330], the metabolic cost of movement can be readily estimated [330], [331], providing approximations to the ground truth data from calorimetry [330], [332]. This way, we can reduce the time demands of HILO by simulating the metabolic cost of walking using musculoskeletal models, while retaining the ability to learn personalised controllers using data collected directly from subjects.

In [333] we used this hybrid approach to support human-in-the-loop optimisation with musculoskeletal modelling. In this work, led by Daniel F. N. Gordon, we were able to show that with the use of musculoskeletal modelling we can potentially reduce the time investment required to observe the effects of controller updates on human locomotion and speed up the convergence of HILO, albeit improvements in the personalisation of the muscle properties of the human model may be necessary for more reliable results.

Curse of dimensionality

The curse of dimensionality clearly affects both HILO and offline model-based optimisation. In the former, a larger search space will inevitably increase the duration of experimental protocol, introduce bias in the readings and affect the convergence of the optimiser, while in the latter, increased modelling complexity will increase both computational demands and the gap between simulation and reality. This, limits the utility of both approaches for the personalisation of more complicated interventions that may include additional controllable agents such as functional electrical stimulation (FES). For the personalisation of an integrated robot-FES system, a novel hierarchical and adaptive component is proposed in the following chapter to provide personalised assistance.

5

HYBRID ADAPTIVE ASSISTANCE

5.1 STATE OF THE ART HYBRID CONTROL

To further enhance the outcomes of physical therapy in robot-assisted rehabilitation, the combination of functional electrical stimulation (FES) with robotic assistance has been proposed [250], [334]. The use of FES can induce muscle contractions and utilise the patient's muscles as actuators. This increased afferent feedback to the patient is associated with increased neuroplasticity [251], [335], while the induced muscle contractions are known to provide improved cardiovascular and metabolic benefits, as well as increased calcium concentration in bones [222]. However, some of the main challenges that arise with the use of FES is the rapid onset of muscle fatigue [244], [245] and the non-linear response of muscles to electrical stimulation, which makes the resultant limb motion hard to control [234], [270]. When combined with robotic assistance, it is possible to overcome these limitations while still preserving the advantages associated with both FES and robotic assistance. However, in this over-actuated system, achieving a seamless triadic collaboration between the user, the robot and the electrical stimulation remains a challenge (Figure 38).

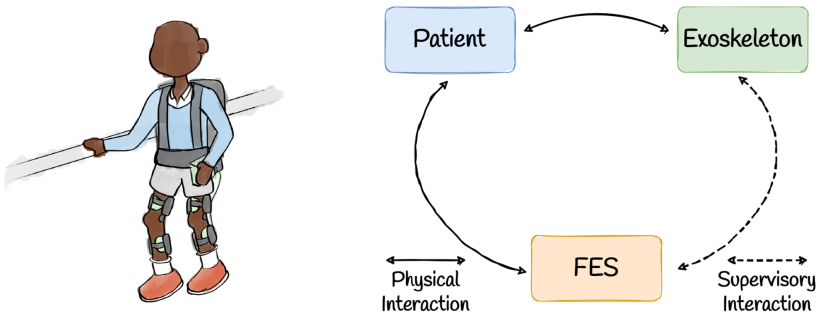

Figure 38: Triadic collaboration between a human and two technological agents, a robot and FES.

Various hybrid controllers have been proposed to deal with the effects of muscle fatigue and the non-linear response of muscles to electrical stimulation. One of the first studies to demonstrate the feasibility of hybrid systems was

presented by Popovic et al. in [336]. Popovic et al. demonstrated that with the use of open-loop FES control and an impedance-controlled orthosis, energy consumption as well as ground reaction forces on crutches can be reduced in an ambulatory patient with spinal cord injury (SCI). Similarly, some of the earliest studies on hybrid systems, tested the feasibility of combining FES with passive wearable orthoses [337]–[339]. However, the passive nature and the dissipative control of these orthoses, implies that the torques induced by FES needed to match or exceed the desired joint torques. Thus, even though these passive orthoses proved to be safe, their inability to be actively controlled to provide assistive torques that would increase the energy of the system limited their capacity to reduce muscle fatigue.

To address this limitation observed by the use of passive exoskeletons, more emphasis was given on combining FES with active electromechanical devices. This led to the exploration of a more diverse pool of assistive controllers with the majority of them incorporating adaptive control for either or both the robot and FES. Examples include the studies by Stauffer et al. [340] and Ha et al. [341] where iterative learning control (ILC) was used to adjust the stimulation intensity of FES in order to minimise the interaction torques between the user and the robot while performing an ambulatory task. ILC was also used in [314] for both the FES controller and the robotic controller. Del-Ama et al. used a dual state controller that switched between a learning state and a monitoring state to adjust the stimulation parameters and the stiffness of the exoskeleton, respectively, in order to respond to muscle fatigue, reduce the interaction between the human and the robot, and maintain an accurate tracking of the desired kinematic trajectory [314].

Studies on hybrid robot-FES cooperation have also been carried out using optimal control and nonlinear control to address the actuation redundancy problem [342]–[345]. In [342], the use of model predictive control (MPC) is proposed for the distribution of torques between FES and robot assistance. This controller was tested in simulation and it was demonstrated that the allocation of controls between robotic assistance and FES in a knee extension task reaches an equilibrium based on the relative weight matrices to find a balance between trajectory tracking error, muscle fatigue, motor effort and electrical stimulation. The use of non-linear model predictive control (NMPC) was also proposed by [343] and was tested on 3 healthy subjects during the knee extension task. In this case, even though muscle fatigue was not included as a cost in

the problem formulation, it was demonstrated that the use of NMPC could allocate controls between robot assistance and FES such that the muscle fatigue experienced by the subjects is less compared to the muscle fatigue observed when a proportional-integral-derivative (PID) controller is used. Similarly, Molazadeh et al. [344] used a bi-level hybrid controller to estimate the needed assistive forces and distribute them between the robotic device and the FES. On the higher level, a neural-network-based iterative learning controller (NNILC) was used which was designed to learn the unknown system dynamics and estimate the required assistive forces, and on the lower level, MPC was used to distribute the assistive torques between the robot and the FES. This bi-level hybrid controller was tested on four healthy subjects, and it was shown to be effective in reducing the trajectory tracking error by reducing the feedback input and increasing the contribution of the learning terms. A slightly different approach was adopted by Alibeji et al. [345] where a hybrid controller was proposed that utilises postural synergies to reduce the dimensions of the control variables. Based on the identified postural synergies, the estimated muscle fatigue, and a Lyapunov-based stability approach, a non-linear control law was derived which achieved accurate trajectory tracking. However, the controller's effect on muscle fatigue could not be analysed due to the limited duration of the experiments. Some interesting torque distribution methods have also been explored in simulation in order to address this actuation redundancy in hybrid control but their effectiveness was not validated experimentally [346], [347].

A common element among these controllers is that the focus is on the neuroprosthetic benefits of hybrid robot-FES systems, while the therapeutic effects of training due to the collaboration between human, robot and FES are not considered. As a result, the voluntary contributions of the human are often neglected or are dealt with as disturbance to the system. However, many studies have highlighted the importance of the patient's engagement in driving neural plasticity [287], [289], [348], [349]. Another common element among these studies is that muscle fatigue is often treated as a discrete event instead of a continuous process, the management of which is usually compensatory and not preventive. As a result, increased stimulation intensity is often used to compensate for the reduced force generated by the fatigued muscles, which is likely to induce even higher levels of muscle fatigue and discomfort.

Here, we design an adaptive hybrid controller for ambulatory patients (i.e. people who retain some voluntary control over their lower limbs) to achieve the triadic collaboration between the human, the robot and FES [350], where the main driver of the system is the patient, and muscle fatigue is addressed in a continuous and preventive fashion. In this controller, we use a hierarchical structure to prioritise the contributions of the three agents in the following order: (1) the voluntary contributions of the patient, (2) the assistance from FES and (3) the assistance from the robot. We use a model-based approach to estimate the level of induced muscle fatigue, and the controller's parameters are adapted to provide personalised assistance. This adaptation happens based on the user's estimated level of muscle fatigue and their ability to follow the desired path. The performance of this hybrid adaptive path controller (HAPC) is verified in simulation using our offline model-based approach (Chapter 3), and it is validated experimentally on one healthy subject. The ability of the controller to adapt to the needs of the user in order to provide assistance as needed and prevent muscle fatigue is analysed and discussed.

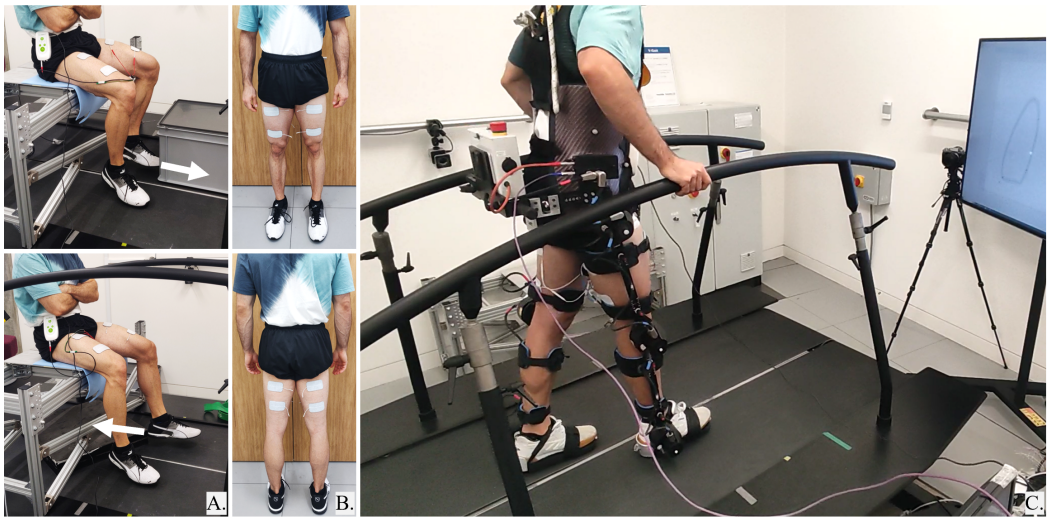

Figure 39: A. Fatigue model identification for quadriceps and hamstrings using FES in isometric conditions (pushing a heavy box on an instrumented treadmill). B. Electrode placement on the quadriceps and hamstrings. C. Experimental validation of hybrid adaptive controller on an instrumented treadmill with real-time visual feedback.

The main contributions here include:

- The design of a cooperative controller where robotic assistance and FES are provided as needed.

- The triadic collaboration between human, FES and robotic assistance in a hierarchical fashion where the voluntary movement of the human is prioritised.
- A novel muscle fatigue management approach that preserves the fitness of the muscles through the adaptation of the intensity of FES and the controls of the robot in a preventive and continuous process.

5.2 HYBRID PATH CONTROL

As our starting point we deploy a HAPC – a controller that follows the principles of Path Control [221], and provides adaptive assistance using a wearable robot and FES (Figure 40). This controller involves a reference kinematic path in joint space, $\mathbf{Q}_{ref} \in \mathbb{R}^{i \times j}$, and a dynamically defined reference point, $\mathbf{q}_{\text{ref}} \in \mathbb{R}^{j}$, as explained in section 2.6.1. To establish a hierarchy between the human, the FES and the robot, a deadband and a FES band of radius, r_{db} and r_{fesb}, respectively, are defined around the reference path. This defines a region where no assistance is provided to the human (deadband), a region where only assistance from FES is provided (FES band) and a region where hybrid robot-FES assistance is provided (hybrid band). Based on these regions, the corresponding joint angle error can be calculated for the FES controller, $\Delta\mathbf{q}_f \in \mathbb{R}^{j}$, and the exoskeleton's controller, $\Delta\mathbf{q}_e \in \mathbb{R}^{j}$, as the difference between the reference point and the human's pose, minus the relevant error tolerance, r, formally expressed as:

$$\Delta\tilde{\mathbf{q}} = \mathbf{q}_{\text{ref}} - \mathbf{q}_{\text{act}}, \tag{45}$$

$$\Delta q^{(j)} = \begin{cases} 0, & |\Delta\tilde{q}^{(j)}| \leq r, \\ \Delta\tilde{q}^{(j)} - r_{\text{db}}, & \Delta\tilde{q}^{(j)} > r, \text{ for } j = 1,2 \\ \Delta\tilde{q}^{(j)} + r_{\text{db}}, & \Delta\tilde{q}^{(j)} < -r, \end{cases} \tag{46}$$

$$r = \begin{cases} r_{\text{db}}, & \text{FES controller}, \\ r_{\text{fesb}}, & \text{Exo controller}. \end{cases} \tag{47}$$

Based on the tracking error, assistance is provided by the FES and the robot, in a direction orthogonal to the reference path in order to promote patient-driven

therapy without temporal constraints. For this purpose, three closed-loop controllers are used: an adaptive controller for the FES, an adaptive controller for the exoskeleton, and an adaptive controller for the width of the FES band. A control diagram of the HAPC is provided in Figure 41.

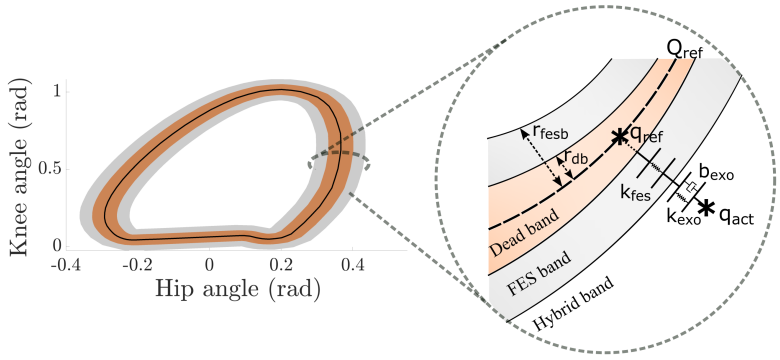

Figure 40: Illustration of the reference kinematic path in joint space, surrounded by the deadband, and the FES band. The magnified region depicts the components of the hybrid path controller for a human configuration, q_{act}.

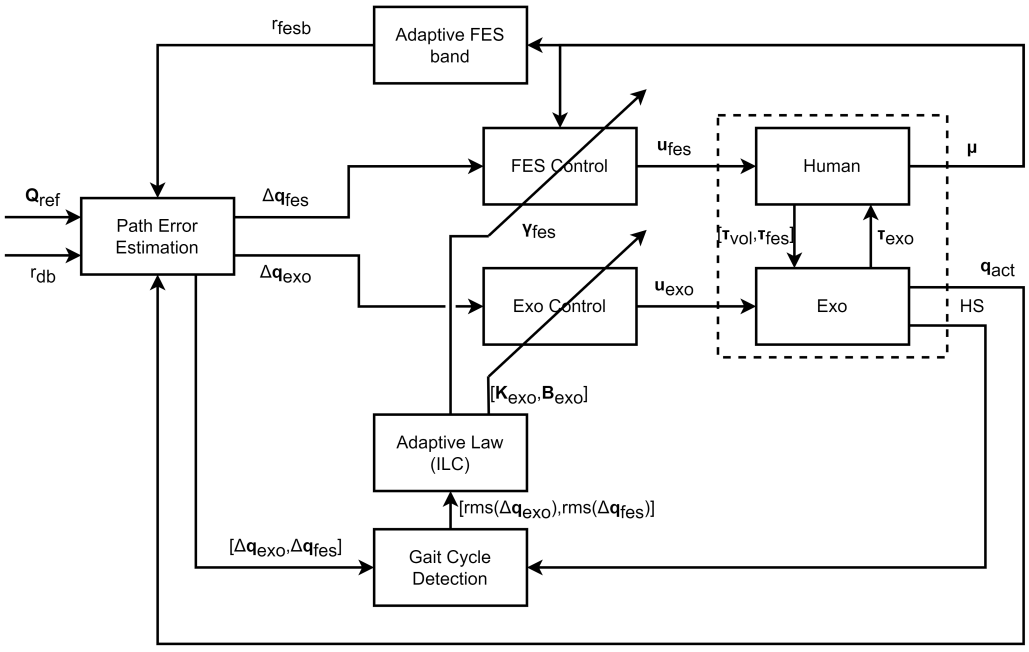

Figure 41: Control diagram of the hybrid adaptive path controller.

5.2.1 *Adaptive FES controller*

To enable the hybrid controller to adjust the intensity of electrical stimulation to the needs of the user, a proportional controller with two adaptive components is defined as:

$$\mathbf{u}_f = \boldsymbol{\mu}\boldsymbol{\gamma}\mathbf{K}_f\Delta\hat{\mathbf{q}}_f, \tag{48}$$

$$\mathbf{K}_f = \frac{(\mathbf{u}_{sat} - \mathbf{u}_{thr})}{2r^0_{\text{fesb}}}, \tag{49}$$

where $\mathbf{u}_f \in \mathbb{R}^k$ is the stimulation intensity, $\boldsymbol{\mu} \in \mathbb{R}^k$ is a measure of muscle fitness (the inverse of muscle fatigue) ranging from [0,1], $\boldsymbol{\gamma} \in \mathbb{R}^k$ is the ILC gain ranging from [0,1], $\mathbf{K}_f \in \mathbb{R}^k$ is a constant stiffness, and $\Delta\hat{\mathbf{q}}_f \in \mathbb{R}^k$ is the kinematic error adjusted by its sign and the stimulated muscles to ensure $\mathbf{u}_f \geq 0$, with k being the number of stimulated muscles. r^0_{fesb} is the initial radius of the FES band (set to 6 degrees), and $\mathbf{u}_{thr}$ and $\mathbf{u}_{sat}$ are the threshold and saturation pulse width for the given stimulation amplitude and frequency, defined as the minimum stimulation pulse width that results in a visible muscle contraction, and the pulse width above which the generated force saturates, respectively.

The first adaptive component involves the adjustment of the stimulation intensity according to muscle fitness. As a result, muscles whose fitness decreases receive less stimulation. To estimate muscle fitness the following model is used [247]:

$$\dot{\mu} = \frac{(\mu_{min} - \mu)\rho(f)a_f}{T_{fat}} + \frac{(1-\mu)(1-\rho(f)a_f)}{T_{rec}}, \tag{50}$$

$$\rho(f) = 1 - \beta_\mu + \beta_\mu\left(\frac{f}{100}\right)^2, \text{ for } f < 100\ Hz, \tag{51}$$

where μ_{min} is the minimum muscle fitness, β_μ is a shape factor, f is the stimulation frequency, and T_{fat} and T_{rec} are the time constants that describe the rate of muscle fatigue and recovery, respectively. The parameter a_f is the activation of the stimulated muscles which is estimated as [347], [351]:

$$\mathbf{a}_f = \mathbf{a}\boldsymbol{\mu}, \tag{52}$$

$$\mathbf{k}_1\ddot{\mathbf{a}} + \mathbf{k}_2\dot{\mathbf{a}} + \mathbf{a} = \mathbf{e}, \tag{53}$$

$$\mathbf{e} = \begin{cases} 0, & \mathbf{u}_f < \mathbf{u}_{thr}, \\ \frac{\mathbf{u}_f - \mathbf{u}_{thr}}{\mathbf{u}_{sat} - \mathbf{u}_{thr}}, & \mathbf{u}_{thr} < \mathbf{u}_f < \mathbf{u}_{sat}, \\ 1, & \mathbf{u}_f > \mathbf{u}_{sat}. \end{cases} \tag{54}$$

where $\mathbf{k}_1$ and $\mathbf{k}_2$ are constants that characterise the response of muscles to electrical stimulation as described in [351] including a rise-time constant, T_{rise}, a fall-time constant, T_{fall}, and the excitation time constant, T_e, where $k_1 = T_e * T$, and $k_2 = T_e + T$ for $T = T_{rise}$, if $e > a$ and $T = T_{fall}$, otherwise.

The second adaptive component of this controller is the stimulation adjustment that occurs iteratively, at every gait cycle, based on the root mean squared error of the user. This adaptive component changes the value of parameter γ according to the performance of the patient. As the performance of the patient improves, parameter γ reduces until the patient can perform the task without any assistance. For this, a finite state machine (FSM) is used to differentiate between the swing phase (SW) and stance phase (ST) where different assistive forces may be appropriate. This is defined as:

$$\gamma_{st}^{z+1} = \phi_f \gamma_{st}^{z} + \boldsymbol{\lambda}_f \text{rms}(\Delta \bar{\mathbf{q}}_f)_{st}^{z}, \tag{55}$$

$$\gamma_{sw}^{z+1} = \phi_f \gamma_{sw}^{z} + \boldsymbol{\lambda}_f \text{rms}(\Delta \bar{\mathbf{q}}_f)_{sw}^{z}, \tag{56}$$

$$\lambda_f = (1 - \phi_f), \tag{57}$$

where ϕ_f and $\boldsymbol{\lambda}_f$ are the forgetting and learning factors of the FES ILC (ϕ_f set to 0.95), $\Delta \bar{\mathbf{q}}_f$ is the error for the FES controller normalised by r_{db} (set to 2 degrees) and z is the number of gait cycles performed.

5.2.2 *Adaptive exoskeleton controller*

For the robotic assistance, an adaptive proportional-derivative (PD) controller is used. This is defined as:

$$\boldsymbol{\tau}_e = \mathbf{K}_e \Delta \mathbf{q}_e + \mathbf{B}_e \Delta \dot{\mathbf{q}}_e, \tag{58}$$

$$\mathbf{B}_e = \mathbf{c}_{cr} \sqrt{\mathbf{K}}, \tag{59}$$

where $\mathbf{K}_e$ and $\mathbf{B}_e$ are the stiffness and damping of the exoskeleton's joints, respectively, and $\mathbf{c}_{cr}$ is the matrix of the critical damping coefficients.

Like the FES controller, the exoskeleton controller also uses a FSM in order to adjust the stiffness of the exoskeleton based on the phase in the gait cycle. On every gait cycle, the root mean squared error of the user is recorded and is used to update the exoskeleton's stiffness as follows:

$$\mathbf{K}_{st}^{z+1} = \phi_e \mathbf{K}_{st}^{z} + \boldsymbol{\lambda}_e \mathbf{K}_e^0 \text{rms}(\Delta \bar{\mathbf{q}}_e)_{st}^{z}, \tag{60}$$

$$\mathbf{K}_{sw}^{z+1} = \phi_e \mathbf{K}_{sw}^{z} + \boldsymbol{\lambda}_e \mathbf{K}_e^0 \text{rms}(\Delta \bar{\mathbf{q}}_e)_{sw}^{z}, \tag{61}$$

$$\lambda_e = (1 - \phi_e), \tag{62}$$

where ϕ_e and $\boldsymbol{\lambda}_e$ are the forgetting and the learning factors of the exoskeleton's ILC (ϕ_e set to 0.95), $\Delta \bar{\mathbf{q}}_e$ is the error for the exoskeleton's controller normalised by r_{db} (set to 2 degrees) and $\mathbf{K}_e^0$ is the baseline stiffness (set to 340 Nm/rad [314]).

5.2.3 *Adaptive FES band*

The adaptation of the width of the FES band is designed in order to achieve the collaboration between the robot and the FES. By reducing the width of the FES band according to the fitness level of the muscles, robotic assistance is combined with FES at smaller levels of trajectory tracking error. This ensures that as muscles start to fatigue and lower stimulation intensities are provided to allow the muscle to recover, more assistance from the robot will be provided to maintain a low tracking error. This adaptation of the FES band is implemented as:

$$r_{\text{fesb}} = r_{\text{fesb}}^0 \tilde{\mu}, \tag{63}$$

where $\tilde{\mu}$ is the mean muscle fitness across the stimulated muscles.

5.3 MODELLING

The initial development and testing of the controller was carried out using musculoskeletal modelling. Using OpenSim [151], [352], a generic lower-limb model, *gait1018*, was scaled to the true dimensions of a healthy adult and was

combined with the lower-limb exoskeleton, Exo-H3, as described in section 3.3.2. The dynamics of this human-exoskeleton model can be expressed as:

$$\mathbf{M}_{hr}(\mathbf{q})\ddot{\mathbf{q}} + \mathbf{C}_{hr}(\mathbf{q}, \dot{\mathbf{q}}) + \mathbf{G}_{hr}(\mathbf{q}) = \boldsymbol{\tau}_h + \boldsymbol{\tau}_r + \mathbf{J}(\mathbf{q})^T \mathbf{f}_{\text{ext}}, \tag{64}$$

where $\boldsymbol{\tau}_h \in \mathbb{R}^n$ represents the human's generated joint torques, which include both the voluntarily generated joint torques and the joint torques induced by the FES.

The exoskeleton assistance was simulated using ideal joint actuators while an estimate of the FES-induced torques was obtained based on Hill-type muscle models [157] and the activation dynamics described in section 5.2.2 for the monoarticular muscles of both the hip joint and the knee joint.

5.3.1 *Muscle dynamics*

To approximate the effect of electrical stimulation on muscle activity, a linear model is used:

$$\boldsymbol{\tau}_h = \boldsymbol{\tau}_v + \boldsymbol{\tau}_f, \tag{65}$$

where $\boldsymbol{\tau}_v$ are the voluntarily generated joint torques and $\boldsymbol{\tau}_{\text{fes}}$ are the FES-induced joint torques. An estimate of the voluntary joint torques is obtained using motion capture technology as described in section 3.3.3, while an estimate of the FES-induced torques is obtained based on equations 52-54 and the Millard 2012 equilibrium Hill-type musculotendon models (Figure 42) available in OpenSim [157] which can be expressed as:

$$f^{M*} = f_0^M(a\mathbf{f}^L(\tilde{l}^M)\mathbf{f}^V(\tilde{v}^M) + \mathbf{f}^{PE}(\tilde{l}^M) + \beta\tilde{v}^M)cos\alpha, \tag{66}$$

$$f^M = \begin{cases} f^{M*} & if f^{M*} > 0, \\ 0 & otherwise, \end{cases} \tag{67}$$

$$\tau_f = f^M r_{ma}(q), \tag{68}$$

where f_0^M is the maximum isometric force of the muscle, a is the muscle activation ranging from [0,1], and $\mathbf{f}^L(\tilde{l}^M)$, $\mathbf{f}^V(\tilde{v}^M)$, $\mathbf{f}^{PE}(\tilde{l}^M)$ are the normalised force functions for the muscle's force-length relationship (L), force-velocity relationship (V), and force-length relationship of the passive element (PE),

respectively. The force functions are normalised by f_0^M and the tilde is used to denote velocities, $\tilde{v}$, and muscle lengths, $\tilde{l}$, that are normalised by the maximum muscle velocity, v_{max}^M, and the length of the muscle at the point of maximum force, l_0^M, respectively. β is a damping coefficient and α is the muscle's pennation angle. Given the calculated muscle force, f^M, the joint torques that result from the activation of the muscles are calculated as the product of the muscle force and the moment arm of the joint, r_{ma}, which is a function of the joint angle, q. The force-length and force-velocity relationships are defined to fit the available data sets observed in Figure 43. In the Millard muscle models available in OpenSim, these curves are implemented using Bezier splines to fit the experimental data [157].

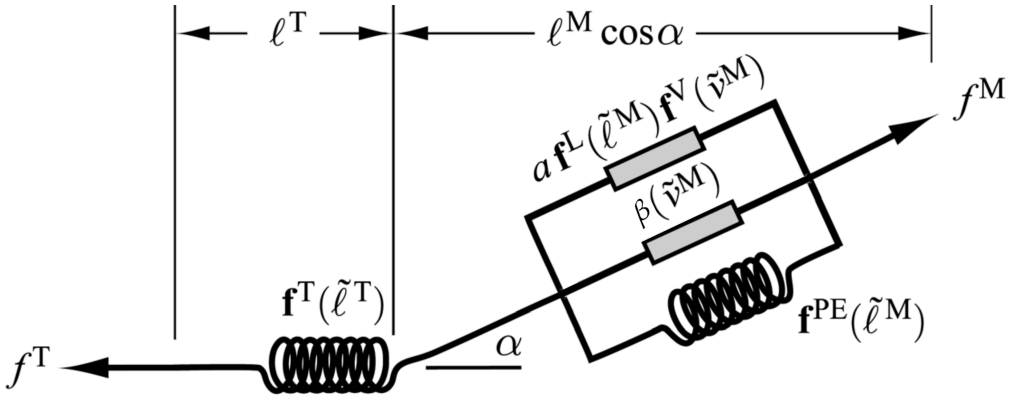

Figure 42: A four element Hill-type model. The contractile element ($= a\mathbf{f}^L(\tilde{l}^M)\mathbf{f}^V(\tilde{v}^M)$) is in parallel with a passive element ($= \mathbf{f}^{PE}(\tilde{l}^M)$) and a damper ($= \beta(\tilde{v}^M)$), which are in series with the tendon unit ($= \mathbf{f}^T(\tilde{l}^T)$) (adapted from [157]).

5.3.2 *Fatigue model identification*

A model-based method was used for the approximation of muscle fatigue as expressed by equations 50-51. To ensure that the estimated fatigue of muscles reflects the fitness level of the participant, a model calibration was carried out as described in [354], [355]. Stimulation signals of variable intensity were used and the force generated by the muscles was measured under isometric conditions. For this, the feet of the participant were placed in contact with a heavy (immovable) box and the generated muscle force (contact force) was measured using the treadmill's force sensors (Figure 44). A symmetric biphasic signal with constant stimulation frequency of 25 Hz and current amplitude of 25 mA was used. Firstly, to identify the threshold stimulation intensity, u_{thr},

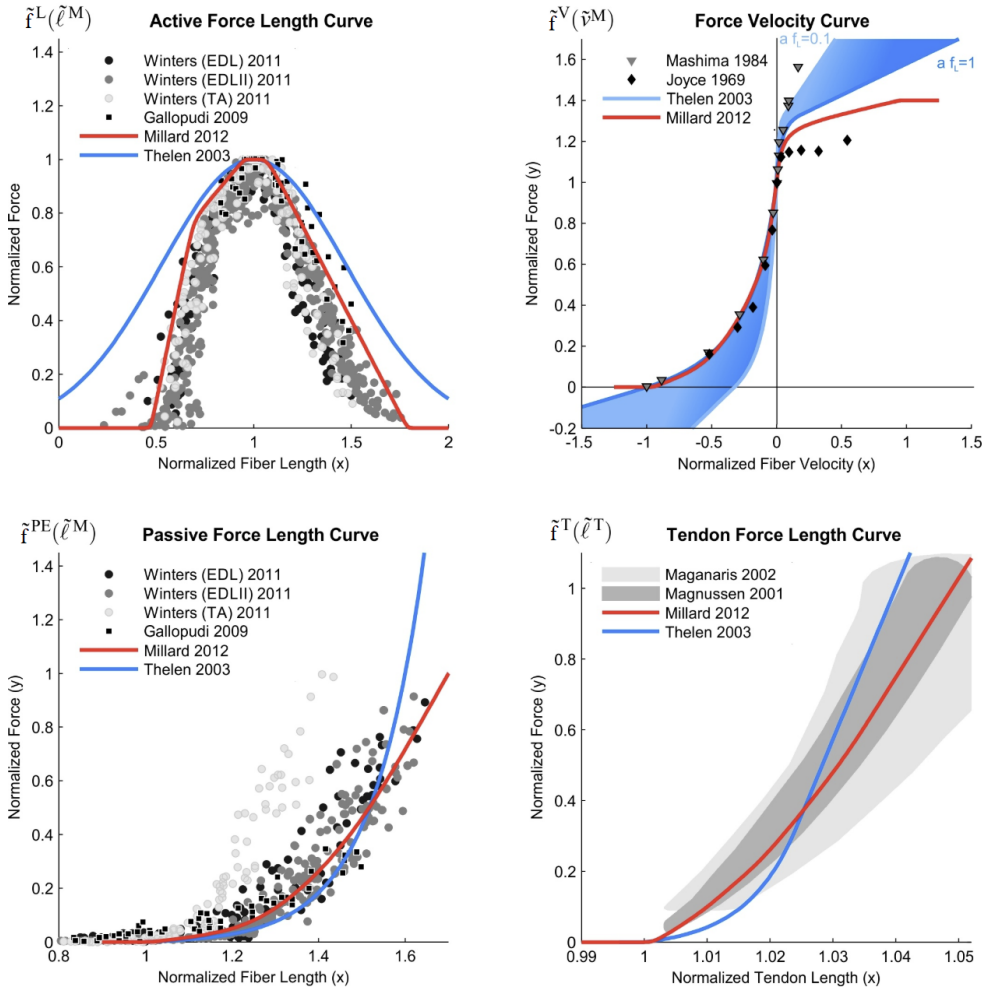

Figure 43: Characteristic curve values for the muscles' force-length relationship, force-velocity relationship, force-length relationship of the passive element and force-length relationship of tendons (extracted from [353]).

and the saturation intensity, u_{sat}, a series of signals were delivered at 50 μs increments until a pulse width of 800 μs was reached. The signal duration was set to 4 s, with a resting period of 20 s. A fatigue test was then carried out using a continuous signal at the saturation intensity for 180 s, followed by a 2-minute recovery test which included pulses of 1 s, with a between-pulse rest of 10 s (Figure 44). The identification of the model parameters was carried out using MATLAB's optimisation tool *fmincon*. The identified parameters are presented in Table 3.

Table 3: Identified parameters for muscle fatigue model.

		$u_{thr}(\mu s)$	$u_{sat}(\mu s)$	$T_{fat}(s)$	$T_{rec}(s)$	$T_{rise}(s)$	$T_{fall}(s)$	$T_e(s)$	μ_{min}	β
Right	Quadriceps	100	700	57.01	59.87	0.2071	0.1370	0	0.07	0.0747
	Hamstring	250	600	64.34	65.27	0.2440	0.0829	0.06	0.13	0.1493
Left	Quadriceps	200	600	36.05	69.56	0.1428	0.2533	0	0.17	0.2453
	Hamstring	250	550	44.58	105.19	0.1963	0.1797	0.002	0.14	0.2347

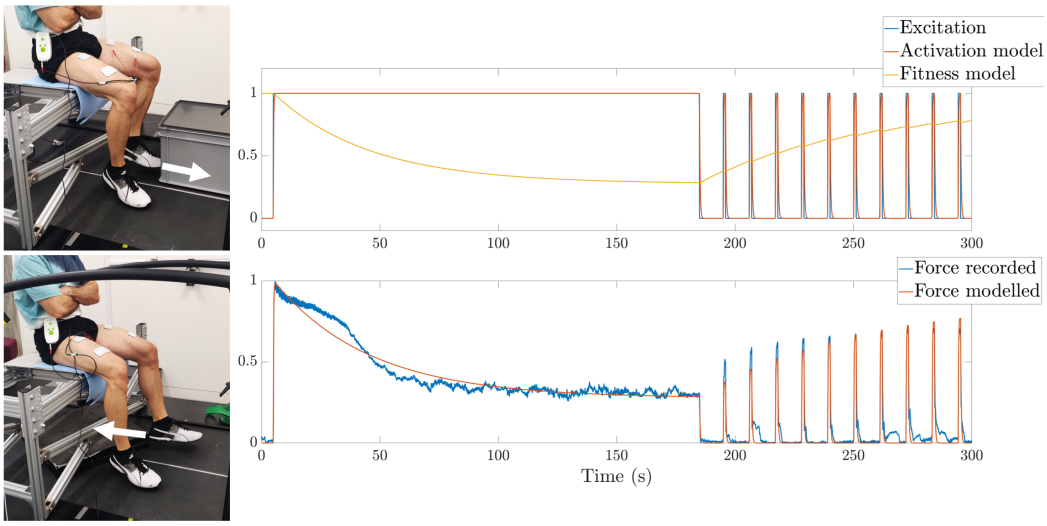

Figure 44: Identification of fatigue model for the quadriceps and the hamstrings using a high-intensity stimulation profile.

5.4 CONTROLLER VALIDATION

5.4.1 *Subject*

The effectiveness of the HAPC was tested both in simulation and experimentally on one healthy volunteer (male, age = 30, weight = 80 kg). The experimental pipeline was approved by the University of Edinburgh, School of Informatics Ethics Committee (ID 2021/46920) and the participant provided written consent.

5.4.2 *Hardware*

The RehaMove3 stimulator (Hasomed, Germany) was used to provide FES using rectangular surface electrodes (5x9 cm). The instrumented treadmill M-Gait (Motek Medical, Netherlands) was used to facilitate the fatigue model identification (section 5.3.2) and to enable self-paced gait during the experiment. The exoskeleton Exo-H3 (Technaid, Spain) was used to provide assistance

during the task and the exoskeleton's joint position sensors were used to record the joint angle of the legs and provide visual feedback to the user (Figure 39c). Simulink Desktop Real Time was used for the real-time control of the exoskeleton and FES at 100 Hz (see sections 2.3.1 and 2.6 for more details about the hardware).

5.4.3 *Simulation setup*

To observe the controller's response to a changing human behaviour, simulations were carried out with two different inputs for the human controls. For the first half of the simulation, a behaviour that corresponds to a high-error trajectory was used as illustrated in Figure 45a. This trajectory is an example of poor performance where exaggerated knee flexion and hip flexion can be observed during the late swing phase. For the second half, a behaviour that corresponds to a low-error trajectory was used as illustrated in Figure 45b. This trajectory is an example of accurate trajectory tracking where lower assistive forces are expected. These trajectories were obtained from our previous study described in section 3.4.4. Using these model controls, a comparison was carried out between the HAPC, its non adaptive equivalent (HPC), and the exoskeleton-only (EPC) and FES-only controllers (FPC). In all cases, 64 cycles were simulated, for which the root-mean-squared (RMS) error, root-mean-squared (RMS) of the assistance and mean fatigue were used for comparison.

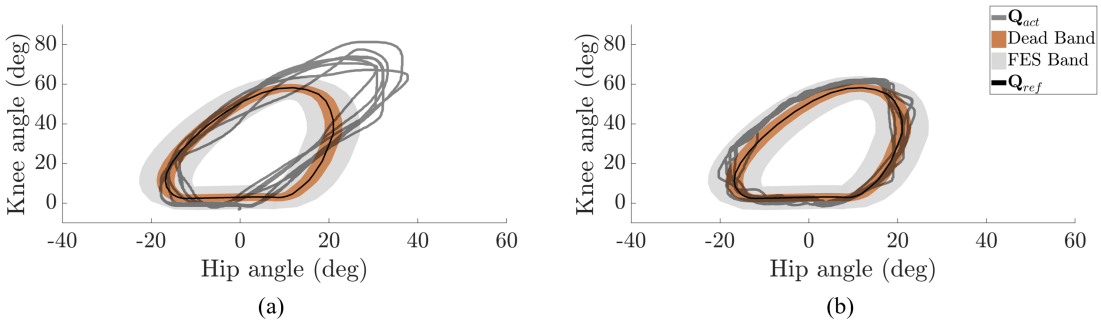

Figure 45: Trajectories used for human behaviour estimation for forward dynamics simulations.

5.4.4 *Experimental Setup*

During the experimental validation of the controller, the participant was fitted with the exoskeleton and was asked to walk at their preferred speed in order to follow the reference path as accurately as possible. Two 10-minute recordings were performed with the aid of visual feedback; one while using the HAPC and one while using the HPC. The participant was blinded to the experimental conditions, meaning they were unaware of which specific controller was tested during each trial to prevent any potential bias in their responses. The non-adaptive controller was tested first and a 5-minute break between trials was included. Hybrid assistance was provided only for the muscles of the knee joint while for the hip joint only robotic assistance was provided (surface electrodes were placed at the quadriceps and hamstrings as shown in Figure 39b). The position of the ankles was adjusted according to the relative position in the gait cycle. The participant's ability to follow the reference path, the assistance they received from both the FES and the robot, and their estimated muscle fatigue were quantified. The sum of these parameters was also calculated in order to evaluate the controller's ability to provide assistance as needed and prevent muscle fatigue. To facilitate the comparison between controllers, the results were normalised such that the costs for the HAPC are equal to 1.

5.5 RESULTS

5.5.1 *Simulation results*

Figure 46 shows the controller's response to the simulated human behaviour described in section 5.4.3. It can be seen that for the first half of the simulation (indicated by a grey dotted line) the adaptive controller results in a reduction in exoskeleton stiffness, exoskeleton assistance (Figure 46a), and FES stiffness through the adaptation of parameter γ (Figure 46b), while the trajectory error follows a periodic pattern (Figure 46b) and muscle fatigue slowly increases (Figure 46c). For the second half of the simulation, the improved performance of the model reduces both the tracking error (Figure 46b) as well as the assistance received from the exoskeleton (Figure 46a) and the FES (Figure 46b-c), which allows the muscles to recover (Figure 46c). In Figure 46b, the

decreasing value of parameter γ, for the hip during stance and for the knee during swing and stance, shows that the root-mean-squared (RMS) values of the trajectory tracking error for FES was kept below 1. For the hip trajectory during swing, the value of parameter γ can be seen to be capped at 1 for the first half of the simulation, which indicates that the root-mean-squared (RMS) value of the trajectory error is higher than 1. It is interesting to note that even though the muscles' fitness level drops during the first half of the simulation, the assistance provided by the exoskeleton for both joints seems to decrease in magnitude. This decrease in the provided assistance combined with a decrease in the trajectory tracking error which is seen in Figure 46b, implies an increased ability to provide assistance as needed due to the controller's adaptation. This is also evident by how the controller adapts to provide less stimulation and less exoskeleton assistance when the human behaviour improves during the second half of the simulation.

In Figure 47 the performance of four different controllers is compared in response to the simulated human behaviour described in section 5.4.3. It can be seen that, compared to the HAPC, the EPC provides almost six times as much robotic assistance to keep the trajectory error lower, while the FPC results in higher trajectory error, higher stimulation intensity and more muscle fatigue than the HAPC. When comparing the HAPC to the HPC, a visible reduction in robotic assistance is observed, while the rest of the parameters are affected less. This indicates that the hybridisation of robotic assistance and FES in this hierarchical order, and the controller's adaptation, provide a substantial reduction in the assistance provided to the user (at the expense of a higher tracking error when compared to the EPC), which overall reduces the sum of error, assistance and muscle fatigue, and implies an improved ability to provide assistance as needed.

5.5.2 *Experimental results*

Figure 48 shows the response of the HAPC to the recorded human behaviour and Figure 49 provides a comparison between the HAPC and its equivalent non adaptive controller (HPC). Based on the results presented in Figure 48a it is evident that due to the controller's adaptation the exoskeleton's stiffness converged towards a lower value than the baseline stiffness for both the hips

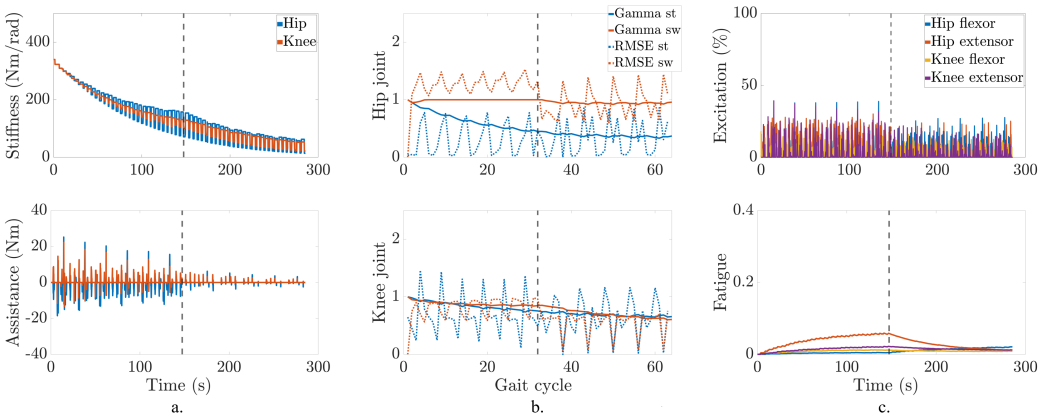

Figure 46: Simulated response of the hybrid controller during poor model performance (before grey dotted line) and more accurate performance (after grey dotted line). (a) Shows the robot stiffness and robot assistance for the hip joint and the knee joint, (b) the trajectory error and adaptation of parameter γ, for the hip joint and the knee joint and (c) the stimulation provided with the adaptive controller and its effect on muscle fatigue.

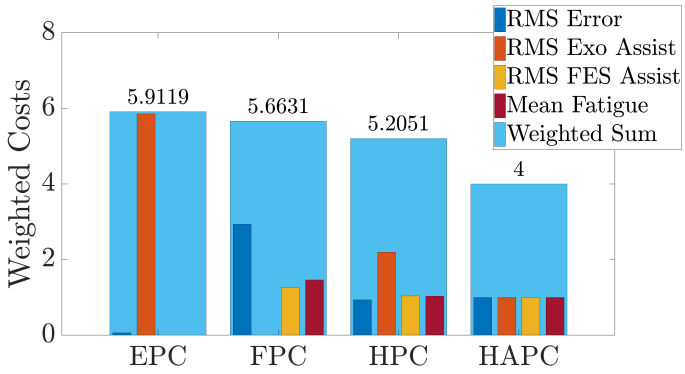

Figure 47: Comparison of the normalised trajectory error, robotic assistance, FES, and muscle fatigue between the exoskeleton-only controller (EPC), the FES-only controller (FPC), the hybrid controller (HPC) and the hybrid adaptive controller (HAPC).

and the knees[1]. This decrease in exoskeleton stiffness was also reflected in the assistance provided by the robot (Figure 48a). It is also evident that the exoskeleton stiffness of the knee joint converged to a smaller value than the exoskeleton stiffness of the hip joint (Figure 48a), which could be indicative of the cooperation between the robot and the FES. Similarly, a reduction in parameter γ is observed, which reduces the stiffness of the FES controller (Figure 48b). This is also reflected in the stimulation provided by the adaptive controller to the knee (Figure 48c). As a result, a decreased muscle fatigue is observed (Figure 49), which for the left leg was more pronounced for the knee

1 Results are shown for the left leg only as the results for the right leg follow similar patterns.

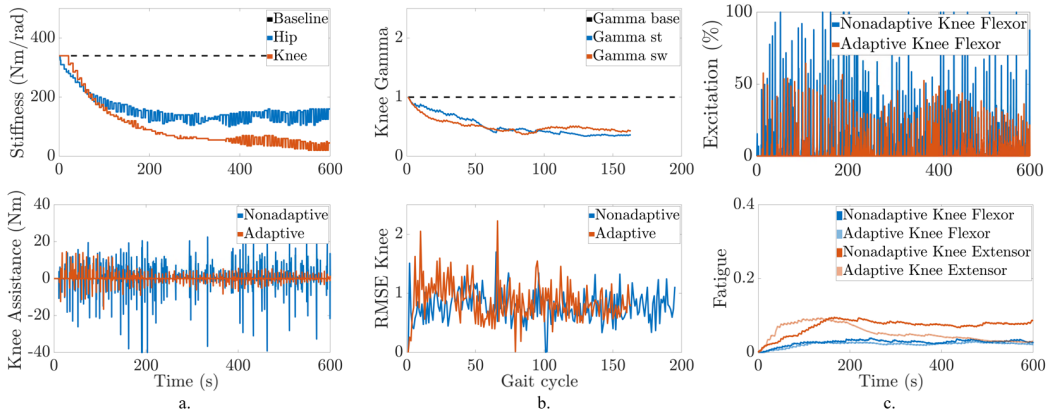

Figure 48: Experimental response of a healthy subject while using the HAPC. Comparison between (a) the robot stiffness and robot assistance, (b) FES controller adaptation and trajectory error, and (c) stimulation provided and resultant muscle fatigue when the adaptive and non adaptive controllers were used.

extensor muscles (Figure 48c). Meanwhile, the trajectory tracking error of the knee joint seems to vary only slightly (Figure 48b).

It can be seen from Figure 49, that the sum of tracking error, assistance received and muscle fatigue, is smaller when the HAPC was used for both joints for both legs. For the hip joint, an average reduction of 49% was recorded in the assistance provided by the exoskeleton across both legs, while the trajectory tracking error was higher by an average of 10% across both legs when the HAPC was used. Similarly, for the knee joint, lower assistive forces were recorded from both the exoskeleton and the FES. The exoskeleton assistance was found to be an average of 58% lower when the HAPC was used and the FES intensity was also lower by an average of 16% across both legs. On the other hand, the tracking error was higher by 8% for the left leg but lower by 8% for the right leg when the HAPC was used. At the same time, the estimated fatigue of the knee muscles was reduced by an average of 37% when the HAPC was used. This noticeable reduction in assistance and muscle fatigue, as compared to the less apparent change in tracking error, indicate the controller's ability to adapt to the user's performance in order to provide assistance as needed and preserve the fitness of the muscles.

5.6 DISCUSSION

The controller's response is verified in a pilot study with a healthy subject. The change in the open parameters of the controller, such as the exoskeleton

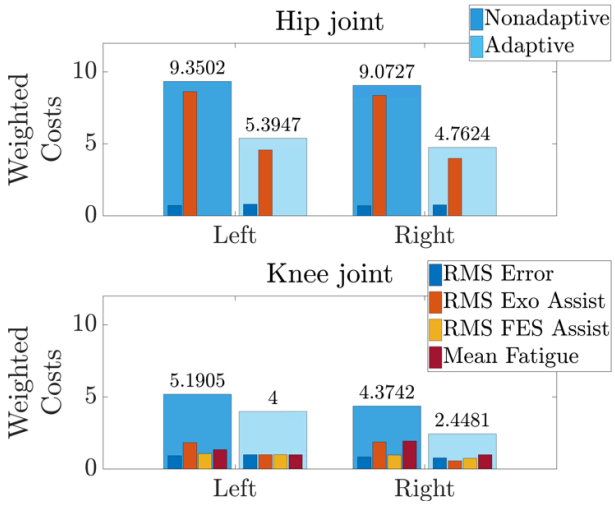

Figure 49: Comparison between the non adaptive and the adaptive controller for the recorded data of the hip and knee joints for both legs (normalised by the data recorded from the left knee joint during the adaptive control).

stiffness and the stiffness of the FES controller, are observed, as well as their effect on the provided assistance and the resultant tracking error of the participant. It was observed, that when the adaptive controller was used, the participant received less assistance from the robot and less assistance from the FES compared to the assistance received when the non-adaptive controller was used. This resulted in a delayed onset of muscle fatigue, while there was no obvious difference between the kinematic tracking error in the two experiments. These results support our hypothesis that the proposed HAPC could potentially provide assistance as needed and delay the onset of muscle fatigue. However, due to the limited number of participants, the statistical power of our analysis is insufficient to draw conclusive support for this hypothesis, and a larger experimental study is required.

Another limitation of our study is the estimation of muscle fatigue. Due to the increased complexity involved with the measurement of muscle fatigue in the presence of both voluntary muscle contractions and electrical stimulation, a model-based estimation of muscle fatigue was used. This model was originally proposed based on experimental data from patients with paraplegia [247], [354], [356]. Here it is assumed that voluntary muscle contractions will not significantly affect the fitness of the muscles or the reliability of the model. Due to the hybridisation of FES and robotic assistance, this assumption is not expected to compromise the safety of the proposed controller or its ability to provide assistance as needed. It may, however, lead to an under-estimation of

muscle fatigue, which may reduce the effectiveness of the assistance provided by the FES, and increase the reliance of the user on the robot. Methods for estimating muscle fatigue using electromyography (EMG) and force sensing have been proposed, but have been tested mostly under isometric conditions [357]–[359]. Accurately measuring muscle fatigue during gait in the presence of both voluntary contractions and functional electrical stimulation remains a challenge. Advancements in this field will improve our understanding of the interactions between FES and voluntary motion, and further improve the effectiveness of our controller.

5.7 CONCLUSION

To conclude, here we presented a hybrid adaptive controller that prioritises the voluntary human contributions and addresses muscle fatigue in a continuous and preventive fashion. This controller is designed to provide assistance as needed in order to encourage the active participation of the user, and preserve muscle fitness in order to prevent discomfort and the premature termination of rehabilitation. It is shown that the controller is able to adapt to the user's movement, and adjust the levels of assistance provided by the robot and the FES in order to maintain an accurate tracking of the desired trajectory and preserve muscle fitness. These encouraging results indicate that the controller's hierarchical structure and adaptive components may be able to provide personalised assistance and prevent muscle fatigue which can be further investigated in the future, in a larger experimental study, including people with neurological disorders.

6

SUMMARY & FUTURE WORK

6.1 SUMMARY

In this thesis, we delve into the exciting intersection of neuroscience, robotics, and rehabilitation. We learn from pioneering research in neuroscience how our nervous system adapts to external stimuli, and we transfer this knowledge to robot-assisted gait training. With a focus on the rehabilitation of ambulatory patients, who retain voluntary control of their lower limbs, we explore methods for the personalisation of robot-assisted training to promote neuroplasticity and enhance the functional outcomes of therapy. Through a series of experiments, we investigate methods for the design of personalised robotic controllers which can be used to encourage the active participation of neurological patients and provide assistance as needed.

Our first study showcased a methodology for the offline design and tuning of robotic controllers using musculoskeletal models. We proposed that by observing the human through the lenses of motion-capture systems, we can construct a personalised model of the human and the wearable device, estimate the effect of external forces on the dynamics of the combined system, and identify the control parameters and/or control structure that will support the human in an optimal way. We were able to show that for each human and their respective kinematics when performing a task, we can obtain a set of individualised controller parameters using offline model-based optimisation, which are expected to significantly increase their performance and reduce the assistance received by the robot. In a subsequent experimental study with eighteen healthy participants, we performed a comparison between the performance of the participants with their personalised parameters and their performance with a baseline set of parameters, which were common across all participants. We observed that this expected improvement in the performance of the participants, as well as the expected reduction in the assistance received by the robot, was not uniform across all participants. Six participants performed better when their personalised parameters were used, seven participants had

no obvious change, and five participants performed worse. High interpersonal and intra-personal variability was observed, potentially originating from modelling inaccuracies, and/or variations in concentration levels, muscle fatigue and motor learning. This highlighted some of the challenges involved with the modelling of such a complex, adaptive, multi-dimensional system and emphasised the need for methods that can capture these subject-specific, time-dependent adaptations at a higher frequency.

This led to our next study, where we explored the potential of optimising robotic controllers to provide assistance as needed using human-in-the-loop optimisation (HILO), which relies a lot less on modelling assumptions. HILO techniques have shown great promise in the field of human augmentation where the objective involves the minimisation of the user's metabolic cost, but their effectiveness in minimising objectives that may be more applicable to rehabilitation have not been explored. Following a continuous optimisation approach over a multi-day experiment using the Covariance Matrix Adaptation Evolution Strategy (CMA-ES), we observed a convergence of the evolutionary strategy towards a unique set of control parameters in six healthy subjects. However, due to high variability in human behaviour, and the small number of participants in our experiment, the measured effect of HILO on the performance of the participants when an assistive rule-based controller is used was not statistically significant. While HILO remains a compelling area to explore further, it suffers from long experimental procedures which are needed to ensure that for each recorded sample, adequate time is provided to allow the human-robot interaction reach steady state. This limits the extent to which HILO can be used, as an increase in the number of decision variables would increase the required experiment duration to reach convergence.

Thus, for our next study, where we considered the addition of neuromuscular electrical stimulation to robot-assisted gait training, we used adaptive control to design a hierarchical controller for the triadic collaboration between human, robot and functional electrical stimulation (FES). While there are several physiological benefits and practical reasons that favour the combination of these two interventions, it remains a major challenge in gait rehabilitation to find the right balance between electrical stimulation and robotic assistance. The challenge lies in ensuring that the user receives adequate support from both the FES and the robot, without overly relying on the robot and without causing undue muscle fatigue with electrical stimulation. In this work, we

implemented a hierarchical control structure which encourages the user to utilise their residual strength, and prioritises assistance from electrical stimulation over robotic assistance. We also used adaptive control to adjust the relative magnitude of the two interventions to achieve the triadic collaboration between human, robot and FES based on the performance of the user and the level of muscle fatigue. In our pilot study with one healthy subject we observed reduced levels of assistance, reduced levels of muscle fatigue and consistent performance when this hierarchical and adaptive configuration was used, as compared to the corresponding non-adaptive controller. These are encouraging results suggesting that the proposed hierarchical adaptive controller may be able to provide personalised assistance as needed, which motivates us to explore this further in a larger experimental study on people with neurological disorders.

These three experimental studies, contribute towards the fine-tuning of collaborative robotic controllers to provide personalised assistance in neurorehabilitation using novel state-of-the-art methodologies. Naturally, this work can be extended to address some of the bottlenecks that were identified and pursue more clinically meaningful results.

6.2 LIMITATIONS & DISCUSSION

In Chapter 3 an offline model-based optimisation pipeline is presented for the design of personalised interventions in gait training. This method capitalises on the advances in musculoskeletal modelling and exploits the power of state-of-the-art modelling platforms that can serve not only as a means of understanding human biomechanics but also as tools for the prototyping and testing of novel interventions. However, even with our increased ability to observe and analyse human motion, our understanding and our ability to model human intention and human response to external forces is limited. This becomes especially hard when, due to experimental protocol, time constraints are imposed that push the limits of computational power and necessitate model reduction. These limitations challenged some of our assumptions regarding the human-robot interactions and proved to be a bottleneck in transferring the benefits of our simulation studies to the real world. With improvements in the computational efficiency in musculoskeletal modelling and with a

better understanding of human-robot interaction dynamics, it is expected that these limitations will be addressed and the benefits of such model-based approaches in the real world will be more attainable. Already, there are several platforms that aim to improve the computational efficiency of musculoskeletal modelling to enable real-time optimal control and facilitate the exploration of learning-based algorithms for the control of wearable robots [360]–[363]. At the same time, pioneering research on the sensing and modelling of voluntary control and neuromuscular stimulation is carried out which will contribute to increased precision and will enhance the utility of model-based optimisation [364], [365].

Chapter 4 discusses the use of HILO for the personalisation of robot-assisted gait training (RAGT). This is another method for the personalisation of RAGT that also relies on optimisation. These different optimisation methods provide an alternative to manual controller tuning, which can be a time-consuming process and as a result it is often carried out on one subject, usually one healthy individual, and kept the same for all subjects. Using optimisation, the aim is to provide an effective and clinically meaningful way of tuning robotic controllers to meet the unique needs of patients in order to improve the functional outcomes of training and accelerate recovery. The only caveat is that even when using optimisation, there is a need to make some design choices and tune the hyperparameters, or the weights of the different costs in the objective function. Due to the composition of the objective, where the weighted sum of a number of normalised rehabilitation objectives is considered, controller tuning through optimisation provides a more intuitive way of making adjustments. Yet, it is not clear what the relative importance of the different costs needs to be in order to maximise recovery, and whether this is yet another patient-specific feature.

Lastly, all presented studies have showcased personalised interventions for gait rehabilitation where a kinematic trajectory is provided as the ideal trajectory to be followed. This is motivated by studies that have shown significant improvements in the gait of neurological patients from kinematic trajectory tracking both in joint space and in end-effector space [366]–[371]. However, it is becoming clearer that each patient may require as a reference, a kinematic trajectory that is tailored to their needs [175], [192], [198], [372]–[374]. How such a trajectory can be obtained for each patient is still an open question. In many cases, people have used the kinematics of healthy people as a reference

[189]–[191], but this does not take into account the potentially limited range of motion of certain patients which may be a result of weakness or spasticity. Research efforts on identifying a personalised kinematic trajectory for each patient or adapting a kinematic trajectory on the fly based on the needs of the patient are presented in [192], [198], [372]–[374]. For the implementation of the methods proposed in this thesis on neurological patients, it is imperative that the appropriate kinematic trajectories are used.

That being said, focusing only on the kinematics of selected joints, may as well be a limited view of a more complicated problem, which may need to be analysed both kinematically and dynamically. An alternative that appears to be insightful in characterising gait, is the study of muscle synergies [375]–[377]. Yet, what constitutes a good reference in terms of muscle synergies to aim for, in the rehabilitation of patients with different levels of neural degeneration, is hard to define. Also, it is not clear what the optimum strategy for progressively improving muscle synergies would be, or how the inertia of wearable robots may affect muscle synergies.

6.3 FUTURE WORK

The immediate steps that follow this work is the extension of the experimental studies that have been presented in Chapters 4 and 5. This includes, the application of the CMA-ES and the hybrid adaptive controller on a larger cohort of healthy subjects and neurological patients to verify that the proposed methods can provide assistance as needed and promote the triadic human-robot-FES collaboration, respectively. Moreover, it is of interest to exploit some of the synergies in our approaches such as the combination of HILO with model-based optimisation, and also address some of the bottlenecks encountered in Chapter 3 to facilitate the utility of offline model-based optimisation.

Optimising surrogate controllers online

One limitation of HILO is the limited samples that can be obtained for convergence in a given time frame. Especially in the case where the aim is to reduce the metabolic cost of locomotion, an average of two minutes per sample are commonly allocated to reach metabolic equilibrium and obtain repres-

entative estimates of energy expenditure. This implies that over an hour of walking, HILO is expected to reach convergence with approximately 30 samples. Consequently, a smart sampling process is required that will speed up the process. An integration of HILO with offline model-based optimisation could facilitate a more accurate approximation of human motion strategies and faster convergence.

Using offline model-based optimisation in parallel with human-in-the-loop (HIL) experiments, could provide evolutionary algorithms such as the CMA-ES with more confidence during exploration. The challenge in this case will be to minimise modelling uncertainties over time using the experimental readings to ensure that the two processes converge to the same point. Experimental readings of the human's response to different levels of assistance can be used to capture time-dependent changes in human motor control and facilitate a more accurate representation of the human model and the human-robot interactions.

Learning personalised human motion strategies

To accurately capture the dynamics of human-robot interaction, it is necessary to better understand the human behaviour and the human adaptation to external assistive forces. In Chapter 3 we implemented a feedforward controller to model human behaviour based on the data obtained from motion capture, and discussed how a more adaptive model could be constructed using inverse optimal control. Even though inverse optimal control is computationally expensive, and relies on the assumption that human locomotion can be described as a multi-objective optimisation problem, constructing personalised models of human motion strategies during gait can be extremely useful in prototyping and optimising personalised interventions that may be applicable to rehabilitation or even human augmentation.

Future work can exploit the power of personalised models obtained through inverse optimal control and can elaborate on the presented model-based optimisation method. This will likely require substantial improvements in the computational efficiency of both offline optimisation and inverse optimal control, and will need an objective function that can reliably capture the

kinematic and dynamic patterns of both healthy gait, pathological gait and robot-assisted gait.

Hybrid systems and soft wearables

In robot-assisted rehabilitation, the selection of the robot can affect the dynamics of gait [378], [379] and can potentially impact the effectiveness of rehabilitation. Ideally, a lightweight robot is preferred as it minimally obstructs the patient's natural motion. However, a lightweight robot often comes with the trade-off of reduced power, which can pose a challenge in RAGT. This type of training frequently necessitates a more powerful device capable of adequately supporting patients with weakened or paralysed muscles. The balance between robot weight and power is crucial, as an overly cumbersome robot can hinder the patient's movement, while an underpowered robot may fail to provide the necessary support.

However, especially when focusing on the rehabilitation of patients who retain voluntary control of their limbs, the use of hybrid robot-FES systems can offer a solution to this dilemma. These systems combine robotic assistance with electrical stimulation, resulting in actuation redundancy. On the one hand this can make control harder, but on the other hand this dual support system allows the use of a lighter, less powerful robot without compromising the efficacy of gait training. The incorporation of soft wearable devices within hybrid systems can further enhance comfort and compliance, offering a promising avenue for more effective and user-friendly rehabilitation.

Reinforcement learning in neurorehabilitation

Another potential path for further investigation is the use of reinforcement learning for the control of wearable robots in neurorehabilitation. While machine learning techniques have been used for the classification of human intention and the intuitive control of wearable lower-limb and upper-limb devices [380]–[383], a more recent application involves the use of reinforcement learning (RL). Coser et al. [384] provide a review of AI-based methodologies that have been applied to exoskeleton-assisted locomotion for either robot control, locomotion classification, intention detection, or joint trajectory prediction.

It is evident that the majority of AI-based methods that have focused on robot control have relied on reinforcement learning.

Both model-based and model-free RL algorithms are being explored in robot-assisted locomotion but not many have investigated the utility of these algorithms in enhancing the collaboration between human and robot, and promoting patient-driven therapy. The model-based approach adopted by Luo et al. [362] to reduce the metabolic cost of locomotion using musculoskeletal modelling is an appealing concept which could be adapted to the assist-as-needed protocols presented here to obtain personalised policies for RAGT. Similarly, the use of model-free methods like the ones described in [385]–[388] could provide viable alternatives to model-based optimisation and HILO for the tuning of adaptive controllers and the design of personalised assistive policies. Yet again, in many cases these approaches seem to suffer from the need of a large amount of data and computational power that make their application to the real world more challenging.

A

APPENDIX A: MODEL SCALING USING MOTION CAPTURE

Model scaling in the context of musculoskeletal modelling is the process of adapting a generic or template musculoskeletal model to match the specific anatomical characteristics of an individual. Musculoskeletal models are often based on averaged data found in the literature, but individuals vary significantly in terms of body size, weight, limb lengths, and other anatomical features. Scaling the model ensures that it more accurately represents the specific person being studied or analysed.

OpenSim offers a Scaling Tool to carry out this process using the data obtained from motion capture. For this, virtual markers are placed on the unscaled model, on anatomical locations that can be systematically identified on different individuals. The same set of markers, referred to as experimental markers, are then placed on the human and their location is recorded using motion capture (Figure 50).

Once the posture of the human is recorded, OpenSim's Scale Tool can be used to adjust the dimensions of the model, the musculotendon properties of the model, the weight of the model, and the location of the model's markers to match the experimental data. To adjust the dimensions of the model's segments, marker pairs are defined, and scale factors are calculated for each segment. Depending on the marker set, it is possible to either uniformly scale a model's segment based on a single marker pair, or use different marker pairs to independently scale a segment in the x-y-z directions. Similarly, the weight of the model can be adjusted by either uniformly distributing the recorded mass of the human based on the mass distribution of the template model, or by distributing the recorded mass of the human based on the calculated scale factors. Then, based on the dimensions of each segment, any length-dependent musculotendon properties, such as optimal fibre length and tendon slack length, are also scaled. However, since muscle strength is not a length-dependent property, it is not scaled and any updates must be carried out manually.

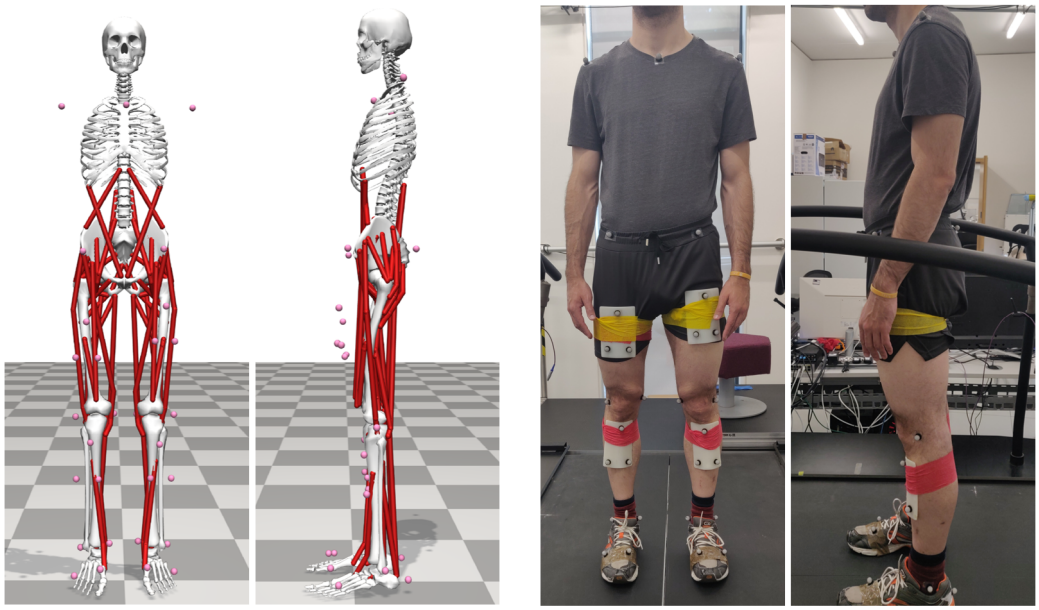

(a) (b)

Figure 50: (a) Front and side view of the musculoskeletal model with the virtual markers. (b) Front and side view of a healthy adult wearing the experimental marker set.

After the model is scaled, OpenSim's Scale Tool offers a Marker Placement process to match the experimental data. A weight can be allocated to each marker and each joint coordinate (if known), and the static pose of the model along with the model's markers are updated using OpenSim's Inverse Kinematics tool (Appendix B) to minimise errors.

B

APPENDIX B: INVERSE KINEMATICS USING OPENSIM

Inverse kinematics in musculoskeletal modelling refers to the process of obtaining joint angles from known marker coordinates. For this, the position of the experimental marker set, $\mathbf{x}^{exp}$, is compared to the position of the virtual marker set, $\mathbf{x}$, and the pose of the model is adjusted to minimise errors. This can be expressed as:

$$\min_{\mathbf{q}} \quad \sum_{i=1}^{N} w_i ||\mathbf{x}_i^{exp} - \mathbf{x}_i(\mathbf{q})||^2 \tag{69}$$

where $\mathbf{q}$ are the generalised coordinates of the model, w are the marker weights, and N is the number of markers.

In the case where estimates of the model's coordinates are available, $\mathbf{q}^{exp}$, this process can be adjusted to minimise both marker errors and coordinate errors. This can be expressed as:

$$\min_{\mathbf{q}} \quad \sum_{i=1}^{N} w_i ||\mathbf{x}_i^{exp} - \mathbf{x}_i(\mathbf{q})||^2 + \sum_{j=1}^{M} \omega_j (q_j^{exp} - q_j)^2 \tag{70}$$

where ω are the coordinate weights and M is the number of coordinates.

The same pipeline can be used during model scaling, to adjust both the model kinematics and the placement of the virtual markers based on experimental data and the respective weights. This process can be expressed as:

$$\min_{\mathbf{q},\mathbf{x}} \quad \sum_{i=1}^{N} w_i ||\mathbf{x}_i^{exp} - \mathbf{x}_i(\mathbf{q})||^2 + \sum_{j=1}^{M} \omega_j (q_j^{exp} - q_j)^2 \tag{71}$$

where the position of the virtual markers, $\mathbf{x}$, is included in the decision variables.

C

APPENDIX C: RESIDUAL REDUCTION ALGORITHM

The Residual Reduction Algorithm (RRA) available in OpenSim aims to minimise the effects of modelling and marker errors that may lead to large non-physiological compensatory forces, called residuals. To do this, RRA relies on forward dynamics that use a tracking controller to follow the kinematics obtained from the experimental data. During this process, residual forces and moments are applied to the pelvis, to ensure that the model's kinematics are more consistent with the ground reaction forces and/or bushing forces acting on the model. This is formulated as an optimisation problem where the aim is to minimise the model's controls, $\mathbf{x}$, and tracking error:

$$\min_{\mathbf{P}} \quad \sum_{i=1}^{N} x_i^2 + \sum_{j=1}^{M} w_j (\ddot{q}_j^* - \ddot{q}_j)^2 \tag{72}$$

where N is the number of actuators, M represents the model's degrees of freedom (DOFs), $\ddot{q}^*$ are the desired joint accelerations, and w are the acceleration weights. At the end of the simulation, the outputs $\mathbf{P}$ include the resultant joint moments and residual forces, along with an updated mass distribution of the model and updated joint kinematics.

Based on these outputs, the average values of the residual moments in the mediolateral direction and anterior-posterior direction can be used to adjust the torso mass center to minimise errors due to inaccuracies in the mass distribution and geometry of the torso in the model. Similarly, the average residual force applied in the inferior-superior direction can then be used to adjust the overall weight of the model to make it more consistent with the external forces acting on the model.

BIBLIOGRAPHY

[1] 'Incidence and prevalence of parkinson's in the uk', *Parkinson's UK*, 2017. [Online]. Available: https://www.parkinsons.org.uk/sites/default/files/2018-01/Prevalence%20%20Incidence%20Report%20Latest_Public_2.pdf (cit. on p. 1).

[2] 'Scottish stroke statistics', *Information Services Division - NHS Scotland*, p. 9, January 2019. [Online]. Available: https://webarchive.nrscotland.gov.uk/20200502171035mp_/https://beta.isdscotland.org/media/1269/2019-01-29-stroke-report.pdf (cit. on p. 1).

[3] 'Scottish multiple sclerosis register - national report 2018', *Information Services Division - NHS Scotland*, 2018. [Online]. Available: http://www.msr.scot.nhs.uk/Reports/Main.html (cit. on p. 1).

[4] E. J. McCaughey, M. Purcell, A. N. Mclean, M. H. Fraser, A. Bewick, R. J. Borotkanics and D. B. Allan, 'Changing demographics of spinal cord injury over a 20-year period: A longitudinal population-based study in scotland', *Spinal Cord*, vol. 54, pp. 270–276, 4 2016, ISSN: 14765624. DOI: 10.1038/sc.2015.167 (cit. on p. 1).

[5] E. Kirk-Wade, *Uk disability statistics: Prevalence and life experiences*, 2022. [Online]. Available: https://commonslibrary.parliament.uk/research-briefings/cbp-9602/ (cit. on p. 1).

[6] M. Zhang, Z. Liang, Y. Li, J. Meng, X. Jiang, B. Xu, H. Li and T. Liu, 'The effect of balance and gait training on specific balance abilities of survivors with stroke: A systematic review and network meta-analysis', *Frontiers in Neurology*, vol. 14, Nov. 2023, ISSN: 1664-2295. DOI: 10.3389/fneur.2023.1234017 (cit. on pp. 1, 23, 24).

[7] S. M. Hatem, G. Saussez, M. della Faille, V. Prist, X. Zhang, D. Dispa and Y. Bleyenheuft, 'Rehabilitation of motor function after stroke: A multiple systematic review focused on techniques to stimulate upper extremity recovery', *Frontiers in Human Neuroscience*, vol. 10, pp. 1–22,

SEP2016 2016, ISSN: 16625161. DOI: 10.3389/fnhum.2016.00442 (cit. on p. 1).

[8] G. Kwakkel, B. Kollen and E. Lindeman, 'Understanding the pattern of functional recovery after stroke: Facts and theories', *Restorative Neurology and Neuroscience*, vol. 22, pp. 281–299, 2004 (cit. on p. 1).

[9] P. Langhorne and P. Duncan, 'Does the organization of postacute stroke care really matter?', *Stroke*, vol. 32, pp. 268–274, 2001 (cit. on p. 1).

[10] T. Patathong, K. Klaewkasikum, P. Woratanarat, S. Rattanasiri, T. Anothaisintawee, T. Woratanarat and A. Thakkinstian, 'The efficacy of gait rehabilitations for the treatment of incomplete spinal cord injury: A systematic review and network meta-analysis', *Journal of Orthopaedic Surgery and Research*, vol. 18, 1 Dec. 2023, ISSN: 1749799X. DOI: 10.1186/s13018-022-03459-w (cit. on p. 1).

[11] G. L. Rosa, M. Avola, T. D. Gregorio, R. S. Calabrò and M. P. Onesta, 'Gait recovery in spinal cord injury: A systematic review with metanalysis involving new rehabilitative technologies', *Brain Sciences*, vol. 13, 5 May 2023, ISSN: 20763425. DOI: 10.3390/brainsci13050703 (cit. on p. 1).

[12] P. J. Reier, D. R. Howland, G. Mitchell, J. R. Wolpaw, D. Hoh and M. A. Lane, 'Spinal cord injury: Repair, plasticity and rehabilitation', in John Wiley & Sons, Ltd, Mar. 2017, pp. 1–12, ISBN: 9780470015902. DOI: 10.1002/9780470015902.a0021403.pub2 (cit. on p. 1).

[13] T. Lam, J. Eng, D. Wolfe, J. Hsieh and M. Whittaker, 'A systematic review of the efficacy of gait rehabilitation strategies for spinal cord injury', *Topics in Spinal Cord Injury Rehabilitation*, vol. 13, pp. 32–57, 1 2007, ISSN: 1082-0744. DOI: 10.1310/sci1301-32 (cit. on p. 1).

[14] A. Barrett, M. Oh-Park, P. Chen and N. L. Ifejika, 'Neurorehabilitation', *Neurology Clinical Practice*, vol. 3, pp. 484–492, 6 Dec. 2013, ISSN: 2163-0402. DOI: 10.1212/01.CPJ.0000437088.98407.fa (cit. on p. 1).

[15] A. Pollock, G. Baer, V. M. Pomeroy and P. Langhorne, 'Physiotherapy treatment approaches for the recovery of postural control and lower

limb function following stroke', in A. Pollock, Ed. John Wiley & Sons, Ltd, Jan. 2007. DOI: 10.1002/14651858.CD001920.pub2 (cit. on p. 1).

[16] Y. Wang, P. Zhang and C. Li, 'Systematic review and network meta-analysis of robot-assisted gait training on lower limb function in patients with cerebral palsy', *Neurological Sciences*, vol. 44, pp. 3863–3875, 11 Nov. 2023, ISSN: 1590-1874. DOI: 10.1007/s10072-023-06964-w (cit. on p. 1).

[17] C. Corrini, E. Gervasoni, G. Perini, C. Cosentino, M. Putzolu, A. Montesano, E. Pelosin, L. Prosperini and D. Cattaneo, 'Mobility and balance rehabilitation in multiple sclerosis: A systematic review and dose-response meta-analysis', *Multiple Sclerosis and Related Disorders*, vol. 69, p. 104 424, Jan. 2023, ISSN: 22110348. DOI: 10.1016/j.msard.2022.104424 (cit. on p. 1).

[18] C. A. Sîrbu, D.-C. Thompson, F. C. Plesa, T. M. Vasile, D. C. Jianu, M. Mitrica, D. Anghel and C. Stefani, 'Neurorehabilitation in multiple sclerosis—a review of present approaches and future considerations', *Journal of Clinical Medicine*, vol. 11, p. 7003, 23 Nov. 2022, ISSN: 2077-0383. DOI: 10.3390/jcm11237003 (cit. on p. 1).

[19] G. Qian, X. Cai, K. Xu, H. Tian, Q. Meng, Z. Ossowski and J. Liang, 'Which gait training intervention can most effectively improve gait ability in patients with cerebral palsy? a systematic review and network meta-analysis', *Frontiers in Neurology*, vol. 13, Jan. 2023, ISSN: 1664-2295. DOI: 10.3389/fneur.2022.1005485 (cit. on pp. 1, 20).

[20] P. Lynch and K. Monaghan, 'Effects of sensory substituted functional training on balance, gait, and functional performance in neurological patient populations: A systematic review and meta-analysis', *Heliyon*, vol. 7, 9 Sep. 2021, ISSN: 24058440. DOI: 10.1016/j.heliyon.2021.e08007 (cit. on p. 1).

[21] G. Kwakkel, C. J. de Goede and E. E. van Wegen, 'Impact of physical therapy for parkinson's disease: A critical review of the literature', *Parkinsonism and Related Disorders*, vol. 13, SUPPL. 3 2007, ISSN: 13538020. DOI: 10.1016/S1353-8020(08)70053-1 (cit. on p. 1).

[22] Z. Gao, Z. Pang, Y. Chen, G. Lei, S. Zhu, G. Li, Y. Shen and W. Xu, 'Restoring after central nervous system injuries: Neural mechanisms and translational applications of motor recovery', *Neuroscience Bulletin*, vol. 38, pp. 1569–1587, 12 Dec. 2022, ISSN: 1673-7067. DOI: 10.1007/s12264-022-00959-x (cit. on pp. 1, 9).

[23] J. M. Cassidy and S. C. Cramer, 'Spontaneous and therapeutic-induced mechanisms of functional recovery after stroke', *Translational Stroke Research*, vol. 8, pp. 33–46, 1 Feb. 2017, ISSN: 1868601X. DOI: 10.1007/s12975-016-0467-5 (cit. on p. 1).

[24] U. Frith, 'Flux of life', *Developmental Cognitive Neuroscience*, vol. 38, p. 100 669, Aug. 2019, ISSN: 18789293. DOI: 10.1016/j.dcn.2019.100669 (cit. on p. 2).

[25] J. A. Kleim and T. A. Jones, 'Principles of experience-dependent neural plasticity: Implications for rehabilitation after brain damage', *Journal of Speech, Language, and Hearing Research*, vol. 51, pp. 225–239, 1 Feb. 2008, ISSN: 1092-4388. DOI: 10.1044/1092-4388(2008/018) (cit. on pp. 2, 9, 10, 24).

[26] M. Maier, B. R. Ballester and P. F. M. J. Verschure, 'Principles of neurorehabilitation after stroke based on motor learning and brain plasticity mechanisms', *Frontiers in Systems Neuroscience*, vol. 13, Dec. 2019, ISSN: 1662-5137. DOI: 10.3389/fnsys.2019.00074 (cit. on pp. 2, 11, 24).

[27] E. Fuchs and G. Flügge, 'Adult neuroplasticity: More than 40 years of research', *Neural Plasticity*, vol. 2014, pp. 1–10, 2014, ISSN: 2090-5904. DOI: 10.1155/2014/541870 (cit. on pp. 2, 7).

[28] R. J. Nudo, 'Recovery after brain injury: Mechanisms and principles', *Frontiers in Human Neuroscience*, vol. 7, DEC Dec. 2013, ISSN: 16625161. DOI: 10.3389/fnhum.2013.00887 (cit. on pp. 2, 9).

[29] Z. Warraich and J. A. Kleim, 'Neural plasticity: The biological substrate for neurorehabilitation', *PM and R*, vol. 2, pp. 208–219, 12 SUPPL 2010, ISSN: 19341482. DOI: 10.1016/j.pmrj.2010.10.016 (cit. on pp. 2, 11).

[30] R. Yamamoto, S. Sasaki, W. Kuwahara, M. Kawakami and F. Kaneko, 'Effect of exoskeleton-assisted body weight-supported treadmill training on gait function for patients with chronic stroke: A scoping review', *Journal of NeuroEngineering and Rehabilitation*, vol. 19, p. 143, 1 Dec. 2022, ISSN: 1743-0003. DOI: 10.1186/s12984-022-01111-6 (cit. on pp. 2, 20).

[31] C. Y. Hsu, Y. H. Cheng, C. H. Lai and Y. N. Lin, 'Clinical non-superiority of technology-assisted gait training with body weight support in patients with subacute stroke: A meta-analysis', *Annals of Physical and Rehabilitation Medicine*, vol. 63, pp. 535–542, 6 Nov. 2020, ISSN: 18770665. DOI: 10.1016/j.rehab.2019.09.009 (cit. on p. 2).

[32] J. Mehrholz, L. A. Harvey, S. Thomas and B. Elsner, 'Is body-weight-supported treadmill training or robotic-assisted gait training superior to overground gait training and other forms of physiotherapy in people with spinal cord injury? a systematic review', *Spinal Cord*, vol. 55, pp. 722–729, 8 Aug. 2017, ISSN: 14765624. DOI: 10.1038/sc.2017.31 (cit. on p. 2).

[33] J. Mehrholz, J. Kugler and M. Pohl, 'Locomotor training for walking after spinal cord injury', *Cochrane Database of Systematic Reviews*, 11 Nov. 2012, ISSN: 14651858. DOI: 10.1002/14651858.CD006676.pub3 (cit. on p. 2).

[34] C. Morawietz and F. Moffat, 'Effects of locomotor training after incomplete spinal cord injury: A systematic review', *Archives of Physical Medicine and Rehabilitation*, vol. 94, pp. 2297–2308, 11 2013, ISSN: 00039993. DOI: 10.1016/j.apmr.2013.06.023 (cit. on p. 2).

[35] M. Alwardat, M. Etoom, S. A. Dajah, T. Schirinzi, G. D. Lazzaro, P. S. Salimei, N. B. Mercuri and A. Pisani, 'Effectiveness of robot-assisted gait training on motor impairments in people with parkinson's disease: A systematic review and meta-analysis', *International Journal of Rehabilitation Research*, vol. 41, pp. 287–296, 4 Dec. 2018, ISSN: 0342-5282. DOI: 10.1097/MRR.0000000000000312 (cit. on p. 2).

[36] S.-W. Yeh, L.-F. Lin, K.-W. Tam, C.-P. Tsai, C.-H. Hong and Y.-C. Kuan, 'Efficacy of robot-assisted gait training in multiple sclerosis: A system-

atic review and meta-analysis', *Multiple Sclerosis and Related Disorders*, vol. 41, p. 102 034, Jun. 2020, ISSN: 22110348. DOI: 10.1016/j.msard.2020.102034 (cit. on pp. 2, 20).

[37] C. J. Hasson, J. Manczurowsky, E. C. Collins and M. Yarossi, 'Neurorehabilitation robotics: How much control should therapists have?', *Frontiers in Human Neuroscience*, vol. 17, 2023, ISSN: 16625161. DOI: 10.3389/fnhum.2023.1179418 (cit. on p. 2).

[38] S. D. Gasperina, L. Roveda, A. Pedrocchi, F. Braghin and M. Gandolla, 'Review on patient-cooperative control strategies for upper-limb rehabilitation exoskeletons', *Frontiers in Robotics and AI*, vol. 8, Dec. 2021, ISSN: 2296-9144. DOI: 10.3389/frobt.2021.745018 (cit. on p. 2).

[39] J. Galvez, G. Kerdanyan, S. Maneekobkunwong, R. Weber, M. Scott, S. Harkema and D. Reinkensmeyer, ''measuring human trainers' skill for the design of better robot control algorithms for gait training after spinal cord injury', IEEE, 2005, pp. 231–234, ISBN: 0-7803-9003-2. DOI: 10.1109/ICORR.2005.1501092 (cit. on p. 2).

[40] 'Gait training', *Epic Physical Therapy Co.*, 2024. [Online]. Available: https://epicptco.com/our-services/gait-training/ (cit. on p. 3).

[41] K. Sirlantzis, L. B. Larsen, L. K. Kanumuru and P. Oprea, 'Robotics', in Elsevier, Jan. 2018, pp. 311–345, ISBN: 9780128124871. DOI: 10.1016/B978-0-12-812487-1.00011-9 (cit. on p. 3).

[42] 'Able exoskeleton', *Exoskeleton Report*, 2024. [Online]. Available: https://exoskeletonreport.com/product/able-exoskeleton/ (cit. on p. 3).

[43] M. R. Rosenzweig, 'Aspects of the search for neural mechanisms of memory', *Annual Review of Psychology*, vol. 47, pp. 1–32, 1 Feb. 1996, ISSN: 0066-4308. DOI: 10.1146/annurev.psych.47.1.1 (cit. on p. 7).

[44] B. de Charles, 'Oeuvres d'histoire naturelle et de philosophie', *Neuchatel: S. Fauche*, 1779 (cit. on p. 7).

[45] H. Scheuerlein, F. Henschke and F. Köckerling, 'Wilhelm von waldeyer-hartz—a great forefather: His contributions to anatomy with particular

attention to "his" fascia', *Frontiers in Surgery*, vol. 4, Dec. 2017, ISSN: 2296-875X. DOI: 10.3389/fsurg.2017.00074 (cit. on p. 7).

[46] S. Finger, 'Santiago ramón y cajal: From nerve nets to neuron doctrine', in Oxford University Press, Mar. 2005, pp. 197–216, ISBN: 9780199865277. DOI: 10.1093/acprof:oso/9780195181821.003.0013 (cit. on p. 7).

[47] J. A. D. Carlos and Z. Molnár, 'Cajal's interactions with sherrington and the croonian lecture', *Anatomical Record*, vol. 303, pp. 1181–1188, 5 May 2020, ISSN: 19328494. DOI: 10.1002/ar.24189 (cit. on p. 7).

[48] C. y Ramon Santiago, 'The croonian lecture - la fine structure des centres nerveux', 1894, pp. 444–468 (cit. on p. 7).

[49] B. G. Cragg, 'Changes in visual cortex on first exposure of rats to light: Effect on synaptic dimensions', *Nature*, vol. 215, pp. 251–253, 5098 Jul. 1967, ISSN: 0028-0836. DOI: 10.1038/215251a0 (cit. on p. 7).

[50] M. C. Diamond, D. Krech and M. R. Rosenzweig, 'The effects of an enriched environment on the histology of the rat cerebral cortex', *Journal of Comparative Neurology*, vol. 123, pp. 111–119, 1 1964, ISSN: 10969861. DOI: 10.1002/cne.901230110 (cit. on p. 7).

[51] A. Globus, M. R. Rosenzweig, E. L. Bennett and M. C. Diamond, 'Effects of differential experience on dendritic spine counts in rat cerebral cortex.', *Journal of Comparative and Physiological Psychology*, vol. 82, pp. 175–181, 2 Feb. 1973, ISSN: 0021-9940. DOI: 10.1037/h0033910 (cit. on p. 7).

[52] R. W. West and W. T. Greenough, 'Effect of environmental complexity on cortical synapses of rats: Preliminary results', *Behavioral Biology*, vol. 7, pp. 279–284, 2 Apr. 1972, ISSN: 00916773. DOI: 10.1016/S0091-6773(72)80207-4 (cit. on p. 7).

[53] R. R. Marchese, A. S. do Pinho, C. Mazutti, K. D. Rech, M. Grzebellus, C. Schäfer, L. G. da Silva and A. de Souza Pagnussat, 'Proprioceptive neuromuscular facilitation induces muscle irradiation to the lower limbs – a cross-sectional study with healthy individuals', *Journal of Bodywork and Movement Therapies*, vol. 27, pp. 440–446, Jul. 2021, ISSN: 15329283. DOI: 10.1016/j.jbmt.2020.12.026 (cit. on p. 8).

[54] S. Hesse, 'Treadmill training with partial body weight support after stroke: A review', *NeuroRehabilitation*, vol. 23, L. Sawaki, Ed., pp. 55–65, 1 Mar. 2008, ISSN: 10538135. DOI: 10.3233/NRE-2008-23106 (cit. on p. 8).

[55] F. B. Wagner, J. B. Mignardot, C. G. L. Goff-Mignardot *et al.*, 'Targeted neurotechnology restores walking in humans with spinal cord injury', *Nature*, vol. 563, pp. 65–93, 7729 2018, ISSN: 14764687. DOI: 10.1038/s41586-018-0649-2 (cit. on p. 9).

[56] A. Shaik and A. Shemjaz, 'The rise of physical therapy: A history in footsteps', *Archives of Medicine and Health Sciences*, vol. 2, p. 257, 2 2014, ISSN: 2321-4848. DOI: 10.4103/2321-4848.144367 (cit. on p. 7).

[57] *Today's physical therapist: A comprehensive review of a 21st-century health care profession*, 2011 (cit. on pp. 7, 8).

[58] M. Moffat, 'The history of physical therapy practice in the united states', *Journal of Physical Therapy Education*, vol. 17, pp. 15–25, 3 2003, ISSN: 0899-1855. DOI: 10.1097/00001416-200310000-00003 (cit. on pp. 7, 8).

[59] J. Carr and R. Shepherd, 'The changing face of neurological rehabilitation', *Revista Brasileira de Fisioterapia*, vol. 10, pp. 147–156, 2 2006, ISSN: 1413-3555. DOI: 10.1590/S1413-35552006000200003 (cit. on pp. 7, 8).

[60] B. Bobath, 'The very early treatment of cerebral palsy', *Develop. Med. Child Neurol.*, vol. 9, pp. 373–390, 1967 (cit. on p. 8).

[61] H. Kabat and M. Knott, 'Proprioceptive facilitation therapy for paralysis', *Physiotherapy*, pp. 8–12, 1954 (cit. on p. 8).

[62] P. R. Surburg and J. W. Schrader, 'Proprioceptive neuromuscular facilitation techniques in sports medicine: A reassessment', *Journal of Athletic Training*, vol. 32, pp. 34–39, 1 1997 (cit. on p. 8).

[63] M. S. Rood, 'Neurophysiological reactions as a basis for physical therapy*', *Physical Therapy*, vol. 34, pp. 444–449, 9 Sep. 1954, ISSN: 0031-9023. DOI: 10.1093/ptj/34.9.444 (cit. on p. 8).

[64] D. H. Hubel and T. N. Wiesel, 'Receptive fields and functional architecture in two nonstriate visual areas (18 and 19) of the cat', *Journal of*

Neurophysiology, vol. 28, pp. 229–289, 2 Mar. 1965, ISSN: 0022-3077. DOI: 10.1152/jn.1965.28.2.229 (cit. on p. 9).

[65] E. Fifková, 'The effect of monocular deprivation on the synaptic contacts of the visual cortex', *Journal of Neurobiology*, vol. 1, pp. 285–294, 3 1969, ISSN: 10974695. DOI: 10.1002/neu.480010304 (cit. on p. 9).

[66] R. A. Reale, J. F. Brugge and J. C. Chan, 'Maps of auditory cortex in cats reared after unilateral cochlear ablation in the neonatal period', *Developmental Brain Research*, vol. 34, pp. 281–290, 2 Aug. 1987, ISSN: 01653806. DOI: 10.1016/0165-3806(87)90215-X (cit. on p. 9).

[67] R. Pascual, M. C. Hervias, M. E. Tohá, A. Valero and H. R. Figueroa, 'Purkinje cell impairment induced by early movement restriction', *Neonatology*, vol. 73, pp. 47–51, 1 1998, ISSN: 1661-7800. DOI: 10.1159/000013959 (cit. on p. 9).

[68] R. Nudo, G. Milliken, W. Jenkins and M. Merzenich, 'Use-dependent alterations of movement representations in primary motor cortex of adult squirrel monkeys', *The Journal of Neuroscience*, vol. 16, pp. 785–807, 2 Jan. 1996, ISSN: 0270-6474. DOI: 10.1523/JNEUROSCI.16-02-00785.1996 (cit. on p. 9).

[69] J. A. Kleim, S. Barbay and R. J. Nudo, 'Functional reorganization of the rat motor cortex following motor skill learning', *Journal of Neurophysiology*, vol. 80, pp. 3321–3325, 6 Dec. 1998, ISSN: 0022-3077. DOI: 10.1152/jn.1998.80.6.3321 (cit. on p. 9).

[70] N. M. Weinberger and J. S. Bakin, 'Learning-induced physiological memory in adult primary auditory cortex: Receptive field plasticity, model, and mechanisms', *Audiology and Neurotology*, vol. 3, pp. 145–167, 2-3 1998, ISSN: 1420-3030. DOI: 10.1159/000013787 (cit. on p. 9).

[71] J. Biernaskie and D. Corbett, 'Enriched rehabilitative training promotes improved forelimb motor function and enhanced dendritic growth after focal ischemic injury', *The Journal of Neuroscience*, vol. 21, pp. 5272–5280, 14 Jul. 2001, ISSN: 0270-6474. DOI: 10.1523/JNEUROSCI.21-14-05272.2001 (cit. on p. 9).

[72] C. Alia, C. Spalletti, S. Lai *et al.*, 'Neuroplastic changes following brain ischemia and their contribution to stroke recovery: Novel approaches in neurorehabilitation', *Frontiers in Cellular Neuroscience*, vol. 11, Mar. 2017, ISSN: 1662-5102. DOI: 10.3389/fncel.2017.00076 (cit. on p. 9).

[73] B. B. Johansson, 'Brain plasticity and stroke rehabilitation', *Stroke*, vol. 31, pp. 223–230, 1 Jan. 2000, ISSN: 0039-2499. DOI: 10.1161/01.STR.31.1.223 (cit. on p. 9).

[74] K. Ganguly and M. ming Poo, 'Activity-dependent neural plasticity from bench to bedside', *Neuron*, vol. 80, pp. 729–741, 3 2013, ISSN: 08966273. DOI: 10.1016/j.neuron.2013.10.028 (cit. on pp. 9, 10).

[75] D. L. Adkins, J. Boychuk, M. S. Remple and J. A. Kleim, 'Motor training induces experience-specific patterns of plasticity across motor cortex and spinal cord', *Journal of Applied Physiology*, vol. 101, pp. 1776–1782, 6 Dec. 2006, ISSN: 8750-7587. DOI: 10.1152/japplphysiol.00515.2006 (cit. on p. 9).

[76] M. A. Perez, B. K. Lungholt, K. Nyborg and J. B. Nielsen, 'Motor skill training induces changes in the excitability of the leg cortical area in healthy humans', *Experimental Brain Research*, vol. 159, pp. 197–205, 2 Nov. 2004, ISSN: 00144819. DOI: 10.1007/s00221-004-1947-5 (cit. on p. 9).

[77] J. A. Kleim, S. Barbay, N. R. Cooper, T. M. Hogg, C. N. Reidel, M. S. Remple and R. J. Nudo, 'Motor learning-dependent synaptogenesis is localized to functionally reorganized motor cortex', *Neurobiology of Learning and Memory*, vol. 77, pp. 63–77, 1 2002, ISSN: 10747427. DOI: 10.1006/nlme.2000.4004 (cit. on p. 9).

[78] M. S. Remple, R. M. Bruneau, P. M. VandenBerg, C. Goertzen and J. A. Kleim, 'Sensitivity of cortical movement representations to motor experience: Evidence that skill learning but not strength training induces cortical reorganization', *Behavioural Brain Research*, vol. 123, pp. 133–141, 2 Sep. 2001, ISSN: 01664328. DOI: 10.1016/S0166-4328(01)00199-1 (cit. on p. 9).

[79] C. D. Wickens, S. Hutchins, T. Carolan and J. Cumming, 'Effectiveness of part-task training and increasing-difficulty training strategies: A meta-analysis approach', *Human Factors*, vol. 55, pp. 461–470, 2 Apr. 2013, ISSN: 00187208. DOI: 10.1177/0018720812451994 (cit. on p. 9).

[80] J. Lisman and N. Spruston, 'Postsynaptic depolarization requirements for ltp and ltd: A critique of spike timing-dependent plasticity', *Nature Neuroscience*, vol. 8, pp. 839–841, 7 Jul. 2005, ISSN: 1097-6256. DOI: 10.1038/nn0705-839 (cit. on p. 9).

[81] M. A. Guadagnoli and T. D. Lee, 'Challenge point: A framework for conceptualizing the effects of various practice conditions in motor learning', *Journal of Motor Behavior*, vol. 36, pp. 212–224, 2 Jul. 2004, ISSN: 0022-2895. DOI: 10.3200/JMBR.36.2.212-224 (cit. on p. 9).

[82] A. Peinemann, B. Reimer, C. Löer, A. Quartarone, A. Münchau, B. Conrad and H. R. Siebner, 'Long-lasting increase in corticospinal excitability after 1800 pulses of subthreshold 5 hz repetitive tms to the primary motor cortex', *Clinical Neurophysiology*, vol. 115, pp. 1519–1526, 7 Jul. 2004, ISSN: 13882457. DOI: 10.1016/j.clinph.2004.02.005 (cit. on p. 9).

[83] E. B. Sandler, K. E. Roach and E. C. Field-Fote, 'Dose-response outcomes associated with different forms of locomotor training in persons with chronic motor-incomplete spinal cord injury', *Journal of Neurotrauma*, vol. 34, pp. 1903–1908, 10 May 2017, ISSN: 0897-7151. DOI: 10.1089/neu.2016.4555 (cit. on p. 9).

[84] C. E. Lang, K. R. Lohse and R. L. Birkenmeier, 'Dose and timing in neurorehabilitation', *Current Opinion in Neurology*, vol. 28, pp. 549–555, 6 Dec. 2015, ISSN: 1350-7540. DOI: 10.1097/WCO.0000000000000256 (cit. on pp. 9, 10).

[85] K. R. Lohse, C. E. Lang and L. A. Boyd, 'Is more better? using metadata to explore dose-response relationships in stroke rehabilitation', *Stroke*, vol. 45, pp. 2053–2058, 7 2014, ISSN: 15244628. DOI: 10.1161/STROKEAHA.114.004695 (cit. on pp. 9, 10).

[86] T. Hornby, D. Straube, C. Kinnaird, C. Holleran, A. Echauz, K. Rodriguez, E. Wagner and E. Narducci, 'Importance of specificity, amount,

and intensity of locomotor training to improve ambulatory function in patients poststroke', *Topics in Stroke Rehabilitation*, vol. 18, pp. 293–307, 4 Jan. 2011, ISSN: 10749357. DOI: 10.1310/tsr1804-293 (cit. on p. 10).

[87] K. A. Leech, R. T. Roemmich, J. Gordon, D. S. Reisman and K. M. Cherry-Allen, 'Updates in motor learning: Implications for physical therapist practice and education', *Physical Therapy*, vol. 102, 1 Jan. 2022, ISSN: 15386724. DOI: 10.1093/ptj/pzab250 (cit. on p. 10).

[88] B. French, L. H. Thomas, J. Coupe, N. E. McMahon, L. Connell, J. Harrison, C. J. Sutton, S. Tishkovskaya and C. L. Watkins, 'Repetitive task training for improving functional ability after stroke', *Cochrane Database of Systematic Reviews*, vol. 2016, 11 Nov. 2016, ISSN: 14651858. DOI: 10.1002/14651858.CD006073.pub3 (cit. on p. 10).

[89] L. Pauwels, S. Chalavi and S. P. Swinnen, 'Aging and brain plasticity', *Aging*, vol. 10, pp. 1789–1790, 8 Aug. 2018, ISSN: 1945-4589. DOI: 10.18632/aging.101514 (cit. on p. 10).

[90] D. C. Park and G. N. Bischof, 'The aging mind: Neuroplasticity in response to cognitive training', *Dialogues in Clinical Neuroscience*, vol. 15, pp. 109–119, 1 Mar. 2013, ISSN: 1958-5969. DOI: 10.31887/DCNS.2013.15.1/dpark (cit. on p. 10).

[91] S. N. Burke and C. A. Barnes, 'Neural plasticity in the ageing brain', *Nature Reviews Neuroscience*, vol. 7, pp. 30–40, 1 Jan. 2006, ISSN: 1471-003X. DOI: 10.1038/nrn1809 (cit. on p. 10).

[92] M. Königs, E. A. Beurskens, L. Snoep, E. J. Scherder and J. Oosterlaan, 'Effects of timing and intensity of neurorehabilitation on functional outcome after traumatic brain injury: A systematic review and meta-analysis', *Archives of Physical Medicine and Rehabilitation*, vol. 99, 1149–1159.e1, 6 Jun. 2018, ISSN: 00039993. DOI: 10.1016/j.apmr.2018.01.013 (cit. on p. 10).

[93] J. Bernhardt, P. Langhorne, R. I. Lindley, A. G. Thrift, F. Ellery, J. Collier, L. Churilov, M. Moodie, H. Dewey and G. Donnan, 'Efficacy and safety of very early mobilisation within 24 h of stroke onset (avert): A randomised controlled trial', *The Lancet*, vol. 386, pp. 46–55, 9988 Jul.

2015, ISSN: 1474547X. DOI: 10.1016/S0140-6736(15)60690-0 (cit. on p. 10).

[94] A. Sundseth, B. Thommessen and O. M. Rønning, 'Outcome after mobilization within 24 hours of acute stroke: A randomized controlled trial', *Stroke*, vol. 43, pp. 2389–2394, 9 Sep. 2012, ISSN: 00392499. DOI: 10.1161/STROKEAHA.111.646687 (cit. on p. 10).

[95] G. S. Griesbach, F. Gomez-Pinilla and D. A. Hovda, 'The upregulation of plasticity-related proteins following tbi is disrupted with acute voluntary exercise', *Brain Research*, vol. 1016, pp. 154–162, 2 Aug. 2004, ISSN: 00068993. DOI: 10.1016/j.brainres.2004.04.079 (cit. on p. 10).

[96] J. Humm, D. A. Kozlowski, S. T. Bland, D. C. James and T. Schallert, 'Use-dependent exaggeration of brain injury: Is glutamate involved?', *Experimental Neurology*, vol. 157, pp. 349–358, 2 Jun. 1999, ISSN: 00144886. DOI: 10.1006/exnr.1999.7061 (cit. on p. 10).

[97] J. Humm, D. A. Kozlowski, D. C. James, J. E. Gotts and T. Schallert, 'Use-dependent exacerbation of brain damage occurs during an early post-lesion vulnerable period', *Brain Research*, vol. 783, pp. 286–292, 2 Feb. 1998, ISSN: 00068993. DOI: 10.1016/S0006-8993(97)01356-5 (cit. on p. 10).

[98] D. A. Kozlowski, D. C. James and T. Schallert, 'Use-dependent exaggeration of neuronal injury after unilateral sensorimotor cortex lesions', *The Journal of Neuroscience*, vol. 16, pp. 4776–4786, 15 Aug. 1996, ISSN: 0270-6474. DOI: 10.1523/JNEUROSCI.16-15-04776.1996 (cit. on p. 10).

[99] L. Speranza, U. di Porzio, D. Viggiano, A. de Donato and F. Volpicelli, 'Dopamine: The neuromodulator of long-term synaptic plasticity, reward and movement control', *Cells*, vol. 10, p. 735, 4 Mar. 2021, ISSN: 2073-4409. DOI: 10.3390/cells10040735 (cit. on p. 10).

[100] Y. Ranjbar-Slamloo and Z. Fazlali, 'Dopamine and noradrenaline in the brain; overlapping or dissociate functions?', *Frontiers in Molecular Neuroscience*, vol. 12, Jan. 2020, ISSN: 16625099. DOI: 10.3389/fnmol.2019.00334 (cit. on p. 10).

[101] A. H. Bazzari and H. R. Parri, 'Neuromodulators and long-term synaptic plasticity in learning and memory: A steered-glutamatergic perspective', *Brain Sciences*, vol. 9, 11 Nov. 2019, ISSN: 20763425. DOI: 10.3390/brainsci9110300 (cit. on p. 10).

[102] K. Tully and V. Y. Bolshakov, 'Emotional enhancement of memory: How norepinephrine enables synaptic plasticity', *Molecular Brain*, vol. 3, p. 15, 1 2010, ISSN: 1756-6606. DOI: 10.1186/1756-6606-3-15 (cit. on p. 10).

[103] M. J. Hylin, A. L. Kerr and R. Holden, 'Understanding the mechanisms of recovery and/or compensation following injury', *Neural Plasticity*, vol. 2017, pp. 1–12, 2017, ISSN: 2090-5904. DOI: 10.1155/2017/7125057 (cit. on p. 11).

[104] N. Takeuchi and S.-I. Izumi, 'Maladaptive plasticity for motor recovery after stroke: Mechanisms and approaches', *Neural Plasticity*, vol. 2012, pp. 1–9, 2012, ISSN: 2090-5904. DOI: 10.1155/2012/359728 (cit. on p. 11).

[105] F. Fregni and A. Pascual-Leone, 'Hand motor recovery after stroke: Tuning the orchestra to improve hand motor function', *Cognitive and Behavioral Neurology*, vol. 19, pp. 21–33, 1 Mar. 2006, ISSN: 1543-3633. DOI: 10.1097/00146965-200603000-00003 (cit. on p. 11).

[106] F. C. Hummel and L. G. Cohen, 'Non-invasive brain stimulation: A new strategy to improve neurorehabilitation after stroke?', *The Lancet Neurology*, vol. 5, pp. 708–712, 8 Aug. 2006, ISSN: 14744422. DOI: 10.1016/S1474-4422(06)70525-7 (cit. on p. 11).

[107] E. M. Khedr, M. A. Ahmed, N. Fathy and J. C. Rothwell, 'Therapeutic trial of repetitive transcranial magnetic stimulation after acute ischemic stroke', *Neurology*, vol. 65, pp. 466–468, 3 Aug. 2005, ISSN: 0028-3878. DOI: 10.1212/01.wnl.0000173067.84247.36 (cit. on p. 11).

[108] C. M. Bütefisch, V. Khurana, L. Kopylev and L. G. Cohen, 'Enhancing encoding of a motor memory in the primary motor cortex by cortical stimulation', *Journal of Neurophysiology*, vol. 91, pp. 2110–2116, 5 May 2004, ISSN: 00223077. DOI: 10.1152/jn.01038.2003 (cit. on p. 11).

[109] M. Power, C. Fraser, A. Hobson, J. C. Rothwell, S. Mistry, D. A. Nicholson, D. G. Thompson and S. Hamdy, 'Changes in pharyngeal corticobulbar excitability and swallowing behavior after oral stimulation', *Am J Physiol Gastrointest Liver Physiol*, vol. 286, pp. 45–50, 2004. DOI: 10.1152/ajpgi (cit. on p. 11).

[110] K. Rosenkranz, M. A. Nitsche, F. Tergau and W. Paulus, 'Diminution of training-induced transient motor cortex plasticity by weak transcranial direct current stimulation in the human', *Neuroscience Letters*, vol. 296, pp. 61–63, 1 Dec. 2000, ISSN: 03043940. DOI: 10.1016/S0304-3940(00)01621-9 (cit. on p. 11).

[111] E. I. Moser, K. A. Krobert, M.-B. Moser and R. G. M. Morris, 'Impaired spatial learning after saturation of long-term potentiation', *Science*, vol. 281, pp. 2038–2042, 5385 Sep. 1998, ISSN: 0036-8075. DOI: 10.1126/science.281.5385.2038 (cit. on p. 11).

[112] J. Robbins, S. G. Butler, S. K. Daniels, R. D. Gross, S. Langmore, C. L. Lazarus, B. Martin-Harris, D. McCabe, N. Musson and J. Rosenbek, 'Swallowing and dysphagia rehabilitation: Translating principles of neural plasticity into clinically oriented evidence', *Journal of Speech, Language, and Hearing Research*, vol. 51, 1 Feb. 2008, ISSN: 1092-4388. DOI: 10.1044/1092-4388(2008/021) (cit. on p. 11).

[113] N. J. Cepeda, H. Pashler, E. Vul, J. T. Wixted and D. Rohrer, 'Distributed practice in verbal recall tasks: A review and quantitative synthesis', *Psychological Bulletin*, vol. 132, pp. 354–380, 3 May 2006, ISSN: 00332909. DOI: 10.1037/0033-2909.132.3.354 (cit. on p. 11).

[114] E. Gerbier and T. C. Toppino, 'The effect of distributed practice: Neuroscience, cognition, and education', *Trends in Neuroscience and Education*, vol. 4, pp. 49–59, 3 Sep. 2015, ISSN: 22119493. DOI: 10.1016/j.tine.2015.01.001 (cit. on p. 11).

[115] H. M. Sisti, A. L. Glass and T. J. Shors, 'Neurogenesis and the spacing effect: Learning over time enhances memory and the survival of new neurons.', *Learning & memory (Cold Spring Harbor, N.Y.)*, vol. 14, pp. 368–375, 5 2007, ISSN: 15495485. DOI: 10.1101/lm.488707 (cit. on p. 11).

[116] M. S. Ameen, M. Petzka, P. Peigneux and K. Hoedlmoser, 'Post-training sleep modulates motor adaptation and task-related beta oscillations', *Journal of Sleep Research*, 2023, ISSN: 13652869. DOI: 10.1111/jsr.14082 (cit. on p. 11).

[117] W. Stee and P. Peigneux, 'Post-learning micro- and macro-structural neuroplasticity changes with time and sleep', *Biochemical Pharmacology*, vol. 191, p. 114 369, Sep. 2021, ISSN: 00062952. DOI: 10.1016/j.bcp.2020.114369 (cit. on p. 11).

[118] S. Y. Wang, K. C. Baker, J. L. Culbreth, O. Tracy, M. Arora, T. Liu, S. Morris, M. B. Collins and E. J. Wamsley, ''sleep-dependent' memory consolidation? brief periods of post-training rest and sleep provide an equivalent benefit for both declarative and procedural memory', *Learning and Memory*, vol. 28, pp. 195–203, 6 Jun. 2021, ISSN: 15495485. DOI: 10.1101/LM.053330.120 (cit. on p. 11).

[119] M. Deantoni, T. Villemonteix, E. Balteau, C. Schmidt and P. Peigneux, 'Post-training sleep modulates topographical relearning-dependent resting state activity', *Brain Sciences*, vol. 11, 4 2021, ISSN: 20763425. DOI: 10.3390/brainsci11040476 (cit. on p. 11).

[120] M. Murphy, R. Stickgold, M. E. Parr, C. Callahan and E. J. Wamsley, 'Recurrence of task-related electroencephalographic activity during post-training quiet rest and sleep', *Scientific Reports*, vol. 8, 1 Dec. 2018, ISSN: 20452322. DOI: 10.1038/s41598-018-23590-1 (cit. on p. 11).

[121] M. Gorgoni, A. D'Atri, G. Lauri, P. M. Rossini, F. Ferlazzo and L. D. Gennaro, 'Is sleep essential for neural plasticity in humans, and how does it affect motor and cognitive recovery?', *Neural Plasticity*, vol. 2013, pp. 1–13, 2013, ISSN: 2090-5904. DOI: 10.1155/2013/103949 (cit. on p. 11).

[122] J. Driver and T. Noesselt, 'Multisensory interplay reveals crossmodal influences on 'sensory-specific' brain regions, neural responses, and judgments', *Neuron*, vol. 57, pp. 11–23, 1 Jan. 2008, ISSN: 08966273. DOI: 10.1016/j.neuron.2007.12.013 (cit. on p. 11).

[123] L. Shams and A. R. Seitz, 'Benefits of multisensory learning', *Trends in Cognitive Sciences*, vol. 12, pp. 411–417, 11 Nov. 2008, ISSN: 13646613. DOI: 10.1016/j.tics.2008.07.006 (cit. on p. 11).

[124] S. J. Sober and P. N. Sabes, 'Multisensory integration during motor planning', *The Journal of Neuroscience*, vol. 23, pp. 6982–6992, 18 Aug. 2003, ISSN: 0270-6474. DOI: 10.1523/JNEUROSCI.23-18-06982.2003 (cit. on p. 11).

[125] R. Sigrist, G. Rauter, R. Riener and P. Wolf, 'Augmented visual, auditory, haptic, and multimodal feedback in motor learning: A review', *Psychonomic Bulletin & Review*, vol. 20, pp. 21–53, 1 2013, ISSN: 1069-9384. DOI: 10.3758/s13423-012-0333-8 (cit. on p. 11).

[126] H. Huang, S. L. Wolf and J. He, 'Recent developments in biofeedback for neuromotor rehabilitation', *Journal of NeuroEngineering and Rehabilitation*, vol. 3, 1 Dec. 2006, ISSN: 1743-0003. DOI: 10.1186/1743-0003-3-11 (cit. on p. 11).

[127] J. A. Grahn, 'Neural mechanisms of rhythm perception: Current findings and future perspectives', *Topics in Cognitive Science*, vol. 4, pp. 585–606, 4 Oct. 2012, ISSN: 17568757. DOI: 10.1111/j.1756-8765.2012.01213.x (cit. on p. 11).

[128] C. Nombela, L. E. Hughes, A. M. Owen and J. A. Grahn, 'Into the groove: Can rhythm influence parkinson's disease?', *Neuroscience & Biobehavioral Reviews*, vol. 37, pp. 2564–2570, 10 Dec. 2013, ISSN: 01497634. DOI: 10.1016/j.neubiorev.2013.08.003 (cit. on p. 11).

[129] E. Moore, R. S. Schaefer, M. E. Bastin, N. Roberts and K. Overy, 'Diffusion tensor mri tractography reveals increased fractional anisotropy (fa) in arcuate fasciculus following music-cued motor training', *Brain and Cognition*, vol. 116, pp. 40–46, Aug. 2017, ISSN: 10902147. DOI: 10.1016/j.bandc.2017.05.001 (cit. on p. 11).

[130] G. E. Yoo and S. J. Kim, 'Rhythmic auditory cueing in motor rehabilitation for stroke patients: Systematic review and meta-analysis', *Journal of Music Therapy*, vol. 53, pp. 149–177, 2 2016, ISSN: 00222917. DOI: 10.1093/jmt/thw003 (cit. on p. 11).

[131] S. Ghai, 'Effects of real-time (sonification) and rhythmic auditory stimuli on recovering arm function post stroke: A systematic review and meta-analysis', *Frontiers in Neurology*, vol. 9, JUL Jul. 2018, ISSN: 1664-2295. DOI: 10.3389/fneur.2018.00488 (cit. on p. 11).

[132] F. Hamzei, C. H. Läppchen, V. Glauche, I. Mader, M. Rijntjes and C. Weiller, 'Functional plasticity induced by mirror training: The mirror as the element connecting both hands to one hemisphere', *Neurorehabilitation and Neural Repair*, vol. 26, pp. 484–496, 5 Jun. 2012, ISSN: 15459683. DOI: 10.1177/1545968311427917 (cit. on p. 11).

[133] K. Arya, 'Underlying neural mechanisms of mirror therapy: Implications for motor rehabilitation in stroke', *Neurology India*, vol. 64, p. 38, 1 Jan. 2016, ISSN: 0028-3886. DOI: 10.4103/0028-3886.173622 (cit. on p. 11).

[134] H. Thieme, N. Morkisch, J. Mehrholz, M. Pohl, J. Behrens, B. Borgetto and C. Dohle, 'Mirror therapy for improving motor function after stroke', *Cochrane Database of Systematic Reviews*, vol. 2018, 7 Jul. 2018, ISSN: 14651858. DOI: 10.1002/14651858.CD008449.pub3 (cit. on p. 11).

[135] R. M. Hardwick, S. Caspers, S. B. Eickhoff and S. P. Swinnen, 'Neural correlates of action: Comparing meta-analyses of imagery, observation, and execution', *Neuroscience & Biobehavioral Reviews*, vol. 94, pp. 31–44, Nov. 2018, ISSN: 01497634. DOI: 10.1016/j.neubiorev.2018.08.003 (cit. on p. 11).

[136] D. Ertelt, S. Small, A. Solodkin, C. Dettmers, A. McNamara, F. Binkofski and G. Buccino, 'Action observation has a positive impact on rehabilitation of motor deficits after stroke', *NeuroImage*, vol. 36, SUPPL. 2 2007, ISSN: 10538119. DOI: 10.1016/j.neuroimage.2007.03.043 (cit. on p. 11).

[137] A. A. Mattar and P. L. Gribble, 'Motor learning by observing', *Neuron*, vol. 46, pp. 153–160, 1 Apr. 2005, ISSN: 08966273. DOI: 10.1016/j.neuron.2005.02.009 (cit. on p. 11).

[138] S. C. Cramer, M. Sur, B. H. Dobkin *et al.*, 'Harnessing neuroplasticity for clinical applications', *Brain*, vol. 134, pp. 1591–1609, 6 2011, ISSN: 00068950. DOI: 10.1093/brain/awr039 (cit. on p. 11).

[139] A. L. Behrman, M. G. Bowden and P. M. Nair, 'Neuroplasticity after spinal cord injury and training: An emerging paradigm shift in rehabilitation and walking recovery', *Physical Therapy*, vol. 86, pp. 1406–1425, 10 2006, ISSN: 0031-9023. DOI: 10.2522/ptj.20050212 (cit. on p. 11).

[140] N. Takeuchi and S.-i. Izumi, 'Rehabilitation with poststroke motor recovery: A review with a focus on neural plasticity', *Stroke Research and Treatment*, vol. 2013, pp. 1–13, 2013, ISSN: 2090-8105. DOI: 10.1155/2013/128641 (cit. on p. 11).

[141] M. Kitagawa and B. Windsor, 'An overview and history of motion capture', in Elsevier, 2008, pp. 1–12. DOI: 10.1016/B978-0-240-81000-3.50004-8 (cit. on p. 12).

[142] D. Regazzoni, G. D. Vecchi and C. Rizzi, 'Rgb cams vs rgb-d sensors: Low cost motion capture technologies performances and limitations', *Journal of Manufacturing Systems*, vol. 33, pp. 719–728, 4 Oct. 2014, ISSN: 02786125. DOI: 10.1016/j.jmsy.2014.07.011 (cit. on p. 12).

[143] C. Gu, W. Lin, X. He, L. Zhang and M. Zhang, 'Imu-based motion capture system for rehabilitation applications: A systematic review', *Biomimetic Intelligence and Robotics*, vol. 3, p. 100 097, 2 Jun. 2023, ISSN: 26673797. DOI: 10.1016/j.birob.2023.100097 (cit. on p. 12).

[144] N. Golestani and M. Moghaddam, 'Wearable magnetic induction-based approach toward 3d motion tracking', *Scientific Reports*, vol. 11, 1 Dec. 2021, ISSN: 20452322. DOI: 10.1038/s41598-021-98346-5 (cit. on p. 12).

[145] K. Das, T. de Paula Oliveira and J. Newell, 'Comparison of markerless and marker-based motion capture systems using 95% functional limits of agreement in a linear mixed-effects modelling framework', *Scientific Reports*, vol. 13, 1 Dec. 2023, ISSN: 20452322. DOI: 10.1038/s41598-023-49360-2 (cit. on p. 12).

[146] N. Zahradka, K. Verma, A. Behboodi, B. Bodt, H. Wright and S. C. Lee, 'An evaluation of three kinematic methods for gait event detection compared to the kinetic-based 'gold standard'', *Sensors (Switzerland)*, vol. 20, pp. 1–15, 18 Sep. 2020, ISSN: 14248220. DOI: 10.3390/s20185272 (cit. on p. 12).

[147] E. Ceseracciu, Z. Sawacha and C. Cobelli, 'Comparison of markerless and marker-based motion capture technologies through simultaneous data collection during gait: Proof of concept', *PLoS ONE*, vol. 9, 3 Mar. 2014, ISSN: 19326203. DOI: 10.1371/journal.pone.0087640 (cit. on p. 12).

[148] D. F. N. Gordon, 'Thesis: Exoskeleton-assisted locomotion: Design, control and evaluation of wearable robotic devices', 2021 (cit. on p. 14).

[149] Vicon, *Vicon nexus user guide*, 2022 (cit. on p. 16).

[150] D. F. Gordon, G. Henderson and S. Vijayakumar, 'Effectively quantifying the performance of lower-limb exoskeletons over a range of walking conditions', *Frontiers Robotics AI*, vol. 5, JUN 2018, ISSN: 22969144. DOI: 10.3389/frobt.2018.00061 (cit. on p. 16).

[151] S. L. Delp, F. C. Anderson, A. S. Arnold, P. Loan, A. Habib, C. T. John, E. Guendelman and D. G. Thelen, 'Opensim: Open-source software to create and analyze dynamic simulations of movement', *IEEE Transactions on Biomedical Engineering*, vol. 54, pp. 1940–1950, 11 2007, ISSN: 00189294. DOI: 10.1109/TBME.2007.901024 (cit. on pp. 17, 93).

[152] M. S. Andersen and J. Rasmussen, 'Anybody modeling system', in Elsevier, Jan. 2023, pp. 143–159. DOI: 10.1016/B978-0-12-823913-1.00007-5 (cit. on pp. 17, 38).

[153] F. C. Anderson and M. G. Pandy, 'A dynamic optimization solution for vertical jumping in three dimensions', *Computer Methods in Biomechanics and Biomedical Engineering*, vol. 2, pp. 201–231, 3 1999, ISSN: 10255842. DOI: 10.1080/10255849908907988 (cit. on pp. 17, 84).

[154] F. C. Anderson and M. G. Pandy, 'Dynamic optimization of human walking', *Journal of Biomechanical Engineering*, vol. 123, pp. 381–390, 5 2001, ISSN: 01480731. DOI: 10.1115/1.1392310 (cit. on pp. 17, 84).

[155] S. Delp, J. Loan, M. Hoy, F. Zajac, E. Topp and J. Rosen, 'An interactive graphics-based model of the lower extremity to study orthopaedic surgical procedures', *IEEE Transactions on Biomedical Engineering*, vol. 37, pp. 757–767, 8 1990, ISSN: 00189294. DOI: 10.1109/10.102791 (cit. on pp. 17, 84).

[156] G. T. Yamaguchi and F. E. Zajac, 'A planar model of the knee joint to characterize the knee extensor mechanism', *Journal of Biomechanics*, vol. 22, pp. 1–10, 1 1989, ISSN: 00219290. DOI: 10.1016/0021-9290(89)90179-6 (cit. on pp. 17, 84).

[157] M. Millard, T. Uchida, A. Seth and S. L. Delp, 'Flexing computational muscle: Modeling and simulation of musculotendon dynamics', *Journal of Biomechanical Engineering*, vol. 135, pp. 1–11, 2 2013, ISSN: 01480731. DOI: 10.1115/1.4023390 (cit. on pp. 17, 94, 95).

[158] D. G. Thelen, 'Adjustment of muscle mechanics model parameters to simulate dynamic contractions in older adults', *Journal of Biomechanical Engineering*, vol. 125, pp. 70–77, 1 2003, ISSN: 01480731. DOI: 10.1115/1.1531112 (cit. on p. 17).

[159] E. Y. Cheung, T. K. Ng, K. K. Yu, R. L. Kwan and G. L. Cheing, 'Robot-assisted training for people with spinal cord injury: A meta-analysis', *Archives of Physical Medicine and Rehabilitation*, vol. 98, 2320–2331.e12, 11 2017, ISSN: 1532821X. DOI: 10.1016/j.apmr.2017.05.015 (cit. on p. 20).

[160] J. Mehrholz, S. Thomas, J. Kugler, M. Pohl and B. Elsner, 'Electromechanical-assisted training for walking after stroke', *Cochrane Database of Systematic Reviews*, vol. 2020, 10 Oct. 2020, ISSN: 14651858. DOI: 10.1002/14651858.CD006185.pub5 (cit. on pp. 20, 35).

[161] C.-Y. Fang, J.-L. Tsai, G.-S. Li, A. S.-Y. Lien and Y.-J. Chang, 'Effects of robot-assisted gait training in individuals with spinal cord injury: A meta-analysis', *BioMed Research International*, vol. 2020, pp. 1–13, Mar. 2020, ISSN: 2314-6133. DOI: 10.1155/2020/2102785 (cit. on pp. 20, 35).

[162] S. Campagnini, P. Liuzzi, A. Mannini, R. Riener and M. C. Carrozza, 'Effects of control strategies on gait in robot-assisted post-stroke lower limb rehabilitation: A systematic review', *Journal of NeuroEngineering and Rehabilitation*, vol. 19, pp. 1–16, 1 2022, ISSN: 1743-0003. DOI: 10.1186/s12984-022-01031-5 (cit. on pp. 20, 35).

[163] S. Hesse, T. Sarkodie-Gyan and D. Uhlenbrock, 'Development of an advanced mechanised gait trainer, controlling movement of the centre of mass, for restoring gait in non-ambulant subjects', *Biomedizinische Technik/Biomedical Engineering*, vol. 44, pp. 194–201, 7-8 1999, ISSN: 0013-5585. DOI: 10.1515/bmte.1999.44.7-8.194 (cit. on p. 21).

[164] H. Schmidt, S. Hesse, R. Bernhardt and J. Krüger, 'Hapticwalker—a novel haptic foot device', *ACM Transactions on Applied Perception*, vol. 2, pp. 166–180, 2 Apr. 2005, ISSN: 1544-3558. DOI: 10.1145/1060581.1060589 (cit. on p. 21).

[165] H. Schmidt, C. Werner, R. Bernhardt, S. Hesse and J. Krüger, 'Gait rehabilitation machines based on programmable footplates', *Journal of NeuroEngineering and Rehabilitation*, vol. 4, 2007, ISSN: 17430003. DOI: 10.1186/1743-0003-4-2 (cit. on p. 21).

[166] S. Freivogel, J. Mehrholz, T. Husak-Sotomayor and D. Schmalohr, 'Gait training with the newly developed 'lokohelp'-system is feasible for non-ambulatory patients after stroke, spinal cord and brain injury. a feasibility study', *Brain Injury*, vol. 22, pp. 625–632, 7-8 2008, ISSN: 1362301X. DOI: 10.1080/02699050801941771 (cit. on p. 21).

[167] H. Yano, T. Masuda, Y. Nakajima, N. Tanaka, S. Tamefusa, H. Saitou and H. Iwata, 'Development of a gait rehabilitation systemwith a spherical immersive projection display', *Journal of Robotics and Mechatronics*, vol. 20, pp. 836–845, 6 Dec. 2008, ISSN: 18838049. DOI: 10.20965/jrm.2008.p0836 (cit. on p. 21).

[168] S. Hussein, H. Schmidt and J. Kruger, 'Adaptive control of an end-effector based electromechanical gait rehabilitation device', IEEE, Jun. 2009, pp. 366–371, ISBN: 978-1-4244-3788-7. DOI: 10.1109/ICORR.2009.5209485 (cit. on p. 21).

[169] J. Y. Kim, J. J. Kim and K. Park, 'Gait training algorithm of an end-effector typed hybrid walking rehabilitation robot', *International Journal of Precision Engineering and Manufacturing*, vol. 20, pp. 1767–1775, 10 Oct. 2019, ISSN: 20054602. DOI: 10.1007/s12541-019-00185-y (cit. on p. 21).

[170] J. L. Emken, R. Benitez and D. J. Reinkensmeyer, 'Human-robot cooperative movement training: Learning a novel sensory motor transformation during walking with robotic assistance-as-needed', *Journal of NeuroEngineering and Rehabilitation*, vol. 4, pp. 1–16, 2007, ISSN: 17430003. DOI: 10.1186/1743-0003-4-8 (cit. on pp. 21, 69).

[171] R. Gassert and V. Dietz, 'Rehabilitation robots for the treatment of sensorimotor deficits: A neurophysiological perspective', *Journal of NeuroEngineering and Rehabilitation*, vol. 15, p. 46, 1 Dec. 2018, ISSN: 1743-0003. DOI: 10.1186/s12984-018-0383-x (cit. on pp. 22, 35).

[172] M. R. Tucker, J. Olivier, A. Pagel, H. Bleuler, M. Bouri, O. Lambercy, J. R. D. Millán, R. Riener, H. Vallery and R. Gassert, 'Control strategies for active lower extremity prosthetics and orthotics: A review', *Journal of NeuroEngineering and Rehabilitation*, vol. 12, 1 2015, ISSN: 17430003. DOI: 10.1186/1743-0003-12-1 (cit. on pp. 21, 22).

[173] J. de Miguel-Fernández, J. Lobo-Prat, E. Prinsen, J. M. Font-Llagunes and L. Marchal-Crespo, 'Control strategies used in lower limb exoskeletons for gait rehabilitation after brain injury: A systematic review and analysis of clinical effectiveness', *Journal of NeuroEngineering and Rehabilitation*, vol. 20, p. 23, 1 Feb. 2023, ISSN: 1743-0003. DOI: 10.1186/s12984-023-01144-5 (cit. on pp. 21, 22, 24).

[174] R. Baud, A. R. Manzoori, A. Ijspeert and M. Bouri, 'Review of control strategies for lower-limb exoskeletons to assist gait', *Journal of NeuroEngineering and Rehabilitation*, vol. 18, p. 119, 1 Dec. 2021, ISSN: 1743-0003. DOI: 10.1186/s12984-021-00906-3 (cit. on pp. 21–23).

[175] B. Chen, C. H. Zhong, X. Zhao, H. Ma, L. Qin and W. H. Liao, 'Reference joint trajectories generation of cuhk-exo exoskeleton for system balance in walking assistance', *IEEE Access*, vol. 7, pp. 33 809–33 821, 2019, ISSN: 21693536. DOI: 10.1109/ACCESS.2019.2904296 (cit. on pp. 22, 23, 108).

[176] S. O. Schrade, K. Dätwyler, M. Stücheli, K. Studer, D. A. Türk, M. Meboldt, R. Gassert and O. Lambercy, 'Development of varileg, an exoskeleton with variable stiffness actuation: First results and user evaluation from the cybathlon 2016 olivier lambercy; roger gassert', *Journal of NeuroEngineering and Rehabilitation*, vol. 15, 1 Mar. 2018, ISSN: 17430003. DOI: 10.1186/s12984-018-0360-4 (cit. on p. 22).

[177] T. Vouga, R. Baud, J. Fasola, M. Bouri and H. Bleuler, 'Twiice — a lightweight lower-limb exoskeleton for complete paraplegics', IEEE, Jul. 2017, pp. 1639–1645, ISBN: 978-1-5386-2296-4. DOI: 10.1109/ICORR.2017.8009483 (cit. on p. 22).

[178] R. Griffin, T. Cobb, T. Craig *et al.*, 'Stepping forward with exoskeletons: Team ihmc?s design and approach in the 2016 cybathlon', *IEEE Robotics and Automation Magazine*, vol. 24, pp. 66–74, 4 Dec. 2017, ISSN: 10709932. DOI: 10.1109/MRA.2017.2754284 (cit. on p. 22).

[179] S. Galle, P. Malcolm, S. H. Collins and D. D. Clercq, 'Reducing the metabolic cost of walking with an ankle exoskeleton: Interaction between actuation timing and power', *Journal of NeuroEngineering and Rehabilitation*, vol. 14, 1 Apr. 2017, ISSN: 17430003. DOI: 10.1186/s12984-017-0235-0 (cit. on p. 22).

[180] J. Zhang, P. Fiers, K. A. Witte, R. W. Jackson, K. L. Poggensee, C. G. Atkeson and S. H. Collins, 'Human-in-the-loop optimization of exoskeleton assistance during walking', *Science*, vol. 356, pp. 1280–1284, 6344 Jun. 2017, ISSN: 0036-8075. DOI: 10.1126/science.aal5054 (cit. on pp. 22, 73).

[181] Z. F. Lerner, G. M. Gasparri, M. O. Bair, J. L. Lawson, J. Luque, T. A. Harvey and A. T. Lerner, 'An untethered ankle exoskeleton improves walking economy in a pilot study of individuals with cerebral palsy', *IEEE Transactions on Neural Systems and Rehabilitation Engineering*, vol. 26, pp. 1985–1993, 10 Oct. 2018, ISSN: 15344320. DOI: 10.1109/TNSRE.2018.2870756 (cit. on pp. 22, 23).

[182] L. Righetti, J. Buchli and A. J. Ijspeert, 'Adaptive frequency oscillators and applications', *The Open Cybernetics & Systemics Journal*, vol. 3, pp. 64–

69, 2 Oct. 2009, ISSN: 1874110X. DOI: 10.2174/1874110X00903020064 (cit. on p. 22).

[183] K. Seo, S. Hyung, B. K. Choi, Y. Lee and Y. Shim, 'A new adaptive frequency oscillator for gait assistance', IEEE, May 2015, pp. 5565–5571, ISBN: 978-1-4799-6923-4. DOI: 10.1109/ICRA.2015.7139977 (cit. on p. 22).

[184] J. Kim, S.-J. Kim and J. Choi, 'Real-time gait phase detection and estimation of gait speed and ground slope for a robotic knee orthosis', IEEE, Aug. 2015, pp. 392–397, ISBN: 978-1-4799-1808-9. DOI: 10.1109/ICORR.2015.7281231 (cit. on p. 22).

[185] D. H. Lim, W. S. Kim, H. J. Kim and C. S. Han, 'Development of real-time gait phase detection system for a lower extremity exoskeleton robot', *International Journal of Precision Engineering and Manufacturing*, vol. 18, pp. 681–687, 5 May 2017, ISSN: 20054602. DOI: 10.1007/s12541-017-0081-9 (cit. on p. 22).

[186] J. Figueiredo, P. Félix, L. Costa, J. C. Moreno and C. P. Santos, 'Gait event detection in controlled and real-life situations: Repeated measures from healthy subjects', *IEEE Transactions on Neural Systems and Rehabilitation Engineering*, vol. 26, pp. 1945–1956, 10 Oct. 2018, ISSN: 15580210. DOI: 10.1109/TNSRE.2018.2868094 (cit. on p. 22).

[187] N. Hogan, 'Impedance control: An approach to manipulation: Part i-theory', *Journal of Dynamic Systems, Measurement and Control, Transactions of the ASME*, vol. 107, pp. 17–24, 1 1985, ISSN: 15289028. DOI: 10.1115/1.3140701 (cit. on p. 23).

[188] N. Hogan, 'Impedance control: An approach to manipulation: Part ii—implementation', *Journal of Dynamic Systems, Measurement, and Control*, vol. 107, pp. 8–16, 1 Mar. 1985, ISSN: 0022-0434. DOI: 10.1115/1.3140713 (cit. on p. 23).

[189] L.-F. Yeung, C. Ockenfeld, M.-K. Pang, H.-W. Wai, O.-Y. Soo, S.-W. Li and K.-Y. Tong, 'Design of an exoskeleton ankle robot for robot-assisted gait training of stroke patients', IEEE, Jul. 2017, pp. 211–215, ISBN:

978-1-5386-2296-4. DOI: 10.1109/ICORR.2017.8009248 (cit. on pp. 23, 109).

[190] S. Wang, L. Wang, C. Meijneke *et al.*, 'Design and control of the mindwalker exoskeleton', *IEEE Transactions on Neural Systems and Rehabilitation Engineering*, vol. 23, pp. 277–286, 2 Mar. 2015, ISSN: 1534-4320. DOI: 10.1109/TNSRE.2014.2365697 (cit. on pp. 23, 109).

[191] M. Bortole, A. Venkatakrishnan, F. Zhu, J. C. Moreno, G. E. Francisco, J. L. Pons and J. L. Contreras-Vidal, 'The h2 robotic exoskeleton for gait rehabilitation after stroke: Early findings from a clinical study', *Journal of NeuroEngineering and Rehabilitation*, vol. 12, pp. 1–14, 1 2015, ISSN: 17430003. DOI: 10.1186/s12984-015-0048-y (cit. on pp. 23, 26, 109).

[192] T. Kagawa and Y. Uno, 'Gait pattern generation for a power-assist device of paraplegic gait', IEEE, Sep. 2009, pp. 633–638, ISBN: 978-1-4244-5081-7. DOI: 10.1109/ROMAN.2009.5326348 (cit. on pp. 23, 108, 109).

[193] N. Aphiratsakun and M. Parnichkun, 'Balancing control of ait leg exoskeleton using zmp based flc', *International Journal of Advanced Robotic Systems*, vol. 6, p. 34, 4 Dec. 2009, ISSN: 1729-8814. DOI: 10.5772/7250 (cit. on p. 23).

[194] S. Qiu, W. Guo, D. Caldwell and F. Chen, 'Exoskeleton online learning and estimation of human walking intention based on dynamical movement primitives', *IEEE Transactions on Cognitive and Developmental Systems*, vol. 13, pp. 67–79, 1 Mar. 2021, ISSN: 23798939. DOI: 10.1109/TCDS.2020.2968845 (cit. on p. 23).

[195] M. Tucker, M. Cheng, E. Novoseller, R. Cheng, Y. Yue, J. W. Burdick and A. D. Ames, 'Human preference-based learning for high-dimensional optimization of exoskeleton walking gaits', Institute of Electrical and Electronics Engineers Inc., Oct. 2020, pp. 3423–3430, ISBN: 9781728162126. DOI: 10.1109/IROS45743.2020.9341416 (cit. on p. 23).

[196] H. Mohamad and S. Ozgoli, 'Online gait generator for lower limb exoskeleton robots: Suitable for level ground, slopes, stairs, and obstacle avoidance', *Robotics and Autonomous Systems*, vol. 160, Feb. 2023, ISSN: 09218890. DOI: 10.1016/j.robot.2022.104319 (cit. on p. 23).

[197] T. Gurriet, S. Finet, G. Boeris, A. Duburcq, A. Hereid, O. Harib, M. Masselin, J. Grizzle and A. D. Ames, 'Towards restoring locomotion for paraplegics: Realizing dynamically stable walking on exoskeletons', IEEE, May 2018, pp. 2804–2811, ISBN: 978-1-5386-3081-5. DOI: 10.1109/ICRA.2018.8460647 (cit. on p. 23).

[198] T. Zheng, J. Gao, S. Zhao, M. Lai, Y. Gao, J. Zhao and Y. Zhu, 'Stable gait generation method for lower-limb exoskeleton based on instrumented crutches', *International Journal of Advanced Robotic Systems*, vol. 20, 4 Jul. 2023, ISSN: 17298814. DOI: 10.1177/17298806231191938 (cit. on pp. 23, 108, 109).

[199] C. L. Lewis and D. P. Ferris, 'Invariant hip moment pattern while walking with a robotic hip exoskeleton', *Journal of Biomechanics*, vol. 44, pp. 789–793, 5 Mar. 2011, ISSN: 00219290. DOI: 10.1016/j.jbiomech.2011.01.030 (cit. on p. 23).

[200] D. Xu, X. Liu and Q. Wang, 'Knee exoskeleton assistive torque control based on real-time gait event detection', *IEEE Transactions on Medical Robotics and Bionics*, vol. 1, pp. 158–168, 3 Aug. 2019, ISSN: 25763202. DOI: 10.1109/TMRB.2019.2930352 (cit. on p. 23).

[201] D. Lee, E. C. Kwak, B. J. McLain, I. Kang and A. J. Young, 'Effects of assistance during early stance phase using a robotic knee orthosis on energetics, muscle activity, and joint mechanics during incline and decline walking', *IEEE Transactions on Neural Systems and Rehabilitation Engineering*, vol. 28, pp. 914–923, 4 Apr. 2020, ISSN: 15580210. DOI: 10.1109/TNSRE.2020.2972323 (cit. on p. 23).

[202] Y. Ding, F. A. Panizzolo, C. Siviy, P. Malcolm, I. Galiana, K. G. Holt and C. J. Walsh, 'Effect of timing of hip extension assistance during loaded walking with a soft exosuit', *Journal of NeuroEngineering and Rehabilitation*, vol. 13, p. 87, 1 Dec. 2016, ISSN: 1743-0003. DOI: 10.1186/s12984-016-0196-8 (cit. on p. 23).

[203] G. Orekhov, Y. Fang, C. F. Cuddeback and Z. F. Lerner, 'Usability and performance validation of an ultra-lightweight and versatile untethered robotic ankle exoskeleton', *Journal of NeuroEngineering and Rehabilitation*,

vol. 18, 1 Dec. 2021, ISSN: 17430003. DOI: 10.1186/s12984-021-00954-9 (cit. on p. 23).

[204] J. D. Miguel-Fernandez, C. Pescatore, A. Mesa-Garrido, C. Rikhof, E. Prinsen, J. M. Font-Llagunes and J. Lobo-Prat, 'Immediate biomechanical effects of providing adaptive assistance with an ankle exoskeleton in individuals after stroke', *IEEE Robotics and Automation Letters*, vol. 7, pp. 7574–7580, 3 Jul. 2022, ISSN: 23773766. DOI: 10.1109/LRA.2022.3183799 (cit. on p. 23).

[205] T. Lenzi, M. C. Carrozza and S. K. Agrawal, 'Powered hip exoskeletons can reduce the user's hip and ankle muscle activations during walking', *IEEE Transactions on Neural Systems and Rehabilitation Engineering*, vol. 21, pp. 938–948, 6 2013, ISSN: 15344320. DOI: 10.1109/TNSRE.2013.2248749 (cit. on p. 23).

[206] E. J. Park, T. Akbas, A. Eckert-Erdheim, L. H. Sloot, R. W. Nuckols, D. Orzel, L. Schumm, T. D. Ellis, L. N. Awad and C. J. Walsh, 'A hinge-free, non-restrictive, lightweight tethered exosuit for knee extension assistance during walking', *IEEE Transactions on Medical Robotics and Bionics*, vol. 2, pp. 165–175, 2 May 2020, ISSN: 25763202. DOI: 10.1109/TMRB.2020.2989321 (cit. on p. 23).

[207] C. Bayón, O. Ramírez, J. I. Serrano *et al.*, 'Development and evaluation of a novel robotic platform for gait rehabilitation in patients with cerebral palsy: Cpwalker', *Robotics and Autonomous Systems*, vol. 91, pp. 101–114, May 2017, ISSN: 09218890. DOI: 10.1016/j.robot.2016.12.015 (cit. on p. 23).

[208] O. Unluhisarcikli, M. Pietrusinski, B. Weinberg, P. Bonato and C. Mavroidis, 'Design and control of a robotic lower extremity exoskeleton for gait rehabilitation', IEEE, Sep. 2011, pp. 4893–4898, ISBN: 978-1-61284-456-5. DOI: 10.1109/IROS.2011.6094973 (cit. on p. 23).

[209] R. Hidayah, L. Bishop, X. Jin, S. Chamarthy, J. Stein and S. K. Agrawal, 'Gait adaptation using a cable-driven active leg exoskeleton (c-alex) with post-stroke participants', *IEEE Transactions on Neural Systems and*

Rehabilitation Engineering, vol. 28, pp. 1984–1993, 9 Sep. 2020, ISSN: 15580210. DOI: 10.1109/TNSRE.2020.3009317 (cit. on p. 23).

[210] N. L. Tagliamonte, F. Sergi, G. Carpino, D. Accoto and E. Guglielmelli, 'Human-robot interaction tests on a novel robot for gait assistance', IEEE, Jun. 2013, pp. 1–6, ISBN: 978-1-4673-6024-1. DOI: 10.1109/ICORR.2013.6650387 (cit. on p. 23).

[211] L. Wang, S. Wang, E. H. F. van Asseldonk and H. van der Kooij, 'Actively controlled lateral gait assistance in a lower limb exoskeleton', IEEE, Nov. 2013, pp. 965–970, ISBN: 978-1-4673-6358-7. DOI: 10.1109/IROS.2013.6696467 (cit. on p. 23).

[212] A. Martínez, B. Lawson and M. Goldfarb, 'A controller for guiding leg movement during overground walking with a lower limb exoskeleton', *IEEE Transactions on Robotics*, vol. 34, pp. 183–193, 1 Feb. 2018, ISSN: 15523098. DOI: 10.1109/TRO.2017.2768035 (cit. on p. 23).

[213] S. K. Banala, S. H. Kim, S. K. Agrawal and J. P. Scholz, 'Robot assisted gait training with active leg exoskeleton (alex)', vol. 17, Feb. 2009, pp. 2–8. DOI: 10.1109/TNSRE.2008.2008280 (cit. on p. 23).

[214] G. Chen, J. Ye, Q. Liu, L. Duan, W. Li, Z. Wu and C. Wang, 'Adaptive control strategy for gait rehabilitation robot to assist-when-needed', IEEE, Aug. 2018, pp. 538–543, ISBN: 978-1-5386-6869-6. DOI: 10.1109/RCAR.2018.8621706 (cit. on p. 23).

[215] D. Zanotto, P. Stegall and S. K. Agrawal, 'Adaptive assist-as-needed controller to improve gait symmetry in robot-assisted gait training', IEEE, May 2014, pp. 724–729, ISBN: 978-1-4799-3685-4. DOI: 10.1109/ICRA.2014.6906934 (cit. on p. 23).

[216] A. Duschau-Wicke, A. Caprez and R. Riener, 'Patient-cooperative control increases active participation of individuals with sci during robot-aided gait training', *Journal of NeuroEngineering and Rehabilitation*, vol. 7, pp. 1–13, 1 2010, ISSN: 17430003. DOI: 10.1186/1743-0003-7-43 (cit. on pp. 23, 24, 35, 46, 59).

[217] K. N. Winfree, P. Stegall and S. K. Agrawal, 'Design of a minimally constraining, passively supported gait training exoskeleton: Alex ii', IEEE, Jun. 2011, pp. 1–6, ISBN: 978-1-4244-9862-8. DOI: 10.1109/ICORR.2011.5975499 (cit. on p. 23).

[218] P. Slade, M. J. Kochenderfer, S. L. Delp and S. H. Collins, 'Personalizing exoskeleton assistance while walking in the real world', *Nature*, vol. 610, pp. 277–282, 7931 2022, ISSN: 14764687. DOI: 10.1038/s41586-022-05191-1 (cit. on pp. 24, 73).

[219] J. Kim, B. T. Quinlivan, L. A. Deprey, D. A. Revi, A. Eckert-Erdheim, P. Murphy, D. Orzel and C. J. Walsh, 'Reducing the energy cost of walking with low assistance levels through optimized hip flexion assistance from a soft exosuit', *Scientific Reports*, vol. 12, pp. 1–13, 1 2022, ISSN: 20452322. DOI: 10.1038/s41598-022-14784-9 (cit. on p. 24).

[220] S. K. Banala, S. K. Agrawal and J. P. Scholz, 'Active leg exoskeleton (alex) for gait rehabilitation of motor-impaired patients', *2007 IEEE 10th International Conference on Rehabilitation Robotics, ICORR'07*, vol. 00, pp. 401–407, c 2007. DOI: 10.1109/ICORR.2007.4428456 (cit. on p. 24).

[221] A. Duschau-Wicke, J. V. Zitzewitz, A. Caprez, L. Lünenburger and R. Riener, 'Path control: A method for patient-cooperative robot-aided gait rehabilitation', *IEEE Transactions on Neural Systems and Rehabilitation Engineering*, vol. 18, pp. 38–48, 1 2010, ISSN: 15344320. DOI: 10.1109/TNSRE.2009.2033061 (cit. on pp. 25, 26, 89).

[222] P. H. Peckham and J. S. Knutson, 'Functional electrical stimulation for neuromuscular applications', *Annual Review of Biomedical Engineering*, vol. 7, pp. 327–360, 1 Aug. 2005, ISSN: 1523-9829. DOI: 10.1146/annurev.bioeng.6.040803.140103 (cit. on pp. 28, 85).

[223] J. S. Knutson, N. S. Makowski, K. L. Kilgore and J. Chae, *Neuromuscular Electrical Stimulation Applications*, Fifth Edit. Elsevier Inc., 2019, 432–439.e3, ISBN: 9780323483230. DOI: 10.1016/B978-0-323-48323-0.00043-3 (cit. on p. 28).

[224] R. G. Carson and A. R. Buick, 'Neuromuscular electrical stimulation-promoted plasticity of the human brain', *The Journal of Physiology*,

vol. 599, pp. 2375–2399, 9 May 2021, ISSN: 0022-3751. DOI: 10.1113/JP278298 (cit. on p. 29).

[225] S. Springer, J.-j. Vatine, R. Lipson, A. Wolf and Y. Laufer, 'Effects of dual-channel functional electrical stimulation on gait performance in patients with hemiparesis', *The Scientific World Journal*, 2012. DOI: 10.1100/2012/530906 (cit. on p. 28).

[226] S. Khamis, R. Martikaro, S. Wientroub and Y. Hemo, 'A functional electrical stimulation system improves knee control in crouch gait', *Journal of Children's Orthopaedics*, pp. 137–143, 2015, ISSN: 1863-2521. DOI: 10.1007/s11832-015-0651-2 (cit. on p. 28).

[227] R. D. N., 'Functional electrical stimulation and rehabilitation—an hypothesis', *Medical Engineering and Physics*, vol. 25, pp. 75–78, 24 2003, ISSN: 11283602. DOI: 10.1016/S (cit. on p. 28).

[228] T. J. Kimberley, S. M. Lewis, E. J. Auerbach, L. L. Dorsey, J. M. Lojovich and J. R. Carey, 'Electrical stimulation driving functional improvements and cortical changes in subjects with stroke', *Experimental Brain Research*, vol. 154, pp. 450–460, 4 2004, ISSN: 00144819. DOI: 10.1007/s00221-003-1695-y (cit. on p. 28).

[229] H. K. Shin, S. H. Cho, H. seon Jeon, Y. H. Lee, J. C. Song, S. H. Jang, C. H. Lee and Y. H. Kwon, 'Cortical effect and functional recovery by the electromyography-triggered neuromuscular stimulation in chronic stroke patients', *Neuroscience Letters*, vol. 442, pp. 174–179, 3 2008, ISSN: 03043940. DOI: 10.1016/j.neulet.2008.07.026 (cit. on p. 28).

[230] D. B. Popović, 'Advances in functional electrical stimulation (fes)', *Journal of Electromyography and Kinesiology*, vol. 24, pp. 795–802, 6 2014, ISSN: 18735711. DOI: 10.1016/j.jelekin.2014.09.008 (cit. on p. 28).

[231] N. A. Maffiuletti, M. A. Minetto, D. Farina and R. Bottinelli, 'Electrical stimulation for neuromuscular testing and training: State-of-the art and unresolved issues', *European Journal of Applied Physiology*, vol. 111, pp. 2391–2397, 10 2011, ISSN: 14396319. DOI: 10.1007/s00421-011-2133-7 (cit. on pp. 28–30).

[232] F. O. Barroso, A. Pascual-Valdunciel, D. Torricelli, J. C. Moreno, A. D. Ama-Espinosa, J. Laczko and J. L. Pons, 'Noninvasive modalities used in spinal cord injury rehabilitation', in IntechOpen, Jan. 2019, pp. 1–20. DOI: 10.5772/intechopen.83654 (cit. on pp. 28, 29).

[233] Y. Hara, 'Rehabilitation with functional electrical stimulation in stroke patients', *International Journal of Physical Medicine & Rehabilitation*, vol. 01, pp. 1–6, 06 2013, ISSN: 23299096. DOI: 10.4172/2329-9096.1000147 (cit. on p. 28).

[234] C. L. Lynch and M. R. Popovic, 'Functional electrical stimulation', *IEEE Control Systems*, vol. 28, pp. 40–50, 2 2008, ISSN: 1066-033X. DOI: 10.1109/MCS.2007.914689 (cit. on pp. 28, 29, 85).

[235] J. Gondin, L. Brocca, E. Bellinzona, G. D'Antona, N. A. Maffiuletti, D. Miotti, M. A. Pellegrino and R. Bottinelli, 'Neuromuscular electrical stimulation training induces atypical adaptations of the human skeletal muscle phenotype: A functional and proteomic analysis', *Journal of Applied Physiology*, vol. 110, pp. 433–450, 2 2011, ISSN: 87507587. DOI: 10.1152/japplphysiol.00914.2010 (cit. on p. 28).

[236] T. Yan, C. W. Y. Hui-Chan and L. S. W. Li, 'Functional electrical stimulation improves motor recovery of the lower extremity and walking ability of subjects with first acute stroke', *Stroke*, vol. 36, pp. 80–85, 1 2005, ISSN: 0039-2499. DOI: 10.1161/01.STR.0000149623.24906.63 (cit. on pp. 28, 29).

[237] S. K. Sabut, C. Sikdar, R. Mondal, R. Kumar and M. Mahadevappa, 'Restoration of gait and motor recovery by functional electrical stimulation therapy in persons with stroke', *Disability and Rehabilitation*, vol. 32, pp. 1594–1603, 19 2010, ISSN: 09638288. DOI: 10.3109/09638281003599596 (cit. on p. 28).

[238] D. Pool, J. Valentine, N. Bear, C. J. Donnelly, C. Elliott and K. Stannage, 'The orthotic and therapeutic effects following daily community applied functional electrical stimulation in children with unilateral spastic cerebral palsy: A randomised controlled trial', *BMC Pediatrics*, vol. 15,

p. 154, 1 Dec. 2015, ISSN: 1471-2431. DOI: 10.1186/s12887-015-0472-y (cit. on pp. 28, 29).

[239] G. H. Creasey, C. H. Ho, R. J. Triolo, D. R. Gater, A. F. DiMarco, K. M. Bogie and M. W. Keith, 'Clinical applications of electrical stimulation after spinal cord injury', *Journal of Spinal Cord Medicine*, vol. 27, pp. 365–375, 4 2004, ISSN: 10790268. DOI: 10.1080/10790268.2004.11753774 (cit. on pp. 28, 29).

[240] O. A. Howlett, N. A. Lannin, L. Ada and C. Mckinstry, 'Functional electrical stimulation improves activity after stroke: A systematic review with meta-analysis', *Archives of Physical Medicine and Rehabilitation*, vol. 96, pp. 934–943, 5 2015, ISSN: 1532821X. DOI: 10.1016/j.apmr.2015.01.013 (cit. on p. 29).

[241] R. B. Stein, D. G. Everaert, A. K. Thompson, S. L. Chong, M. Whittaker, J. Robertson and G. Kuether, 'Long-term therapeutic and orthotic effects of a foot drop stimulator on walking performance in progressive and nonprogressive neurological disorders', *Neurorehabilitation and Neural Repair*, vol. 24, pp. 152–167, 2 2010, ISSN: 15459683. DOI: 10.1177/1545968309347681 (cit. on p. 29).

[242] S. M. El-Shamy and A. A. M. Abdelaal, 'Walkaide efficacy on gait and energy expenditure in children with hemiplegic cerebral palsy: A randomized controlled trial', *American Journal of Physical Medicine and Rehabilitation*, vol. 95, pp. 629–638, 9 2016, ISSN: 15377385. DOI: 10.1097/PHM.0000000000000514 (cit. on p. 29).

[243] J. C. Moreno, S. Mohammed, N. Sharma and A. J. del-Ama, *Hybrid Wearable Robotic Exoskeletons for Human Walking*. INC, 2020, pp. 347–364, ISBN: 9780128146590. DOI: 10.1016/b978-0-12-814659-0.00018-7 (cit. on p. 29).

[244] M. O. Ibitoye, N. A. Hamzaid, N. Hasnan, A. K. A. Wahab and G. M. Davis, 'Strategies for rapid muscle fatigue reduction during fes exercise in individuals with spinal cord injury: A systematic review', *PLoS ONE*, vol. 11, pp. 1–28, 2 2016, ISSN: 19326203. DOI: 10.1371/journal.pone.0149024 (cit. on pp. 29, 30, 85).

[245] C. S. Bickel, C. M. Gregory and J. C. Dean, 'Motor unit recruitment during neuromuscular electrical stimulation: A critical appraisal', *European Journal of Applied Physiology*, vol. 111, pp. 2399–2407, 10 Oct. 2011, ISSN: 1439-6319. DOI: 10.1007/s00421-011-2128-4 (cit. on pp. 29, 85).

[246] S. Dorgan and M. O'Malley, 'A nonlinear mathematical model of electrically stimulated skeletal muscle', *IEEE Transactions on Rehabilitation Engineering*, vol. 5, pp. 179–194, 2 Jun. 1997, ISSN: 1063-6528. DOI: 10.1109/86.593289 (cit. on p. 29).

[247] R. Riener and T. Fuhr, 'Patient-driven control of fes-supported standing up: A simulation study', *IEEE Transactions on Rehabilitation Engineering*, vol. 6, pp. 113–124, 2 1998, ISSN: 10636528. DOI: 10.1109/86.681177 (cit. on pp. 29, 91, 103).

[248] M. Gobbo, N. A. Maffiuletti, C. Orizio and M. A. Minetto, 'Muscle motor point identification is essential for optimizing neuromuscular electrical stimulation use', *Journal of NeuroEngineering and Rehabilitation*, vol. 11, p. 17, 1 Dec. 2014, ISSN: 1743-0003. DOI: 10.1186/1743-0003-11-17 (cit. on p. 29).

[249] R. K. Shields, S. Dudley-Javoroski and K. R. Cole, 'Feedback-controlled stimulation enhances human paralyzed muscle performance', *Journal of Applied Physiology*, vol. 101, pp. 1312–1319, 5 2006, ISSN: 87507587. DOI: 10.1152/japplphysiol.00385.2006 (cit. on p. 29).

[250] F. Anaya, P. Thangavel and H. Yu, 'Hybrid fes–robotic gait rehabilitation technologies: A review on mechanical design, actuation, and control strategies', *International Journal of Intelligent Robotics and Applications*, vol. 2, pp. 1–28, 1 2018, ISSN: 2366-5971. DOI: 10.1007/s41315-017-0042-6 (cit. on pp. 29, 31, 85).

[251] C. Marquez-Chin and M. R. Popovic, 'Functional electrical stimulation therapy for restoration of motor function after spinal cord injury and stroke: A review', *BioMedical Engineering Online*, vol. 19, pp. 1–25, 1 2020, ISSN: 1475925X. DOI: 10.1186/s12938-020-00773-4 (cit. on pp. 30, 85).

[252] J. P. Miller, S. Eldabe, E. Buchser, L. M. Johanek, Y. Guan and B. Linderoth, 'Parameters of spinal cord stimulation and their role in electrical charge delivery: A review', *Neuromodulation*, vol. 19, pp. 373–384, 4 Jun. 2016, ISSN: 15251403. DOI: 10.1111/ner.12438 (cit. on p. 30).

[253] S. Godfrey, J. E. Butler, L. Griffin and C. K. Thomas, 'Differential fatigue of paralyzed thenar muscles by stimuli of different intensities', *Muscle and Nerve*, vol. 26, pp. 122–131, 1 2002, ISSN: 0148639X. DOI: 10.1002/mus.10173 (cit. on pp. 30, 31).

[254] M. B. Kebaetse, S. C. Lee, T. E. Johnston and S. A. Binder-Macleod, 'Strategies that improve paralyzed human quadriceps femoris muscle performance during repetitive, nonisometric contractions', *Archives of Physical Medicine and Rehabilitation*, vol. 86, pp. 2157–2164, 11 Nov. 2005, ISSN: 00039993. DOI: 10.1016/j.apmr.2005.06.011 (cit. on pp. 30, 31).

[255] C. K. Thomas, L. Griffin, S. Godfrey, E. Ribot-ciscar and J. E. Butler, 'Fatigue of paralyzed and control thenar muscles induced by variable or constant frequency stimulation', *Journal of Neurophysiology*, vol. 89, pp. 2055–2064, 2003. DOI: 10.1152/jn.01002.2002. (cit. on p. 30).

[256] W. B. Scott, S. C. K. Lee, T. E. Johnston and S. A. Binder-Macleod, 'Switching stimulation patterns improves performance of paralyzed human quadriceps muscle', *Muscle & Nerve*, vol. 31, pp. 581–588, 5 May 2005, ISSN: 0148-639X. DOI: 10.1002/mus.20300 (cit. on p. 30).

[257] G. Deley, J. Denuziller, N. Babault and J. A. Taylor, 'Effects of electrical stimulation pattern on quadriceps isometric force and fatigue in individuals with spinal cord injury', *Muscle & Nerve*, vol. 52, pp. 260–264, 2 Aug. 2015, ISSN: 0148639X. DOI: 10.1002/mus.24530 (cit. on p. 30).

[258] D. Graupe, P. Suliga, C. Prudiant and K. H. Kohn, 'Stochastically-modulated stimulation to slow down muscle fatigue at stimulated sites in paraplegics using functional electrical stimulation for leg extension', *Neurological Research*, vol. 22, pp. 703–704, 2000 (cit. on p. 30).

[259] G. Graham, T. Thrasher and M. Popovic, 'The effect of random modulation of functional electrical stimulation parameters on muscle fatigue', *IEEE Transactions on Neural Systems and Rehabilitation Engineering*, vol. 14,

pp. 38–45, 1 Mar. 2006, ISSN: 1534-4320. DOI: 10.1109/TNSRE.2006.870490 (cit. on p. 30).

[260] A. S. Gorgey, C. D. Black, C. P. Elder and G. A. Dudley, 'Effects of electrical stimulation parameters on fatigue in skeletal muscle', *Journal of Orthopaedic & Sports Physical Therapy*, vol. 39, pp. 684–692, 9 Sep. 2009, ISSN: 0190-6011. DOI: 10.2519/jospt.2009.3045 (cit. on p. 30).

[261] R. Jailani and M. O. Tokhi, 'The effect of functional electrical stimulation (fes) on paraplegic muscle fatigue', *Proceedings - 2012 IEEE 8th International Colloquium on Signal Processing and Its Applications, CSPA 2012*, pp. 500–504, 2012. DOI: 10.1109/CSPA.2012.6194780 (cit. on p. 30).

[262] S. Jezernik, 'The effect of stimulation frequency on the closed-loop control of quadriceps stimulation: Experimental results', *IFAC Proceedings Volumes*, vol. 36, pp. 151–155, 15 Aug. 2003, ISSN: 14746670. DOI: 10.1016/S1474-6670(17)33491-2 (cit. on p. 30).

[263] R. J. Downey, M. J. Bellman, H. Kawai, C. M. Gregory and W. E. Dixon, 'Comparing the induced muscle fatigue between asynchronous and synchronous electrical stimulation in able-bodied and spinal cord injured populations', *IEEE Transactions on Neural Systems and Rehabilitation Engineering*, vol. 23, pp. 964–972, 6 Nov. 2015, ISSN: 1534-4320. DOI: 10.1109/TNSRE.2014.2364735 (cit. on p. 30).

[264] G. P. Braz, M. Russold and G. M. Davis, 'Functional electrical stimulation control of standing and stepping after spinal cord injury: A review of technical characteristics', *Neuromodulation: Technology at the Neural Interface*, vol. 12, pp. 180–190, 3 Jul. 2009, ISSN: 10947159. DOI: 10.1111/j.1525-1403.2009.00213.x (cit. on p. 30).

[265] V. C. K. Cheung, C. M. Niu, S. Li, Q. Xie and N. Lan, 'A novel fes strategy for poststroke rehabilitation based on the natural organization of neuromuscular control', *IEEE Reviews in Biomedical Engineering*, vol. 12, pp. 154–167, 2019, ISSN: 1937-3333. DOI: 10.1109/RBME.2018.2874132 (cit. on p. 30).

[266] N. Kapadia, K. Masani, B. C. Craven, L. M. Giangregorio, S. L. Hitzig, K. Richards and M. R. Popovic, 'A randomized trial of functional electrical

stimulation for walking in incomplete spinal cord injury: Effects on walking competency', *Journal of Spinal Cord Medicine*, vol. 37, pp. 511–524, 5 2014, ISSN: 20457723. DOI: 10.1179/2045772314Y.0000000263 (cit. on p. 31).

[267] E. Chaplin, 'Functional neuromuscular stimulation for mobility in people with spinal cord injuries. the parastep i system', *The Journal of Spinal Cord Medicine*, vol. 19, pp. 99–106, 2 1996 (cit. on p. 31).

[268] H. Chizek, R. Kobetic, E. Marsolais, J. Abbas, I. Donner and E. Simon, 'Control of functional neuromuscular stimulation systems for standing and locomotion in paraplegics', *Proceedings of the IEEE*, vol. 76, pp. 1155–1165, 9 Sep. 1988, ISSN: 0018-9219. DOI: 10.1109/5.9661 (cit. on p. 31).

[269] M. O. Ibitoye, N. A. Hamzaid, M. Hayashibe, N. Hasnan and G. M. Davis, 'Restoring prolonged standing via functional electrical stimulation after spinal cord injury: A systematic review of control strategies', *Biomedical Signal Processing and Control*, vol. 49, pp. 34–47, Mar. 2019, ISSN: 17468094. DOI: 10.1016/j.bspc.2018.11.006 (cit. on p. 31).

[270] T. Schauer, 'Sensing motion and muscle activity for feedback control of functional electrical stimulation: Ten years of experience in berlin', *Annual Reviews in Control*, vol. 44, pp. 355–374, 2017, ISSN: 13675788. DOI: 10.1016/j.arcontrol.2017.09.014 (cit. on pp. 31, 85).

[271] P. Müller, A. J. D. Ama, J. C. Moreno and T. Schauer, 'Adaptive multichannel fes neuroprosthesis with learning control and automatic gait assessment', *Journal of NeuroEngineering and Rehabilitation*, vol. 17, pp. 1–20, 1 2020, ISSN: 17430003. DOI: 10.1186/s12984-020-0640-7 (cit. on p. 31).

[272] C. Cousin, V. Duenas and W. Dixon, 'Fes cycling and closed-loop feedback control for rehabilitative human–robot interaction', *Robotics*, vol. 10, 2 2021, ISSN: 22186581. DOI: 10.3390/robotics10020061 (cit. on p. 31).

[273] C. C. Lin, W. C. Liu, C. C. Chan and M. S. Ju, 'Fuzzy control with amplitude/pulse-width modulation of nerve electrical stimulation for muscle force control', *Journal of Neural Engineering*, vol. 9, 2 Apr. 2012, ISSN: 17412560. DOI: 10.1088/1741-2560/9/2/026026 (cit. on p. 31).

[274] B. K. K. Ibrahim, M. Tokhi, M. Huq and S. Gharooni, 'Fuzzy logic based cycle-to-cycle control of fes-induced swinging motion', IEEE, Jun. 2011, pp. 60–64, ISBN: 978-1-61284-229-5. DOI: 10.1109/INECCE.2011.5953850 (cit. on p. 31).

[275] H. Rouhani, M. Same, K. Masani, Y. Q. Li and M. R. Popovic, 'Pid controller design for fes applied to ankle muscles in neuroprosthesis for standing balance', *Frontiers in Neuroscience*, vol. 11, JUN 2017, ISSN: 1662453X. DOI: 10.3389/fnins.2017.00347 (cit. on p. 31).

[276] J. Quintern, R. Riener and S. Rupprecht, 'Comparison of simulation and experiments of different closed-loop strategies for functional electrical stimulation: Experiments in paraplegics', *Artificial Organs*, vol. 21, pp. 232–235, 3 1997, ISSN: 0160564X. DOI: 10.1111/j.1525-1594.1997.tb04656.x (cit. on p. 31).

[277] S. Jezernik, R. G. Wassink and T. Keller, 'Sliding mode closed-loop control of fes: Controlling the shank movement', *IEEE Transactions on Biomedical Engineering*, vol. 51, pp. 263–272, 2 Feb. 2004, ISSN: 00189294. DOI: 10.1109/TBME.2003.820393 (cit. on p. 31).

[278] D. B. Popovic and M. B. Popovic, 'Design of a control for a neural prosthesis for walking: Use of artificial neural networks', IEEE, 2006, pp. 121–128, ISBN: 1-4244-0432-0. DOI: 10.1109/NEUREL.2006.341193 (cit. on p. 31).

[279] J. Riess and J. Abbas, 'Adaptive neural network control of cyclic movements using functional neuromuscular stimulation', *IEEE Transactions on Rehabilitation Engineering*, vol. 8, pp. 42–52, 1 Mar. 2000, ISSN: 10636528. DOI: 10.1109/86.830948 (cit. on p. 31).

[280] B. A. Osuagwu, E. Whicher and R. Shirley, 'Active proportional electromyogram controlled functional electrical stimulation system', *Scientific Reports*, vol. 10, pp. 1–15, 1 2020, ISSN: 20452322. DOI: 10.1038/s41598-020-77664-0 (cit. on p. 31).

[281] A. Selfslagh, S. Shokur, D. S. Campos, A. R. Donati, S. Almeida, S. Y. Yamauti, D. B. Coelho, M. Bouri and M. A. Nicolelis, 'Non-invasive, brain-controlled functional electrical stimulation for locomotion rehabil-

itation in individuals with paraplegia', *Scientific Reports*, vol. 9, pp. 1–17, 1 2019, ISSN: 20452322. DOI: 10.1038/s41598-019-43041-9 (cit. on p. 31).

[282] S. Huang, Y. Zhang, P. Liu, Y. Chen, B. Gao, C. Chen and Y. Bai, 'Effectiveness of contralaterally controlled functional electrical stimulation vs. neuromuscular electrical stimulation for recovery of lower extremity function in patients with subacute stroke: A randomized controlled trial', *Frontiers in Neurology*, vol. 13, p. 133, Dec. 2022, ISSN: 1664-2295. DOI: 10.3389/fneur.2022.1010975 (cit. on p. 31).

[283] W. Meng, Q. Liu, Z. Zhou, Q. Ai, B. Sheng and S. S. Xie, 'Recent development of mechanisms and control strategies for robot-assisted lower limb rehabilitation', *Mechatronics*, vol. 31, pp. 132–145, 2015, ISSN: 09574158. DOI: 10.1016/j.mechatronics.2015.04.005 (cit. on p. 35).

[284] C. T. Craven, H. Gollee, S. Coupaud, M. A. Purcell and D. B. Allan, 'Investigation of robotic-assisted tilt-table therapy for early-stage spinal cord injury rehabilitation', *Journal of Rehabilitation Research and Development*, vol. 50, pp. 367–378, 3 2013, ISSN: 07487711. DOI: 10.1682/JRRD.2012.02.0027 (cit. on p. 35).

[285] K. J. Hunt, L. P. Jack, A. Pennycott, C. Perret, M. Baumberger and T. H. Kakebeeke, 'Control of work rate-driven exercise facilitates cardiopulmonary training and assessment during robot-assisted gait in incomplete spinal cord injury', *Biomedical Signal Processing and Control*, vol. 3, pp. 19–28, 1 2008, ISSN: 17468094. DOI: 10.1016/j.bspc.2007.10.002 (cit. on p. 35).

[286] L. Marchal-Crespo and D. J. Reinkensmeyer, 'Review of control strategies for robotic movement training after neurologic injury', *Journal of NeuroEngineering and Rehabilitation*, vol. 6, 1 2009, ISSN: 17430003. DOI: 10.1186/1743-0003-6-20 (cit. on p. 35).

[287] S. Paolucci, A. D. Vita, R. Massicci, M. Traballesi, I. Bureca, A. Matano, M. Iosa and C. Guariglia, 'Impact of participation on rehabilitation results: A multivariate study.', *European journal of physical and rehabilitation*

medicine, vol. 48, pp. 455–66, 3 Sep. 2012, ISSN: 1973-9095 (cit. on pp. 35, 87).

[288] A. Pennycott, D. Wyss, H. Vallery, V. Klamroth-Marganska and R. Riener, 'Towards more effective robotic gait training for stroke rehabilitation: A review', *Journal of NeuroEngineering and Rehabilitation*, vol. 9, pp. 1–13, 1 2012, ISSN: 17430003. DOI: 10.1186/1743-0003-9-65 (cit. on p. 35).

[289] A. Kaelin-Lane, L. Sawaki and L. G. Cohen, 'Role of voluntary drive in encoding an elementary motor memory', *Journal of Neurophysiology*, vol. 93, pp. 1099–1103, 2 2005, ISSN: 00223077. DOI: 10.1152/jn.00143.2004 (cit. on pp. 35, 87).

[290] M. Lotze, C. Braun, N. Birbaumer, S. Anders and L. G. Cohen, 'Motor learning elicited by voluntary drive', *Brain*, vol. 126, pp. 866–872, 4 2003, ISSN: 00068950. DOI: 10.1093/brain/awg079 (cit. on p. 35).

[291] E. Shahriari, D. Zardykhan, A. Koenig, E. Jensen and S. Haddadin, 'Energy-based adaptive control and learning for patient-aware rehabilitation', *IEEE International Conference on Intelligent Robots and Systems*, pp. 5671–5678, 2019, ISSN: 21530866. DOI: 10.1109/IROS40897.2019.8968249 (cit. on p. 35).

[292] A. Taherifar, G. Vossoughi and A. S. Ghafari, 'Variable admittance control of the exoskeleton for gait rehabilitation based on a novel strength metric', *Robotica*, vol. 36, pp. 427–447, 3 2018, ISSN: 14698668. DOI: 10.1017/S0263574717000480 (cit. on p. 35).

[293] S. Hussain, P. K. Jamwal, M. H. Ghayesh and S. Q. Xie, 'Assist-as-needed control of an intrinsically compliant robotic gait training orthosis', *IEEE Transactions on Industrial Electronics*, vol. 64, pp. 1675–1685, 2 2017, ISSN: 02780046. DOI: 10.1109/TIE.2016.2580123 (cit. on p. 35).

[294] A. E. Russi and M. A. Brown, 'Robotic assist-as-needed as an alternative to therapist- assisted gait rehabilitation', *Int J Phys Med Rehabil*, vol. 165, pp. 255–269, 2 2016, ISSN: 1527-5418. DOI: 10.1016/j.trsl.2014.08.005.The (cit. on p. 35).

[295] S. L. Delp, F. C. Anderson, A. S. Arnold, P. Loan, A. Habib, C. T. John, E. Guendelman and D. G. Thelen, 'Opensim: Open-source software to create and analyze dynamic simulations of movement', *IEEE Transactions on Biomedical Engineering*, vol. 54, pp. 1940–1950, 11 2007, ISSN: 00189294. DOI: 10.1109/TBME.2007.901024 (cit. on p. 38).

[296] N. Šarabon, Ž. Kozinc and M. Perman, 'Establishing reference values for isometric knee extension and flexion strength', *Frontiers in Physiology*, vol. 12, Oct. 2021, ISSN: 1664-042X. DOI: 10.3389/fphys.2021.767941 (cit. on p. 40).

[297] M. M. Krantz, M. Åström and A. M. Drake, 'Strength and fatigue measurements of the hip flexor and hip extensor muscles: Test-retest reliability and limb dominance effect', *International Journal of Sports Physical Therapy*, vol. 15, pp. 967–976, 6 Dec. 2020, ISSN: 2159-2896. DOI: 10.26603/ijspt20200967 (cit. on p. 40).

[298] A. Moraux, A. Canal, G. Ollivier, I. Ledoux, V. Doppler, C. Payan and J. Y. Hogrel, 'Ankle dorsi- and plantar-flexion torques measured by dynamometry in healthy subjects from 5 to 80 years', *BMC Musculoskeletal Disorders*, vol. 14, 2013, ISSN: 14712474. DOI: 10.1186/1471-2474-14-104 (cit. on p. 40).

[299] R. S. Maeda, P. L. Gribble and J. A. Pruszynski, 'Learning new feedforward motor commands based on feedback responses', *Current Biology*, vol. 30, 1941–1948.e3, 10 May 2020, ISSN: 18790445. DOI: 10.1016/j.cub.2020.03.005 (cit. on p. 41).

[300] I. Pisotta and M. Molinari, 'Cerebellar contribution to feedforward control of locomotion', *Frontiers in Human Neuroscience*, vol. 8, JUNE Jun. 2014, ISSN: 1662-5161. DOI: 10.3389/fnhum.2014.00475 (cit. on p. 41).

[301] A. M. Haith and J. W. Krakauer, 'Model-based and model-free mechanisms of human motor learning', *Advances in Experimental Medicine and Biology*, vol. 782, pp. 1–21, 2013, ISSN: 00652598. DOI: 10.1007/978-1-4614-5465-6_1 (cit. on p. 41).

[302] R. D. Seidler, D. C. Noll and G. Thiers, 'Feedforward and feedback processes in motor control', *NeuroImage*, vol. 22, pp. 1775–1783, 4 Aug.

2004, ISSN: 10538119. DOI: 10.1016/j.neuroimage.2004.05.003 (cit. on p. 41).

[303] K. P. Tee, D. W. Franklin, M. Kawato, T. E. Milner and E. Burdet, 'Concurrent adaptation of force and impedance in the redundant muscle system', *Biological Cybernetics*, vol. 102, pp. 31–44, 1 Jan. 2010, ISSN: 03401200. DOI: 10.1007/s00422-009-0348-z (cit. on pp. 41, 69).

[304] R. A. Scheidt, J. B. Dingwell and F. A. Mussa-Ivaldi, 'Learning to move amid uncertainty', *Journal of Neurophysiology*, vol. 86, pp. 971–985, 2 2001, ISSN: 00223077. DOI: 10.1152/jn.2001.86.2.971 (cit. on pp. 41, 69).

[305] K. A. Thoroughman and R. Shadmehr, 'Learning of action through adaptive combination of motor primitives', *Nature*, vol. 407, pp. 742–747, 6805 Oct. 2000, ISSN: 0028-0836. DOI: 10.1038/35037588 (cit. on pp. 41, 69).

[306] D. F. N. Gordon, A. Christou, T. Stouraitis, M. Gienger and S. Vijayakumar, 'Learning personalised human sit-to-stand motion strategies via inverse musculoskeletal optimal control', vol. 2023-May, IEEE, May 2023, pp. 10 497–10 503, ISBN: 979-8-3503-2365-8. DOI: 10.1109/ICRA48891.2023.10160411 (cit. on pp. 41, 42).

[307] B. Q. Hoa, V. Padois, F. Benamar and E. Desailly, 'A two-step optimization-based synthesis of squat movements', in Springer Science and Business Media Deutschland GmbH, 2021, vol. 12777 LNCS, pp. 122–138, ISBN: 9783030778163. DOI: 10.1007/978-3-030-77817-0_11 (cit. on p. 41).

[308] V. Q. Nguyen, R. T. Johnson, F. C. Sup and B. R. Umberger, 'Bilevel optimization for cost function determination in dynamic simulation of human gait', *IEEE Transactions on Neural Systems and Rehabilitation Engineering*, vol. 27, pp. 1426–1435, 7 2019, ISSN: 15580210. DOI: 10.1109/TNSRE.2019.2922942 (cit. on p. 41).

[309] M. Geravand, P. Z. Korondi, C. Werner, K. Hauer and A. Peer, 'Human sit-to-stand transfer modeling towards intuitive and biologically-inspired robot assistance', *Autonomous Robots*, vol. 41, pp. 575–592, 3

Mar. 2017, ISSN: 15737527. DOI: 10.1007/s10514-016-9553-5 (cit. on p. 41).

[310] S. Ren, W. Wang, Z. G. Hou, B. Chen, X. Liang, J. Wang and L. Peng, 'Personalized gait trajectory generation based on anthropometric features using random forest', *Journal of Ambient Intelligence and Humanized Computing*, vol. 14, pp. 15 597–15 608, 12 Dec. 2023, ISSN: 18685145. DOI: 10.1007/s12652-019-01390-3 (cit. on p. 46).

[311] V. B. Semwal, R. Jain, P. Maheshwari and S. Khatwani, 'Gait reference trajectory generation at different walking speeds using lstm and cnn', *Multimedia Tools and Applications*, vol. 82, pp. 33 401–33 419, 21 Sep. 2023, ISSN: 15737721. DOI: 10.1007/s11042-023-14733-2 (cit. on p. 46).

[312] P. I. Frazier, 'A tutorial on bayesian optimization', pp. 1–22, Section 5 2018 (cit. on pp. 52, 74).

[313] H. M. Gutmann, 'A radial basis function method for global optimization', *Journal of Global Optimization*, vol. 19, pp. 201–227, 3 2001, ISSN: 09255001. DOI: 10.1023/A:1011255519438 (cit. on pp. 52, 59).

[314] A. J. Del-Ama, Á. Gil-Agudo, J. L. Pons and J. C. Moreno, 'Hybrid fes-robot cooperative control of ambulatory gait rehabilitation exoskeleton', *Journal of NeuroEngineering and Rehabilitation*, vol. 11, pp. 1–15, 1 2014, ISSN: 17430003. DOI: 10.1186/1743-0003-11-27 (cit. on pp. 53, 59, 86, 93).

[315] M. Khamar, M. Edrisi and M. Zahiri, 'Human-exoskeleton control simulation, kinetic and kinematic modeling and parameters extraction', *MethodsX*, vol. 6, pp. 1838–1846, December 2018 2019, ISSN: 22150161. DOI: 10.1016/j.mex.2019.08.014 (cit. on p. 68).

[316] B. Ren, J. Liu and J. Chen, 'Simulating human–machine coupled model for gait trajectory optimization of the lower limb exoskeleton system based on genetic algorithm', *International Journal of Advanced Robotic Systems*, vol. 16, pp. 1–15, 6 2019, ISSN: 17298814. DOI: 10.1177/1729881419893493 (cit. on p. 68).

[317] K. A. Inkol and J. McPhee, 'Assessing control of fixed-support balance recovery in wearable lower-limb exoskeletons using multibody dynamic modelling', IEEE, Nov. 2020, pp. 54–60, ISBN: 978-1-7281-5907-2. DOI: 10.1109/BioRob49111.2020.9224430 (cit. on p. 68).

[318] D. Torricelli, C. Cortés, N. Lete, Á. Bertelsen, J. E. Gonzalez-Vargas, A. J. Del-Ama, I. Dimbwadyo, J. C. Moreno, J. Florez and J. L. Pons, 'A subject-specific kinematic model to predict human motion in exoskeleton-assisted gait', *Frontiers in Neurorobotics*, vol. 12, pp. 1–11, APR 2018, ISSN: 16625218. DOI: 10.3389/fnbot.2018.00018 (cit. on p. 68).

[319] Q. Chen, H. Cheng, C. Yue, R. Huang and H. Guo, 'Dynamic balance gait for walking assistance exoskeleton', *Applied Bionics and Biomechanics*, p. 10, 2018. DOI: 10.1155/2018/7847014 (cit. on p. 68).

[320] S. Hosseini-Zahraei, M. S. Tali, M. H. Saberi, I. Kardan and A. Akbarzadeh, 'A simple opensim-simulink interface for cascaded zero-force control of human-robot interaction in a hip exoskeleton robot', IEEE, Nov. 2022, pp. 55–60, ISBN: 978-1-6654-5452-0. DOI: 10.1109/ICRoM57054.2022.10025309 (cit. on p. 68).

[321] M. K. Duong, H. Cheng, H. T. Tran and Q. Jing, 'Minimizing human-exoskeleton interaction force using compensation for dynamic uncertainty error with adaptive rbf network', *Journal of Intelligent and Robotic Systems: Theory and Applications*, vol. 82, pp. 413–433, 3-4 2016, ISSN: 15730409. DOI: 10.1007/s10846-015-0251-x (cit. on p. 68).

[322] G. Serrancoli, A. Falisse, C. Dembia, J. Vantilt, K. Tanghe, D. Lefeber, I. Jonkers, J. D. Schutter and F. D. Groote, 'Subject-exoskeleton contact model calibration leads to accurate interaction force predictions', *IEEE Transactions on Neural Systems and Rehabilitation Engineering*, vol. 27, pp. 1597–1605, 8 Aug. 2019, ISSN: 1534-4320. DOI: 10.1109/TNSRE.2019.2924536 (cit. on p. 69).

[323] J. L. Emken, J. E. Bobrow and D. J. Reinkensmeyer, 'Robotic movement training as an optimization problem: Designing a controller that assists only as needed', vol. 2005, IEEE, 2005, pp. 307–312, ISBN: 0780390032. DOI: 10.1109/ICORR.2005.1501108 (cit. on p. 69).

[324] K. L. Poggensee and S. H. Collins, 'How adaptation, training, and customization contribute to benefits from exoskeleton assistance', *Science Robotics*, vol. 6, p. 2021.04.25.440289, 58 Sep. 2021, ISSN: 2470-9476. DOI: 10.1126/scirobotics.abf1078 (cit. on pp. 73, 75).

[325] G. M. Bryan, P. W. Franks, S. Song, A. S. Voloshina, R. Reyes, M. P. O'Donovan, K. N. Gregorczyk and S. H. Collins, 'Optimized hip–knee–ankle exoskeleton assistance at a range of walking speeds', *Journal of NeuroEngineering and Rehabilitation*, vol. 18, 1 Dec. 2021, ISSN: 17430003. DOI: 10.1186/s12984-021-00943-y (cit. on p. 73).

[326] S. Song and S. H. Collins, 'Optimizing exoskeleton assistance for faster self-selected walking', *IEEE Transactions on Neural Systems and Rehabilitation Engineering*, vol. 29, pp. 786–795, 2021, ISSN: 15580210. DOI: 10.1109/TNSRE.2021.3074154 (cit. on p. 73).

[327] N. Hansen, 'The cma evolution strategy: A tutorial', Apr. 2016 (cit. on pp. 76–78).

[328] J. C. Selinger and J. M. Donelan, 'Estimating instantaneous energetic cost during non-steady-state gait', *Journal of Applied Physiology*, vol. 117, pp. 1406–1415, 11 Dec. 2014, ISSN: 15221601. DOI: 10.1152/japplphysiol.00445.2014 (cit. on p. 84).

[329] B. R. Umberger, K. G. Gerritsen and P. E. Martin, 'A model of human muscle energy expenditure.', *Computer methods in biomechanics and biomedical engineering*, vol. 6, pp. 99–111, 2 2003, ISSN: 10255842. DOI: 10.1080/1025584031000091678 (cit. on p. 84).

[330] T. K. Uchida, J. L. Hicks, C. L. Dembia and S. L. Delp, 'Stretching your energetic budget: How tendon compliance affects the metabolic cost of running', *PLoS ONE*, vol. 11, 3 Mar. 2016, ISSN: 19326203. DOI: 10.1371/journal.pone.0150378 (cit. on p. 84).

[331] C. L. Dembia, A. Silder, T. K. Uchida, J. L. Hicks and S. L. Delp, 'Simulating ideal assistive devices to reduce the metabolic cost of walking with heavy loads', *PLoS ONE*, vol. 12, 7 Jul. 2017, ISSN: 19326203. DOI: 10.1371/journal.pone.0180320 (cit. on p. 84).

[332] A. D. Koelewijn, D. Heinrich and A. J. van den Bogert, 'Metabolic cost calculations of gait using musculoskeletal energy models, a comparison study', *PLoS ONE*, vol. 14, 9 Sep. 2019, ISSN: 19326203. DOI: 10.1371/journal.pone.0222037 (cit. on p. 84).

[333] D. F. N. Gordon, C. McGreavy, A. Christou and S. Vijayakumar, 'Human-in-the-loop optimization of exoskeleton assistance via online simulation of metabolic cost', *IEEE Transactions on Robotics*, vol. 38, pp. 1410–1429, 3 Jun. 2022, ISSN: 1552-3098. DOI: 10.1109/TRO.2021.3133137 (cit. on p. 84).

[334] A. J. Del-Ama, A. D. Koutsou, J. C. Moreno, A. De-los-Reyes, N. Gil-Agudo and J. L. Pons, 'Review of hybrid exoskeletons to restore gait following spinal cord injury', *The Journal of Rehabilitation Research and Development*, vol. 49, p. 497, 4 2012, ISSN: 0748-7711. DOI: 10.1682/JRRD.2011.03.0043 (cit. on p. 85).

[335] M. R. Popovic, K. Masani and S. Micera, 'Functional electrical stimulation therapy: Recovery of function following spinal cord injury and stroke', in Springer International Publishing, 2016, vol. 16, pp. 513–532, ISBN: 9789400720596. DOI: 10.1007/978-3-319-28603-7_25 (cit. on p. 85).

[336] D. Popovic, R. Tomovic and L. Schwirtlich, 'Hybrid assistive system - the motor neuroprosthesis', *Transactions on Biomedical Engineering*, vol. 36, pp. 729–737, 7 1989 (cit. on p. 86).

[337] M. Goldfarb and W. K. Durfee, 'Design of a controlled-brake orthosis for regulating fes-aided gait', *IEEE Transactions on Rehabilitation Engineering*, vol. 4, pp. 13–24, 1 Mar. 1996 (cit. on p. 86).

[338] R. Kobetic, C. S. To, J. R. Schnellenberger, M. L. Audu, T. C. Bulea, R. Gaudio, G. Pinault, S. Tashman and R. J. Triolo, 'Development of hybrid orthosis for standing, walking, and stair climbing after spinal cord injury', *The Journal of Rehabilitation Research and Development*, vol. 46, p. 447, 3 2009, ISSN: 0748-7711. DOI: 10.1682/JRRD.2008.07.0087 (cit. on p. 86).

[339] N. Sharma, V. Mushahwar and R. Stein, 'Dynamic optimization of fes and orthosis-based walking using simple models', *IEEE Transactions on Neural Systems and Rehabilitation Engineering*, vol. 22, pp. 114–126, 1 2014, ISSN: 15344320. DOI: 10.1109/TNSRE.2013.2280520 (cit. on p. 86).

[340] Y. Stauffer, 'Control strategies for a verticalized rehabilitation robot', *Tesis de Doctorado*, vol. 4392, p. 270, 2009 (cit. on p. 86).

[341] K. H. Ha, S. A. Murray and M. Goldfarb, 'An approach for the cooperative control of fes with a powered exoskeleton during level walking for persons with paraplegia', *IEEE Transactions on Neural Systems and Rehabilitation Engineering*, vol. 24, pp. 455–466, 4 2016. DOI: 10.1109/TNSRE.2015.2421052 (cit. on p. 86).

[342] X. Bao, N. Kirsch and N. Sharma, 'Dynamic control allocation of a feedback linearized hybrid neuroprosthetic system', *Proceedings of the American Control Conference*, vol. 2016-July, pp. 3976–3981, 2016, ISSN: 07431619. DOI: 10.1109/ACC.2016.7525534 (cit. on p. 86).

[343] N. Kirsch, N. Alibeji and N. Sharma, 'Nonlinear model predictive control of functional electrical stimulation', *Control Engineering Practice*, vol. 58, pp. 319–331, 2017, ISSN: 09670661. DOI: 10.1016/j.conengprac.2016.03.005 (cit. on p. 86).

[344] V. Molazadeh, Q. Zhang, X. Bao, B. E. Dicianno and N. Sharma, 'Shared control of a powered exoskeleton and functional electrical stimulation using iterative learning', *Frontiers in Robotics and AI*, vol. 8, pp. 1–13, November 2021, ISSN: 22969144. DOI: 10.3389/frobt.2021.711388 (cit. on pp. 86, 87).

[345] N. A. Alibeji, V. Molazadeh, B. E. Dicianno and N. Sharma, 'A control scheme that uses dynamic postural synergies to coordinate a hybrid walking neuroprosthesis: Theory and experiments', *Frontiers in Neuroscience*, vol. 12, pp. 1–15, APR 2018, ISSN: 1662453X. DOI: 10.3389/fnins.2018.00159 (cit. on pp. 86, 87).

[346] H. Vallery, T. Stützle, M. Buss and D. Abel, 'Control of a hybrid motor prosthesis for the knee joint', *IFAC Proceedings Volumes (IFAC-*

PapersOnline), vol. 38, pp. 76–81, 1 2005, ISSN: 14746670. DOI: 10.3182/20050703-6-cz-1902.01415 (cit. on p. 87).

[347] F. Romero-Sánchez, J. Bermejo-García, J. Barrios-Muriel and F. J. Alonso, 'Design of the cooperative actuation in hybrid orthoses: A theoretical approach based on muscle models', *Frontiers in Neurorobotics*, vol. 13, pp. 1–15, July 2019, ISSN: 16625218. DOI: 10.3389/fnbot.2019.00058 (cit. on pp. 87, 91).

[348] A. A. Blank, J. A. French, A. U. Pehlivan and M. K. O'Malley, 'Current trends in robot-assisted upper-limb stroke rehabilitation: Promoting patient engagement in therapy', *Current Physical Medicine and Rehabilitation Reports*, vol. 2, pp. 184–195, 3 2014, ISSN: 21674833. DOI: 10.1007/s40141-014-0056-z (cit. on p. 87).

[349] L. E. Kahn, P. S. Lum, W. Z. Rymer and D. J. Reinkensmeyer, 'Robot-assisted movement training for the stroke-impaired arm: Does it matter what the robot does?', *Journal of Rehabilitation Research and Development*, vol. 43, pp. 619–629, 5 2006, ISSN: 07487711. DOI: 10.1682/JRRD.2005.03.0056 (cit. on p. 87).

[350] D. F. N. Gordon, A. Christou, T. Stouraitis, M. Gienger and S. Vijayakumar, 'Adaptive assistive robotics: A framework for triadic collaboration between humans and robots', *Royal Society Open Science*, vol. 10, 6 Jun. 2023, ISSN: 2054-5703. DOI: 10.1098/rsos.221617 (cit. on p. 88).

[351] M. Gfohler, T. Angeli and P. Lugner, 'Modeling of artificially activated muscle and application to fes cycling', *Journal of Mechanics in Medicine and Biology*, vol. 04, pp. 77–92, 01 2004, ISSN: 0219-5194. DOI: 10.1142/S0219519404000850 (cit. on pp. 91, 92).

[352] A. Seth, J. L. Hicks, T. K. Uchida *et al.*, 'Opensim: Simulating musculoskeletal dynamics and neuromuscular control to study human and animal movement', *PLOS Computational Biology*, vol. 14, D. Schneidman, Ed., e1006223, 7 2018, ISSN: 1553-7358. DOI: 10.1371/journal.pcbi.1006223 (cit. on p. 93).

[353] D. Stanev, 'Biomechanical simulation of virtual physiological humans: Modeling of musculoskeletal kinematic and dynamic redundancy using coordinate projection methods', 2018 (cit. on p. 96).

[354] R. Riener, J. Quintern and G. Schmidt, 'Biomechanical model of the human knee evaluated by neuromuscular stimulation', *Journal of Biomechanics*, vol. 29, pp. 1157–1167, 9 1996, ISSN: 00219290. DOI: 10.1016/0021-9290(96)00012-7 (cit. on pp. 95, 103).

[355] N. Sharma, N. A. Kirsch, N. A. Alibeji and W. E. Dixon, 'A non-linear control method to compensate for muscle fatigue during neuromuscular electrical stimulation', *Frontiers Robotics AI*, vol. 4, DEC 2017, ISSN: 22969144. DOI: 10.3389/frobt.2017.00068 (cit. on p. 95).

[356] R. Riener and J. Quintern, 'A physiologically based model of muscle activation verified by electrical stimulation', *Bioelectrochemistry and Bioenergetics*, vol. 43, pp. 257–264, 2 1997, ISSN: 03024598. DOI: 10.1016/S0302-4598(96)05191-4 (cit. on p. 103).

[357] N. Makowski, J. Knutson, J. Chae and P. Crago, 'Interaction of poststroke voluntary effort and functional neuromuscular electrical stimulation', *The Journal of Rehabilitation Research and Development*, vol. 50, p. 85, 1 2013, ISSN: 0748-7711. DOI: 10.1682/JRRD.2011.04.0068 (cit. on p. 104).

[358] R. Perumal, A. S. Wexler, T. M. Kesar, A. Jancosko, Y. Laufer and S. A. Binder-Macleod, 'A phenomenological model that predicts forces generated when electrical stimulation is superimposed on submaximal volitional contractions', *Journal of Applied Physiology*, vol. 108, pp. 1595–1604, 6 2010, ISSN: 87507587. DOI: 10.1152/japplphysiol.01231.2009 (cit. on p. 104).

[359] E. Langzam, Y. Nemirovsky, E. Isakov and J. Mizrahi, 'Muscle enhancement using closed-loop electrical stimulation: Volitional versus induced torque', *Journal of Electromyography and Kinesiology*, vol. 17, pp. 275–284, 3 2007, ISSN: 10506411. DOI: 10.1016/j.jelekin.2006.03.001 (cit. on p. 104).

[360] H. Wang, V. Caggiano, G. Durandau, M. Sartori and V. Kumar, 'Myosim: Fast and physiologically realistic mujoco models for musculoskeletal

and exoskeletal studies', IEEE, May 2022, pp. 8104–8111, ISBN: 978-1-7281-9681-7. DOI: 10.1109/ICRA46639.2022.9811684 (cit. on p. 108).

[361] A. Ikkala and P. Hämäläinen, 'Converting biomechanical models from opensim to mujoco', in Springer Science and Business Media Deutschland GmbH, 2022, vol. 28, pp. 277–281. DOI: 10.1007/978-3-030-70316-5_45 (cit. on p. 108).

[362] S. Luo, G. Androwis, S. Adamovich, E. Nunez, H. Su and X. Zhou, 'Robust walking control of a lower limb rehabilitation exoskeleton coupled with a musculoskeletal model via deep reinforcement learning', *Journal of NeuroEngineering and Rehabilitation*, vol. 20, pp. 1–20, 1 2023, ISSN: 17430003. DOI: 10.1186/s12984-023-01147-2 (cit. on pp. 108, 112).

[363] S. Luo, G. Androwis, S. Adamovich, H. Su, E. Nunez and X. Zhou, 'Reinforcement learning and control of a lower extremity exoskeleton for squat assistance', *Frontiers in Robotics and AI*, vol. 8, pp. 1–17, July 2021, ISSN: 22969144. DOI: 10.3389/frobt.2021.702845 (cit. on p. 108).

[364] C. R. Taylor, S. S. Srinivasan, S. H. Yeon, M. K. O'Donnell, T. J. Roberts and H. M. Herr, 'Magnetomicrometry', *Science Robotics*, vol. 6, 57 Aug. 2021, ISSN: 2470-9476. DOI: 10.1126/scirobotics.abg0656 (cit. on p. 108).

[365] S. S. Srinivasan, B. E. Maimon, M. Diaz, H. Song and H. M. Herr, 'Closed-loop functional optogenetic stimulation', *Nature Communications*, vol. 9, 1 Dec. 2018, ISSN: 20411723. DOI: 10.1038/s41467-018-07721-w (cit. on p. 108).

[366] L. N. Awad, J. Bae, K. O'Donnell *et al.*, 'A soft robotic exosuit improves walking in patients after stroke', *Science Translational Medicine*, vol. 9, 400 Jul. 2017, ISSN: 1946-6234. DOI: 10.1126/scitranslmed.aai9084 (cit. on p. 108).

[367] J. Chua, J. Culpan and E. Menon, 'Efficacy of an electromechanical gait trainer poststroke in singapore: A randomized controlled trial', *Archives of Physical Medicine and Rehabilitation*, vol. 97, pp. 683–690, 5 May 2016, ISSN: 1532821X. DOI: 10.1016/j.apmr.2015.12.025 (cit. on p. 108).

[368] W. H. Chang, M. S. Kim, J. P. Huh, P. K. Lee and Y. H. Kim, 'Effects of robot-assisted gait training on cardiopulmonary fitness in subacute stroke patients: A randomized controlled study', *Neurorehabilitation and Neural Repair*, vol. 26, pp. 318–324, 4 May 2012, ISSN: 15459683. DOI: 10.1177/1545968311408916 (cit. on p. 108).

[369] S. Fisher, L. Lucas and T. Thrasher, 'Robot-assisted gait training for patients with hemiparesis due to stroke', *Topics in Stroke Rehabilitation*, vol. 18, pp. 269–276, 3 Jan. 2011, ISSN: 10749357. DOI: 10.1310/tsr1803-269 (cit. on p. 108).

[370] T. G. Hornby, D. D. Campbell, J. H. Kahn, T. Demott, J. L. Moore and H. R. Roth, 'Enhanced gait-related improvements after therapist- versus robotic-assisted locomotor training in subjects with chronic stroke: A randomized controlled study', *Stroke*, vol. 39, pp. 1786–1792, 6 Jun. 2008, ISSN: 00392499. DOI: 10.1161/STROKEAHA.107.504779 (cit. on p. 108).

[371] M. Pohl, C. Warner, M. Holzgraefe, G. Kroczek, J. Mehrholz, I. Wingerdorf, G. Hölig, R. Koch and S. Hesse, 'Repetitive locomotor training and physiotherapy improve walking and basic activities of daily living after stroke: A single-blind, randomised multicentre trial (deutsche gangtrainerstudie, degas)', *Clinical Rehabilitation*, vol. 21, pp. 17–27, 1 Jan. 2007, ISSN: 02692155. DOI: 10.1177/0269215506071281 (cit. on p. 108).

[372] M. Shushtari, R. Nasiri and A. Arami, 'Online reference trajectory adaptation: A personalized control strategy for lower limb exoskeletons', *IEEE Robotics and Automation Letters*, vol. 7, pp. 128–134, 1 Jan. 2022, ISSN: 2377-3766. DOI: 10.1109/LRA.2021.3115572 (cit. on pp. 108, 109).

[373] Z. Zhou, B. Liang, G. Huang, B. Liu, J. Nong and L. Xie, 'Individualized gait generation for rehabilitation robots based on recurrent neural networks', *IEEE Transactions on Neural Systems and Rehabilitation Engineering*, vol. 29, pp. 273–281, 2021, ISSN: 15580210. DOI: 10.1109/TNSRE.2020.3045425 (cit. on pp. 108, 109).

[374] H. Vallery, E. H. V. Asseldonk, M. Buss and H. V. D. Kooij, 'Reference trajectory generation for rehabilitation robots: Complementary limb

motion estimation', vol. 17, Feb. 2009, pp. 23–30. DOI: 10.1109/TNSRE.2008.2008278 (cit. on pp. 108, 109).

[375] R. E. Singh, K. Iqbal, G. White and T. E. Hutchinson, 'A systematic review on muscle synergies: From building blocks of motor behavior to a neurorehabilitation tool', *Applied Bionics and Biomechanics*, vol. 2018, 2018, ISSN: 17542103. DOI: 10.1155/2018/3615368 (cit. on p. 109).

[376] D. Torricelli, F. Barroso, M. Coscia, C. Alessandro, F. Lunardini, E. B. Esteban and A. d'Avella, 'Muscle synergies in clinical practice: Theoretical and practical implications', in Springer International Publishing, 2016, vol. 10, pp. 251–272. DOI: 10.1007/978-3-319-24901-8_10 (cit. on p. 109).

[377] S. Safavynia, G. Torres-Oviedo and L. Ting, 'Muscle synergies: Implications for clinical evaluation and rehabilitation of movement', *Topics in Spinal Cord Injury Rehabilitation*, vol. 17, pp. 16–24, 1 May 2011, ISSN: 10820744. DOI: 10.1310/sci1701-16 (cit. on p. 109).

[378] C. Siviy, L. M. Baker, B. T. Quinlivan, F. Porciuncula, K. Swaminathan, L. N. Awad and C. J. Walsh, 'Opportunities and challenges in the development of exoskeletons for locomotor assistance', *Nature Biomedical Engineering*, vol. 7, pp. 456–472, 4 Dec. 2022, ISSN: 2157-846X. DOI: 10.1038/s41551-022-00984-1 (cit. on p. 111).

[379] P. Parik-Americano, J. P. Pinho, F. C. D. Santos, C. Taira, G. S. Umemura and A. Forner-Cordero, 'Walking and standing with an exoskeleton for the lower limbs: Effects of mass and inertia on gait and postural control', in *Proceedings of the IEEE RAS and EMBS International Conference on Biomedical Robotics and Biomechatronics*, vol. 2022-August, IEEE Computer Society, 2022, ISBN: 9781665458498. DOI: 10.1109/BioRob52689.2022.9925521 (cit. on p. 111).

[380] A. C. Villa-Parra, D. Delisle-Rodriguez, T. Botelho, J. J. V. Mayor, A. L. Delis, R. Carelli, A. F. Neto and T. F. Bastos, 'Control of a robotic knee exoskeleton for assistance and rehabilitation based on motion intention from semg', *Research on Biomedical Engineering*, vol. 34, pp. 198–210, 3 2018, ISSN: 24464740. DOI: 10.1590/2446-4740.07417 (cit. on p. 111).

[381] A. R. Donati, S. Shokur, E. Morya *et al.*, 'Long-term training with a brain-machine interface-based gait protocol induces partial neurological recovery in paraplegic patients', *Scientific Reports*, vol. 6, Aug. 2016, ISSN: 20452322. DOI: 10.1038/srep30383 (cit. on p. 111).

[382] A. Krasoulis and K. Nazarpour, 'Myoelectric digit action decoding with multi-output, multi-class classification: An offline analysis', *Scientific Reports*, vol. 10, 1 Dec. 2020, ISSN: 20452322. DOI: 10.1038/s41598-020-72574-7 (cit. on p. 111).

[383] A. Krasoulis, I. Kyranou, M. S. Erden, K. Nazarpour and S. Vijayakumar, 'Improved prosthetic hand control with concurrent use of myoelectric and inertial measurements', *Journal of NeuroEngineering and Rehabilitation*, vol. 14, 1 Jul. 2017, ISSN: 17430003. DOI: 10.1186/s12984-017-0284-4 (cit. on p. 111).

[384] O. Coser, C. Tamantini, P. Soda and L. Zollo, 'Ai-based methodologies for exoskeleton-assisted rehabilitation of the lower limb: A review', *Frontiers in Robotics and AI*, vol. 11, Feb. 2024, ISSN: 2296-9144. DOI: 10.3389/frobt.2024.1341580 (cit. on p. 111).

[385] G. Bingjing, H. Jianhai, L. Xiangpan and Y. Lin, 'Human–robot interactive control based on reinforcement learning for gait rehabilitation training robot', *International Journal of Advanced Robotic Systems*, vol. 16, pp. 1–16, 2 2019, ISSN: 17298814. DOI: 10.1177/1729881419839584 (cit. on p. 112).

[386] S. G. Khan, M. Tufail, S. H. Shah and I. Ullah, 'Reinforcement learning based compliance control of a robotic walk assist device', *Advanced Robotics*, vol. 33, pp. 1281–1292, 24 Dec. 2019, ISSN: 15685535. DOI: 10.1080/01691864.2019.1690574 (cit. on p. 112).

[387] Z. Peng, H. Cheng, R. Huang, J. Hu, R. Luo, K. Shi and B. K. Ghosh, 'Adaptive event-triggered motion tracking control strategy for a lower limb rehabilitation exoskeleton', in *Proceedings of the IEEE Conference on Decision and Control*, vol. 2021-December, Institute of Electrical and Electronics Engineers Inc., 2021, pp. 1795–1801, ISBN: 9781665436595. DOI: 10.1109/CDC45484.2021.9682822 (cit. on p. 112).

[388] L. Rose, M. C. Bazzocchi and G. Nejat, 'A model-free deep reinforcement learning approach for control of exoskeleton gait patterns', *Robotica*, vol. 40, pp. 2189–2214, 7 Jul. 2022, ISSN: 14698668. DOI: 10.1017/S0263574721001600 (cit. on p. 112).